Design requirements for a mobile high-voltage substation to (partly) bypass permanent substations to reduce planned outages.

J.T.H. Klein

Technische Universiteit Delft

TU Delft Delft University of Technology

Challenge the future

Design requirements for a mobile high-voltage substation to (partly) bypass permanent substations to reduce planned outages.

by

J.T.H. Klein

in partial fulfilment of the requirements for the degree of

Master of Science

in Electrical Engineering - Electrical Power Engineering

at the Delft University of Technology,
faculty of Electrical Engineering, Mathematics and Computer Science,

to be defended publicly on September 16, 2022 at 10:00 AM

Student number:	4474384	
Project duration:	December 1, 2021 – September 16, 2022	
Supervisors:	Prof. ir. P. T. M. Vaessen	TU Delft, supervisor
	Dr. Ir. M. Ghaffarian Niasar	TU Delft, daily supervisor
	Ir. C. S. Engelbrecht,	TU Delft daily supervisor
	Ir. E. van der Sluis,	TenneT daily supervisor
Thesis committee:	Prof. ir. P. T. M. Vaessen	TU Delft
	Dr. Ir. M. Ghaffarian Niasar	TU Delft
	Ir. E. van der Sluis,	TenneT Arnhem
	Dr. A. Lekic	TU Delft

This thesis is confidential and cannot be made public until September 16, 2023.

An electronic version of this thesis is available at `http://repository.tudelft.nl/`.

TU Delft

TenneT

Abstract

The energy transition requires massive expansion and reinforcement of the transmission grid which is challenging because of its high utilization, and regular maintenance, replacement, and repair. The difficulty of performing maintenance on high-voltage equipment and especially the substations lies in the fact that a big part of the substation needs to be taken out of service for the maintenance crew to work safely. When a part of a substation is taken out of service this influences the capacity and redundancy and thus the reliability of the grid. A planned outage is required to take a part of a substation out of service, these planned outages are limited in frequency and duration due to a shortage of especially trained and skilled people in combination with the high utilization of the grid.

The objective of this master thesis is to investigate important design aspects for mobile transmission stations to reduce/prevent planned outages during maintenance, replacement, and expansion projects on TenneT's (the Dutch transmission system operator) permanent substations. A mobile substation is a fully equipped substation mounted on one or multiple trailers to be easily transported. The mobile substation provides a bypass during maintenance on permanent substations allowing continued service without requiring planned outage.

A case study in this work shows that using a mobile substation during maintenance, replacement, and expansion projects on substations can possibly save TenneT several hundred million euros per year. Using the mobile substation on a 380 kV or 220 kV substation would make it possible to work on multiple 380 or 220 kV substations at the same time. It would also be easier to get a planned outage permit for the 150 kV and 110 kV substations. The use of a mobile substation would thus increase the efficiency of the projects and would reduce the amount of required critical resources.

Besides the case study, this work investigates the design requirements for mobile substations. The mobile substation should be able to (partly) bypass all TenneT substations and should contain mobile power transformers. The weight of the mobile substation is limited by road regulations. The transformers will be the heaviest components in the substation thus special attention is needed for their design. For the power transformers, a shell-type core design would be preferred with (high temperature) hybrid-insulation, due to its compact design and robustness for transportation. To comply with road regulations without special permits six 83.33 MVA single-phase transformers with an approximate weight of 36 tonne need to be connected in two banks of three single-phase transformers to reach the standardized capacity of 500 MVA.

The insulation distance in the mobile substation will greatly influence the size of the substation when deployed and during transport. Therefore, this insulation distance is an important design aspect which is covered in this work. The standards for insulation distances were analyzed. This analysis gave rise to doubts if these distances would apply to compact substations with large electrodes. An experiment was conducted at the TU Delft Electrical Sustainable Power Lab to determine the dielectric strength of large electrodes with sharp points in compact substations, and to verify if the insulation distances as specified in the standards should be applied to mobile substations.

It was found that the large electrodes with sharp points have similar breakdown voltages as a rod-rod gap setup. A higher breakdown voltage was found for the large spheres with protrusions compared to the rod-conductor gap which is used by the IEC standard. This indicates that the IEC standard insulation distances would be sufficient for use in a compact substation. Whether the substation can be made more compact by reducing the insulation distances should be investigated by executing experiments on an actual skid in a future study.

Acknowledgements

Firstly, I would like to thank my supervisor Peter Vaessen for providing me with the opportunity to work with TenneT and for his guidance and support throughout the course of my thesis. I would also like to thank my company supervisor Erik van der Sluis for his advice and support.

I would like to take this opportunity to thank Mohamad Ghaffarian Niasar for his continuous guidance and support during the project. I would also like to take this opportunity to express my gratitude to Christiaan Engelbrecht for assisting me and sharing his rich technical experience and expertise during the experiments and writing of the thesis.

I would like to express gratitude to Paul van Nes, Wim Termorshuizen, Geert Jan Kamphuis, and Luis Castro Heredia from The TU Delft Electrical Sustainable Power Lab, for their warm hospitality and assistance during the experimental stage of this thesis.

I would like to express my sincere thanks to all my friends and family. Especially, I would like to thank Olger Siebinga for his constant and immense support throughout the course of my thesis.

Contents

1 Introduction

In the Netherlands, 110 TWh of electrical energy was used in 2020 [8]. This enormous amount of energy needs to be transported to the users. the Dutch electricity grid has a total connected generation of 31.5 GW connecting approximately 8 million homes, businesses, and industries [77]. To be able to transport the high amount of electrical energy throughout the country high-voltage is used. By using higher voltages the same amount of power can be transported with lower currents thus reducing the losses. For the Dutch power grid voltages of 110 kV and 150 kV are called high-voltage (HV), 220 kV and 380 kV are called extra-high-voltage (EHV). The high and extra-high-voltage grid in the Netherlands and part of Germany is owned and operated by the Transmission System Operator (TSO) TenneT. Close to the customers, the high voltage is converted to lower voltages and delivered to the users by the Distribution System Operators (DSO).

The TenneT (extra) high-voltage grid consists of electrical transformer stations to step up or down the voltage, and transmission lines, cables, and switching stations to connect different circuits. To ensure continuous operation and prevent blackouts, all these components must be kept in a good condition. Therefore, regular maintenance, replacement, and repair is required. A big part of the high voltage network in the dutch grid was built in the 1960s and is therefore at the end of its expected technical life [68][40]. Besides these challenges in maintaining the existing grid, TenneT also faces a growing demand for new connections due to the transition to distributed energy resources (e.g. wind and solar farms) and growing energy demand e.g. for data centers [40]. For example, before 2030 TenneT plans to build 55 new substations, replace 150 substations and build 1350 km of new connections in the Netherlands [70]. To meet these new demands, the existing infrastructure needs to be expanded, which poses an additional challenge.

Performing maintenance on HV equipment, and especially the substations, is difficult because a big part of the substation needs to be decoupled from the grid and grounded to be able to work safely. When a part of a substation is taken out of service this influences the capacity and redundancy and thus reliability of the grid. For TenneT it is required that even during maintenance there is N-1 redundancy. This means that the grid must be capable of handling an outage of a single transmission line, cable, or transformer without suffering from interruptions in the electricity supply. This means that maintenance can only be performed when sufficient capacity remains available in the grid when the maintained part is taken out of service [69]. To meet the N-1 requirement during substation maintenance, this outage should be planned in advance to make sure that the system overall remains redundant and reliable. TenneT calls these planned outages VNB's (Voorziene Niet Beschikbaarheid). For planning these VNB's the expected loading of the grid is taken into account as well as other maintenance projects in the grid. It often occurs that these planned outages are canceled due to maintenance with higher priority or due to unexpected high utilization of the grid, causing long delays and extra costs for the canceled projects. These planned outages in general need to be requested months in advance. It is getting increasingly more difficult to obtain a planned outage permit due to the high utilization, maintenance, replacement, and repair of the grid.

This thesis will investigate the use of a mobile high-voltage substation to reduce the amount and duration of planned outages during maintenance, replacement, and expansion in TenneT substations. The aim is to bypass parts (bays) or a whole substation using the mobile substation. When the part of the substation is by-

passed maintenance could be performed without influencing the redundancy of the substation. Only during the connection of the mobile substation, a planned outage needs to be scheduled which greatly reduces the total time of planned outages. This mobile substation must fit normal road transport and should not require special permits during transport.

The goal of the thesis is to investigate important design aspects for mobile transmission stations to reduce/prevent planned outages during maintenance, replacement, and expansion projects on TenneT substations. The focus of the thesis is on mobile transformers and insulation distances in the mobile substation.

The main research question is:

What are the important design aspects for a mobile high-voltage substation to (partly) bypass a TenneT substation during maintenance, replacement, and expansion projects to reduce/prevent planned outages?

This main question can be split up into several questions:

- What are the characteristics of a TenneT substation?
- How is maintenance, replacement, and expansion currently performed, and what are the problems?
- To what extent will the use of a mobile substation to bypass a high-voltage substation reduce the required amount of critical resources, VNB time, and re-dispatch costs?
- What are the important design requirements for a mobile power transformer to bypass a TenneT substation and to be transported using regular road transport?
- How does the breakdown voltage between large electrodes with sharp points in compact air-insulated substations relate to gap length and are the minimal insulation distances as specified by the IEC 60071-1 [32] applicable to these compact substation?

1.1. Outline of the Thesis

First, Chapter 2 investigates a typical TenneT substation and its components to give an overview of what needs to be bypassed by a mobile substation. In Chapter 3, the planned outage permit process is explained and the different methods of performing maintenance, replacement, and expansion are investigated. A case study is performed to determine the advantages of a mobile substation for TenneT this is covered in Chapter 4. Finally, Chapter 5 gives an overview of two existing mobile substations.

The rest of this thesis is divided into two parts. Part I discusses the design considerations for a mobile power transformer. Part II covers the insulation distances in a compact mobile substation and a high-voltage breakdown test for air-insulated components.

Part I

An important limitation of using public roads without a special permit is the maximum weight of a loaded vehicle. The power transformer is the heaviest and most bulky component of a mobile substation. Therefore, the design requirements of the mobile power transformer are covered in Part I. Chapter 7 covers the state-of-the-art mobile transformer designs. Chapter 8 investigates the advantages and disadvantages of different transformer types to determine the most suitable transformer design for a mobile substation.

Part II

The insulation distances in an air-insulated mobile substation will greatly influence the substation dimensions when deployed and during transport. Therefore, the insulation distances are the main topic of Part II. Chapter 10 covers two different types of high voltage insulation that can be used for a mobile substation. Chapters 11 and 12 cover the (theoretical) background on insulation coordination. In Chapter 13 the Gap Factor will be introduced as a method to approximate the insulation distance in a substation. The theory behind the influence of overvoltage-wave shape and electrode size on the breakdown in air is discussed in Chapter 14. Chapter 15 discusses a high-voltage breakdown test that is performed at a TU Delft test facility to determine the breakdown voltage for large electrodes with small protrusions.

2

Background

This chapter will introduce the different (extra) high-voltage substations owned by TenneT and give an overview of the components in these substations.

2.1. TenneT

TenneT is the transmission system operator in the Netherlands and part of Germany. The Dutch part of the company is controlled and owned by the Dutch government. TenneT is responsible for the 380, 220, 150, and 110 kV networks in the Netherlands. The interconnections to other countries are also the responsibility of TenneT. The company owns around 300 high-voltage substations throughout the Netherlands.

Within the high-voltage network, there are connections between the high-voltage lines and cables of equal and different voltages. These connections are the so-called substations, consisting of bus-bars, power transformers, instrument transformers, protection and control equipment, circuit breakers, disconnectors, and earthing switches. These substations must guarantee the continuity of the electricity supply in all circumstances. To guarantee the continuity of supply the equipment needs to be protected from faults, such as short circuits or lightning overvoltages. Also, the power flow through the network is controlled by these substations.

The substations can be divided into three categories:

- **Transformer stations**
  A transformer station connects two or more circuits with different voltages using AC transformers. They also contain high-voltage switching equipment which is used to connect or isolate and ground parts of the system for fault clearance, maintenance, and control of the power flow through the network. Most transformer stations also have a switching function, connecting incoming and outgoing lines or cables of the same voltages.
- **Switching substations**
  Switching stations connect two or more circuits with the same voltage and thus there are no transformers present. The main function of a switching station is connecting or disconnecting transmission lines to and from the system. This can be done for fault clearance or to redirect power flows over different lines.
- **Converter substations**
  Converter stations are able to convert AC to DC and vice-versa, this is required at connections between HVDC lines and HVAC circuits but can also be used for the connection of two asynchronous AC circuits. TenneT only owns converter substations for the connection between HVDC and HVAC.

For the Dutch power grid, strict rules are laid down in legislation for grid design and operation. The network design specifications are given by the "Nederlandse Electriciteitswet" (Dutch Electricity law) in art.16 lid 4 [76], which requires the network to be always N-1 redundant. Thus even during maintenance, the system should be N-1 redundant.

TenneT strives to have, as far as possible, a standard substation layout for both the Extra high-voltage (EHV) and high-voltage (HV) grid. The reason for this is the large number of substations that must be re-

newed in the coming years because for a big share of the EHV and HV stations the primary equipment is over 50 years old [68].

2.2. Transformer station

In this section a transformer station will be covered in detail, it is chosen to describe only a transformer station because it is quite similar to a switching station where the presence of power transformers is the main difference.

There are a lot of different transformer stations in the Netherlands, for which the biggest differences are the voltage levels to which they connect. TenneT owns substations that connect their different transmission grid voltages (380 kV, 220 kV, 150 kV, and 110 kV) and substations that connect to the distribution system operators with voltages below 110 kV. The most important components of a substation will be covered in this chapter.

As a case study the TenneT station Eindhoven 380 (EHV380) will be used. This substation is chosen because there is a big maintenance project planned for 2024. An aerial overview of this substation is given in Figure 2.1. There are five 380 kV connections to this substation, one of the bays connecting a 380 kV line to the substation is marked with a blue rectangle. One of the four transformer bays which converts the 380 kV to 150 kV is marked with the red rectangle in Figure 2.1.

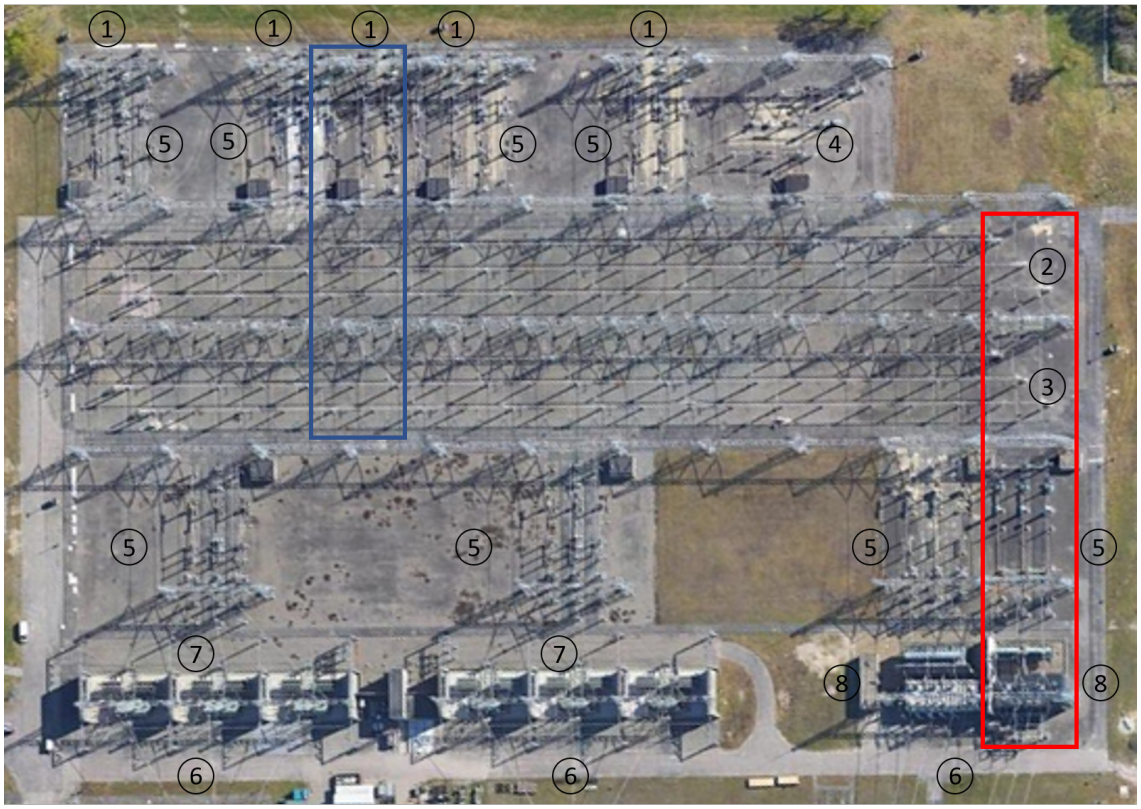

Figure 2.1: Aerial view of the TenneT substation Eindhoven 380.

1: 380 kV line-connections
2. Bus-bar A
3. Bus-bar B
4. Bus-coupler
5. Measurement equipment
6. 150 kV line connections
7. Bank of three single-phase power transformers
8. Three-phase power transformers

2.2.1. connections

The high-voltage side of a substation is called the primary side, this is the connection of the substation with the high-voltage lines or cables. In Figure 2.1 the primary side of station EHV380 is marked with (1). There are five 380 kV overhead line connections to this substation. The lower voltage side of a substation is called the secondary side, this is marked with (6) in Figure 2.1 there are four 150 kV line connections.

The EHV380 substation is an air-insulated substation. When the incoming connection is an overhead line the connection is made through the air. Gantry structures are used to connect the lines to the substation, these are steel supports that are used to carry the tension from the lines. When the substation needs to be connected to a cable circuit high-voltage cable-terminations are used to connect the cables to the substation.

2.2.2. Protection

To ensure correct operation and monitoring of the high-voltage equipment protection and measurement devices are required [73]. The devices are used to protect people and prevent damage to the equipment due to overloading, short circuits, and transient overvoltages caused by lightning or switching. The protection should be **Reliable**, **Redundant** and **Selective**. Selective means that only the part of the system where the fault occurred is isolated, as quickly as possible, while the unaffected part of the system remains in operation. The protection and measurement devices are located at (5). The most important components of the protection system will be described in this section.

Voltage transformers (VT) are used to step down the high-voltage to a voltage level that can be measured [73]. VTs are connected in parallel to the line or device that needs to be measured. There are three primary types of VTs: Electromagnetic, capacitive, and optical voltage transformers. The electromagnetic VT converts a primary voltage (high-voltage) to a secondary voltage using electromagnetic induction, this lower voltage can be measured. The capacitive voltage transformer (CVT) uses the principle of a restive divider, it consists of two series capacitors with different capacitances. The lower voltage over the largest capacitor can then be measured. The third one the optical voltage transformer makes use of the Pockels effect of rotating polarized light [10]. It produces a low-power optical signal which is processed by the measurement device. TenneT uses at this time only captive voltage transformers for 380 kV and inductive voltage transformers for the remaining voltages (110, 150, 220 kV).

Current transformers (CT) are placed in series with the components or lines that they monitor or protect. They are used to scale down the current to a measurable level and isolate the measuring instrument from the high voltage [73]. The CT consists of a primary winding which is often a single winding around the high-voltage conductor and secondary windings which are connected to the measurement device. The alternating current in the primary circuit induces an alternating magnetic field which induces a lower alternating current in the secondary winding. This lower current can then be used safely by the protection relays or measurement devices.

Circuit breakers (CB) are used to open and close a connection while current is flowing [73]. They can be used during normal operation and when faults occur. When a current-carrying connection is opened arcing will take place between the contacts. high-voltage circuit breakers make use of quenching mediums like vacuum or SF_6 to extinguish this arc and effectively break the connection. Circuit breakers are triggered by protective relays when a fault is detected to protect the equipment connected to the circuit breaker. Circuit breakers are also used by the control center to connect and disconnect lines and equipment to and from the network.

Disconnector switches are used to connect or disconnect a bay to one of the substation bus-bars [73]. These disconnector switches can only be operated when there is no current flowing. The circuit must thus be disconnected by a circuit breaker before opening the disconnector. This is due to the fact that the disconnector switches operate relatively slow and are not able to extinguish an arc. The disconnector switches also present a visual confirmation that the circuit is disconnected which increases the safety of working on high-voltage equipment.

Earthing switches are used to connect the high-voltage parts to the grounding grid of the high-voltage station [73]. This is used to de-energize the equipment before maintenance, and also to assure the mainte-

nance crew that the circuit is effectively earthed. Often these earthing switches are marked with colored tape to make them stand out against the other components in the substation.

Protective relays are used to control the circuit breakers in a substation to isolate a part of the grid on which a fault has occurred as fast as possible [73]. This is done to guarantee the continuity of the energy supply as much as possible and to restrict the damage. The relay receives the measurements from the CT and VT. When the measured and calculated values exceed some predetermined values the protective relay gives the circuit breaker a trip command, which then isolates the fault. There are a few different types of protective relays, the newest digital relays are able to perform multiple tasks in one device [73]:

- Overcurrent protection:
  When the measured current exceeds the set limit of the equipment which is monitored by the relay a trip command will be given to the CB. This is done to protect the connected equipment from overloading and possible heat damage.
- Differential protection:
  Differential protection compares the in-flowing current with the out-flowing current, thus two CTs are required. When more current is flowing into an area or device than is flowing out of this area or device there is a fault between the two measurement points and a trip signal is given to the related CBs. This differential protection is used to protect high-voltage lines or cables and transformers.
- Distance protection:
  Distance protection makes use of two measurements; voltage (VT) and current (CT) measurements, from this it is able to determine the impedance of a line for example. When the measured impedance of the line drops below the set-value (nominal impedance) a fault is detected and the relay gives a trip signal to the related CB.

Surge arresters are devices that are used to protect high-voltage equipment against transient overvoltages [73]. These overvoltages can be caused by external factors such as lighting strikes directly or in the vicinity of a conductor. But also the switching of high-voltage equipment can cause transient overvoltages.

A surge arrester is placed in parallel with the equipment which it needs to protect. The voltage is limited by the surge arrester by discharging or bypassing the surge current. The device does not absorb or stop lighting current, it diverts the lightning surge, limits the voltage and so protects the equipment installed in parallel.

2.2.3. Switchyard

The main function of a switchyard is to transmit and distribute the power through the substation [73]. TenneT uses two different types of insulation in its substations. The simplest one is the air-insulated substation (AIS), which uses air to insulate the high-voltage parts. When space is limited Gas insulated substations (GIS) can be used. GIS uses special pressurized gases for insulation, which have a much higher dielectric strength compared to air. This higher dielectric strength allows for making the system much more compact.

Bus-bars are used to connect the different bays inside the substation. For AIS systems the bus-bars are air-insulated and supported by insulating pillars. This makes it possible to tap into these bus-bars at different places without making new joints. Because the power system is a three-phase system the bus-bar system always consists of three parallel bus-bars.

TenneT uses a double bus-bar layout which consists of two identical parallel bus-bar systems often called rail A and B. In Figure 2.1 bus-bar A is marked with (2) and bus-bar B with (3). The two parallel bus-bars can be coupled using the bus-coupler (Figure 2.1 (4)). The equipment can be connected to both bus-bar A and B which makes the system more flexible and even redundant when one of the bus-bars malfunctions.

It is also possible to perform maintenance on one of the bus-bars while the other is in service however then there is no redundancy anymore. A solution could be a third rail system where there are three parallel bus-bar systems, then during maintenance on one rail there is still a backup rail, this will be covered in Section 3.

2.2.4. Power transformers

Power transformers are able to transform AC voltages to different levels. The basic functions of a power transformer are;

- Connecting different voltage levels in a high-voltage grid to enable power transmission.
- Keep the grid voltage level constant in the high-voltage grid with varying loads.
- Earthing of the grid.

In Figure 2.1 the banks of three single-phase power transformers are marked with (7) and the three-phase power transformers are marked with (8). TenneT uses single-phase and three-phase transformers with different voltage levels, ratings, cooling types, bushings, and tank types. All transformers used in the Dutch power grid are standardized and built according to the IEC standards with ONAN (oil natural air natural) and ONAF (oil natural air forced) cooling. ONAN means that there is no active cooling and the transformer is cooled due to the natural flow of the oil and ambient air. While for ONAF the natural flow of the oil is used in combination with forced air to cool the oil by using a radiator and fans.

The following standardized power transformers are used by TenneT [41];

- 380/220/50 kV 750/750/100 MVA 7 units (Autotransformers)
- 380/150/50 kV 500/500/167 MVA 52 units
- 380/110/50 kV 370/370/115 MVA 6 units
- 220/110/20 kV 370/370/105 MVA 12 units

As can be seen, the transformers have three rated voltages and three windings per phase. These transformers are called three-winding transformers. The first two voltages are the primary and secondary voltages. These voltages are used to transport the power and thus have the same and highest power ratings. The third voltage rating is the same for all four transformers, this is called the tertiary winding.

The tertiary winding can be used for multiple purposes for example;

- Three different systems with different operating voltages can be connected [3][78].
- The tertiary wire can be used as a power supply for the substation equipment such as lighting and the cooling of the transformer [3].
- When the primary and secondary windings are both Y-connected a Δ connected tertiary can be used to stabilize voltages, to provide grounding bank action, it can supply third harmonic currents to magnetize the transformer core and filters third harmonics from the system [78][3].

The tertiary winding may serve several of these functions at the same time [78]. For example, when connected in Δ on a Y-Y transformer that is grounded on its primary and secondary side it helps to stabilize the primary and secondary voltage and provides grounding bank action to partially shield the primary circuit from the secondary ground currents. But at the same time, it can supply the auxiliary power for the transformer and/or substation. A grounding bank is used to provide a path for the ground currents (zero sequence).

3

Maintenance at TenneT substations

3.1. Introduction

The goal of the thesis is to investigate important design aspects for mobile transmission stations to reduce/prevent planned outages of TenneT substations during maintenance, replacement, and expansion projects. In this chapter first, it will be determined how TenneT can reduce the amount and duration of planned outages on substations. Present and new methods to perform maintenance, replacement, and expansion need to be assessed to determine the possibility for planned outage reduction.

This chapter will first cover the planning of scheduled unavailability to perform maintenance, replacement, and expansion projects. Thereafter the maintenance strategies of TenneT will be covered. Finally, new methods to perform maintenance replacement and expansion projects on the high and extra-high-voltage grid of TenneT will be covered.

3.2. Planned Outage

A planned outage or scheduled unavailability of an Asset is a period for which part of a substation is taken out of service to be able to work inside the substation for example to perform maintenance, repair, and expansion. When a project requires such a planned outage a request is filed by the project team to the System Operation department of TenneT. This department makes use of a network model in PowerFactory [13] combined with extensive power generation and demand models to determine if that part of the network can be taken out of service at the requested moment without exceeding safety requirements. Only when the system operation department approves the planned outage the (part of) the substation can be taken out of service. Due to the increased energy demand and thus high utilization of the transport capacity, it is becoming increasingly difficult to obtain these planned outage permits. Also when a planned outage permit is granted it can be canceled when maintenance or repair with a higher priority needs to be performed or due to unexpected high utilization of the grid for example. This causes the other projects to be delayed.

3.2.1. Permit process

In TenneT scheduled unavailability of an Asset is called: "Voorziene Niet Beschikbaarheid" (VNB) there is a special permit process for these VNBs. The VNB process is divided into two parts;

1. VNB short-term planning: This is the VNB week and annual planning for the period of the coming 18 months. These requests are handled by the regional VNB planners.
2. VNB long-term planning: This is the planning for VNBs which are planned 18 months ahead of the request. These requests are handled by the long-term VNB planners.

The first step of the VNB process is the request for a planned outage by a TenneT project team or a subcontractor/DSO. Depending on the priority of the project different deadlines for this request are set:

- **Priority 1:** VNB requests for tie-line connections, projects with a longer give-back time (Section 3.3.1; 110/150kV > 6 hours, 220/380kV > 3 hours), and projects with a VNB time longer than 2 weeks are examples of VNB requests with the highest priority. These VNB requests need to be initiated before 1 September in the year before the project, and before 1 December the request needs to be finalized.

- **Priority 2:** Projects with a VNB time between 1 and 2 weeks and VNB requests for power transformers in the 220 kV and 380 kV network are examples of priority 2 VNBs. These requests need to be finalized 6 weeks before the start of the project.
- **Priority 3:** All VNBs which are not priority 1 or 2 are priority 3, these requests need to be filed 2 weeks before the start of the project and will be approved or rejected at last on Wednesday before the start of the project.

When all requests are submitted the VNB-planner responsible for the 220/380 kV network first puts these VNBs in the PowerFactory (PF) week model. The PF model is used to perform a safety analysis on the 220/380 kV system and determines if the operational criteria of the network are met.

When the operational criteria for the 220/380 kV network are met the VNBs for the remaining 110/150 kV sub-part of the network are added and a second safety analysis is performed on these parts. From this safety analysis, it is determined if the VNBs can be granted, if it is not possible to give permission for the VNB the System Operation department will try to postpone the VNB to another week.

A model of the dutch power grid is used in PF which is combined with a generation and load demand profile. The requested VNBs are put in this model using their start and end time. All generator stops with production above 100 MW are mentioned on the ENTSO-E site [20] and are also used in the PF network analysis. Also planned outages on tie-line connections to neighboring countries are put in the PF model. The security analysis is performed for a week. The security analysis takes special dutch holidays into account during simulation. The simulation can be run 3 months in the past and 3 years in the future thus long-term VNB planning can also be simulated using PF.

For the security analysis three peak-load scenarios are used;

- Weekdays: The load on Monday of the week in which you perform the simulation at 11:00 am is used.
- Saturdays: The load on Saturday from the previous week at 11:00 am is used.
- Sunday: The load on Sunday from the previous week at 11:00 am is used.

PF generates a report which mentions the "High and Low voltage violations" and "voltage deviations" for all scenarios which are tested. It is possible to switch on and off capacitor banks and compensation coils in the network model to compensate the reactive power and get a better voltage profile[14]. When the load-flow calculations are in-between the boundaries, contingencies can be added to the model. A contingency is the loss or failure of a small part of the power grid or the loss/failure of individual components such as a generator or transformer. The model simulates these contingency's to check the N-1 situations. Now the model can be simulated again and the "Contingency Branch Loadings" report is generated. This report gives the number of times the rating of a network element is exceeded.

According to the regulations from ENTSO-E Operations Guideline (SO GL), every European TSO needs to participate in outage planning and coordination. This process gives information about the status of relevant assets and the coordination of the availability of these assets in relation to the VNB planning, to guarantee the security of the European grid.

3.3. Maintenance strategy

From conversations with the Asset Management Team (AMT) from TenneT it is found that in the past, TenneT based its maintenance strategy on populations of components. For example, TenneT first determined the life expectancy of a commonly used voltage transformer (VT). When these VTs reached their maximum lifetime a replacement project was initiated to replace these VTs in all substations. For this replacement project, the substation needs to be taken out of service and has to be grounded. Therefore, the project team has to request a VNB. A lot of these permits were required because all of the same type of VTs were replaced in all substations.

Also, it occurred that when all VTs were replaced it was later found that also the rail systems reached their maximum lifetime, and again a replacement project was started and new VNBs needed to be issued for the same substations. This resulted in the need for a lot of VNB which are difficult to plan, and also often were postponed by system operations resulting in delays in the project.

A newly proposed method is to look at all components in a substation that would reach their maximum lifetime in the coming 10/15 years and replace/maintain all these components at the same time. Using this method only one VNB is required for multiple components and the efficiency of maintenance is increased. Also, only once every 10/15 years a maintenance project is required at a substation.

3.3.1. Third-rail

A special maintenance strategy is used on the Eindhoven 380 substation which is mentioned in Section 2.2. TenneT substations have a double rail system which makes the rail N-1 redundant. To be able to perform maintenance on this substation and its rail system while still being N-1 during maintenance a third rail is added. The rail system is then N-1 during maintenance and one rail can be taken out of service for a longer time. With the third rail there are fewer critical resources required and the redispatch costs will be lower.

Critical resources are the specially skilled crews that need to be present during the maintenance and commissioning of a substation (bay). Because the rail now is N-1 during maintenance it can be taken out of service for a longer time and these people do not need to work through the night and on weekends.

Redispatch means that the TSO (TenneT) requests the generation units to alter their power feed-in to the network to resolve congestion issues. During maintenance, redispatch is used to reduce the power flow over the substation which needs to be taken out of service. For this redispatch TenneT needs to compensate the generation unit and these costs are called the redispatch costs.

It should be noted that even with the usage of the third rail the maintenance crew needs to be able to give back the substation to system operation within the time mentioned in Table 3.1. Thus in case of an emergency elsewhere in the network during the maintenance project, the substation needs to be brought back into service within these times to return back to the N-1 situation.

220 kV & 380 kV	110 kV & 150 kV
3 hours	6 hours

Table 3.1: Give-back times for TenneT VNB

An important benefit of the third rail is that it increases the redundancy of the substation to N-2 because at this time all other substation components are already N-2. This thus also increases the redundancy after the maintenance project and is beneficial to the total system security of the TenneT network.

To replace the transformers in the Eindhoven 380 substation first a new transformer with its connection bay is built next to the already present transformers. When this new transformer is taken into service one of the three old transformers can be decommissioned and on the location of the old transformer, a new transformer can be installed. This process will be repeated three times until three new transformers are installed. Then one location of an old transformer will remain vacant and can be used for a new connection or for an expansion of the substation for example. By using this method there will be enough capacity present at the substation to keep it at N-2 during maintenance, and thus no give-back time is required on the transformers.

A problem with the third-rail strategy is the fact that it requires more space inside a substation which is not always available. Also during the installation of the third rail, a considerable amount of VNB time is required. To keep the system N-1 during maintenance there can only be worked on one substation bay at a time which is not very efficient. This bay is also located in between substation bays that are in operation imposing danger to the crew.

3.3.2. Bay-replacement Program

The Bay-Replacement Program (BRP) is developed by TenneT as a new concept for the 110 and 150 kV substations to enable adding new bays to existing substations and replacing its aging substations at a higher rate. The BRP standardized the TenneT substations and makes use of modular substation components (Figure 3.1). These modular sections are built and tested in the factory and are transported to the substation location where the modules only have to be connected together. This substantially reduces the replacement time, reduces the safety risk for the crew, and reduces the costs by setting up assembly lines. When the preparations on site are finished, a substation bay can be installed and connected in two days. During the BRP TenneT only replaces the switching part of the substations and not the transformers. The skids can be slid out of the substation to perform maintenance, and people no longer have to work in a partly energized substation. Also because of the modularity, when a part of the substation fails this part can easily be replaced by a spare module and the failing components can be repaired at a factory location.

During the BRP TenneT uses mobile Gas-Insulated Substation (GIS) units mounted on skids to temporarily take over the switching function of the substation. This makes it possible to remove and replace the complete switching part of the substation at once. Only a short time of VNB will be required during the connection

and disconnection of the mobile GIS units. Thus during the replacement of the bays, no VNB is required and the giveback times do not need to be considered. However, the mobile GIS only takes over the switching equipment and no power transformers.

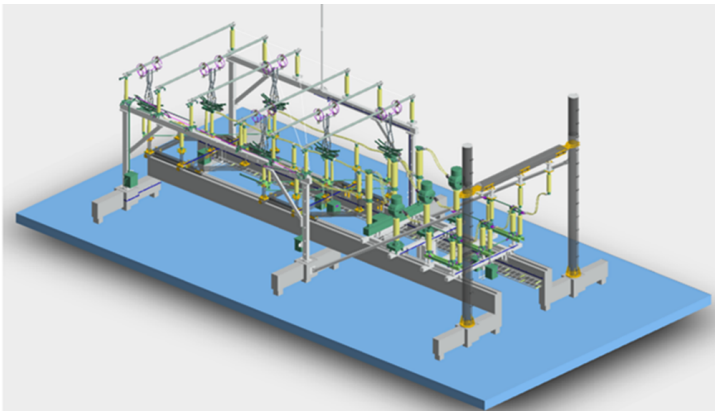

Figure 3.1: Three BRP skids from TenneT connected to form a switching-bay [40]

3.3.3. Mobile Substation

A different method to reduce the amount and duration of planned outages during maintenance, replacement, and expansion in TenneT substations would be the use of a mobile substation. This mobile substation should be able to bypass a complete substation with voltages up to 380 kV. When the substation which needs to be maintained or replaced is bypassed, the redundancy is the same as for the original substation thus no VNB is required during the project. Only when the mobile substation is connected and disconnected VNB is required. During the connecting and disconnecting of the mobile substation, the give-back times mentioned in Table 3.1 need to be considered. There are no requirements on the give-back time during the project, which makes it possible to remove a part or the complete old substation and build an entirely new one. No especially skilled crew members are required during this part of the project because the complete substation is out of service. This thus saves valuable critical resources. There is no reduction in the capacity of the substation and thus there are no redispatch costs. The efficiency of the project is increased because there can be worked on the complete substation at the same time. An additional benefit is the safety of the maintenance crew, because the complete substation/bay is taken out of service the risk of incidents with live high-voltage components is reduced.

The mobile substation should be able to take over a TenneT substation while the redundancy remains the same. Thus it should contain, a double-rail system with switching equipment, power transformers, measurement transformers, and control and protection equipment. The difference between the Bay replacement project and a mobile substation is that the mobile substation also contains mobile power transformers and thus is a complete substitution, where the BRP only takes over the switching part of the substation.

It should be kept in mind that a mobile substation that is able to take over a complete substation will require a rather large area, which in a lot of TenneT substations is not readily available. Also, temporary permits will be required to set up a mobile substation outside the substation area.

Table 3.2 summarises the differences between the Third-rail, Bay Replacement Project, and the mobile substations. In the following chapters, the mobile substation will be covered in more detail, and design criteria will be determined.

	Third-rail	**Bay Replacement Program**	**Mobile-Substation**
VNB time is required during maintenance, replacement, and expansion projects.	Yes, during the full project time.	Minimal when working on the switching part of the substation, only during connection of the temporary GIS-skid. For working on the power transformers still, VNB is required.	Minimal, only during (dis)connection of (mobile) substation.
Redundancy is affected during the project.	Yes	Only for the power transformers, not for the switching part.	No
Critical resources are required during the project.	Yes, during full project time.	Less, Only during connection temporary GIS-skid and for working on the power transformers.	Minimal, only during (dis)connection of (mobile) substation.
Safety	Worst, working in brownfield (partly energized substation).	Better, all switching equipment is disconnected, however, transformers are still in operation.	Best, the complete substation is out of service and grounded.
Redispatch-costs	Worst, during full project time.	Less, Only during connection temporary GIS-skid and when working on the power transformers.	Minimal, only during connection of substation.
Efficiency	Worst, field by field.	Better, assembly and testing of switching bays at the factory location.	Best, possible to work on complete substation at once. Possibly combination with the standard modules of BRP is very efficient.
-	Replacement, consecutive; field by field.	Replacement, removing old substation and placing new switch bays. No transformer replacement. (Up till this time) Only for 110 and 150 kV.	Complete substation for all TenneT voltage levels (110 kV up to 380 kV) can be replaced at once including the transformer.

Table 3.2: Comparison between three different maintenance, replacement, and expansion methods of TenneT.

3.4. conclusion

New methods to perform maintenance, replacement, and expansion projects on the high and extra-high-voltage grid of TenneT to reduce the amount and duration of planned outages are discussed. TenneT already developed different methods of which the bay replacement program (BRP) is a promising solution for the 110 and 150 kV grid. Less planned outages are required because a part of the substation is bypassed during the project. However, with the BRP only the switching part of the substation is bypassed. When a mobile substation that also contains power transformers is used the complete substation can be bypassed and thus no VNB would be required during the project. There is only VNB required for the connection of the mobile substation.

In the following chapter, a case study will be discussed which is performed to determine the possible advantages of a mobile substation for TenneT.

4

Advantages of a mobile substation for TenneT

4.1. Introduction

In the previous chapter, it is concluded that mobile high-voltage substations could be used to reduce the amount and duration of planned outages required to perform maintenance, replacement, and expansion projects on substations. In this chapter, a case study will be discussed which is performed to determine the possible advantages of a mobile substation for TenneT.

4.2. Case study

4.2.1. Increase efficiency

Presently, for the 380 and 220 kV networks, it is only possible to work on one substation per network at the same time, due to VNB restrictions. However, there are more substations in these two networks that need to be maintained or expanded, and thus these restrictions cause delays. During a VNB of a 380 or 220 kV substation, it is also more difficult to get VNBs for the underlying 110 and 150 kV substations due to the reduced redispatch capacity. When a mobile substation would be used to bypass a 380 or 220 kV substation during its maintenance, replacement, and/or expansion no VNB would be required for this substation during the project. It would then be possible to work on multiple 380 kV or 220 kV substations at the same time and it would also be less of a problem to get a VNB permit for the underlying 110 and 150 kV substations. This could thus increase the speed and efficiency of maintenance, replacement, and expansion projects in the complete TenneT network.

As an example, TenneT is planning to perform maintenance on station Eindhoven 380 as mentioned in Section 2.2. Due to VNB restrictions, the Eindhoven 380 project can only start when the project at station Diemen 380 is finished. Station Eindhoven has four transformer bays with a capacity of 450 MVA each. Thus with a mobile substation with four transformer bays of 450 MVA each the complete station in terms of transformer capacity could be bypassed. When station Eindhoven 380 is bypassed there are no VNB restrictions during the project and the amount of 380 kV substations on which can be worked at the same time could be doubled. Only during the connection of the mobile substation, a short VNB time is required.

4.2.2. Cost savings

TenneT can reduce its costs considerably by using a mobile substation as explained in this section. It should be noted that precise information is not available and thus some assumptions are made based on expert knowledge.

According to the 2021 annual report of TenneT, the total redispatch costs have increased to €339.7 million/year [72]. It is assumed that approximately 50 % of these redispatch costs are caused during VNB and

the other 50 % is caused by congestion in the grid. Thus the redispatch costs due to VNB will be in the order of €100-200 million/year.

It is assumed according to expert knowledge that 20 % of the substations are responsible for 80 % of the VNB time, this 80 % of the VNB time could thus be reduced when a mobile substation is used at these substations. This could save approximately €80 to 160 million/year in redispatch costs.

When a part of the grid is not available the power needs to be redirected along other lines and cables in the grid. The current flowing through these parts of the grid will increase and thus also the losses will increase. TenneT transports approximately 110 TWh/year [8], of which 4.7 TWh are grid losses [65] in cables and transformers for example. Assuming an average energy price of €50/MWh [18] it costs TenneT €235 million/year to compensate for the losses. If we assume that we can reduce these losses by 5% by reducing the redispatch during projects on TenneT substations this could save TenneT approximately €12 million/year. When the losses in the network are reduced less energy needs to be generated and thus also the CO_2 emissions from the power plants will reduce. The CO_2 emissions of TenneT comprise 95 % of grid losses [57], thus reducing these losses could considerably reduce the CO_2 footprint of TenneT.

TenneT has approximately 3000 employees in the Netherlands, of which it is assumed that 5% are critical resources. When these people cost TenneT €100.000,- per person/year this adds up to €15 million/year. Thus when the VNB time is reduced by 80 % also less critical resources are required and this could save TenneT up to €12 million/year.

Presently there is a shortage of specially skilled people in the Netherlands. When these critical resources are not available a VNB needs to be postponed or canceled which causes delays for the project and eventually increases the costs. Thus when less VNB time is required this could reduce these delays and their associated costs.

As discussed before the system operations department of TenneT can cancel a VNB permit a short time before the work begins when due to unforeseen circumstances extra grid capacity is required. Because the subcontractors have planned to work on the substation and are maybe already present at the substation location TenneT is required to compensate these companies for the cancellation. Also, these companies need to be paid for the new planned working period. These additional costs are called stagnation costs. When no VNB is required during a project these costs could be averted.

In total TenneT could thus save a few hundred million euros every year by reducing the planned outages during maintenance, replacement, and expansion projects. Due to the complexity of the electricity grid, and maintenance, replacement, and expansion planning of TenneT it was not determined in this thesis how many mobile substations are required to accomplish these savings. It is not determined what the investment and operational costs of a mobile substation will be and thus the mentioned savings are not net savings.

4.3. Conclusion

With the use of a mobile substation with sufficient capacity (MVA) to bypass a 380 or 220 kV substation, it would be possible to work on multiple 380 or 220 kV substations at the same time, it would also make it easier to get VNB permits for projects in the 110 and 150 kV network. This would increase the efficiency of maintenance, replacement, and expansion projects in the complete grid.

It is assumed that the total VNB time could be reduced by 80 % when TenneT uses mobile substations to bypass 20 % of its substations during maintenance, replacement, and expansion projects. This could save TenneT a few hundred million euros every year and would also reduce the CO_2 footprint of TenneT. It is not determined what the investment and operational costs of the mobile substation will be and thus these savings are not net savings.

5

Mobile High-Voltage Substations

In the previous chapters, it is concluded that mobile high-voltage substations can be used to reduce the amount and duration of VNB's (planned outages) required to perform maintenance, replacement, and expansion projects on substations. From a case study, it is concluded that this reduction in VNB's could potentially save several hundred million euros every year and reduce the CO_2 footprint of TenneT.

These mobile substations should be able to take over the function of a part or possibly an entire substation. When this mobile substation is in operation the bypassed or taken-over (part of the) substation can be grounded and maintenance can be performed safely without the need for a VNB. This chapter will cover the definition and requirements of mobile substations which could be used by TenneT.

5.1. Definition

A mobile substation is a fully equipped substation mounted on one or multiple trailers to be easily transported [43]. Mobile substations are generally used to reduce the duration of unexpected outages by bypassing a complete substation or part thereof. The equipment can also be used to perform maintenance to substations while the net service is continued by bypassing the substation [44].

To be able to take over the function of (a part of) a substation a mobile substation should contain the following components:

- High-Voltage (HV) equipment such as circuit breakers and bus-bar systems for connection between the HV incoming line or cable and the power transformer.
- Power transformer
- Medium-Voltage (MV) equipment such as circuit breakers and bus-bar systems for connection between the power transformer and the MV line or cables.
- Control and Protection equipment, including voltage and current transformers.

Because the substation should be easily transportable the flowing limitations should be taken into account:

- Dimensions
- Weight
- It should be able to withstand frequent transportation

The mobile substation needs to be installed in existing substations where space is often limited, thus the electrical clearances when the substation is deployed should be taken into account and should be minimized.

Several criteria for the mobile substations are specified by TenneT:

- The mobile high-voltage substation must be easy and quick to transport. It should be small and light enough to be allowed to be transported without special road permits.
- The mobile high-voltage substation must be environmentally friendly.
- The lifetime may be shorter than ordinary stationary high-voltage substations.

- The mobile high voltage substation should be able to be used at all of the TenneT (E)HV substations.
- The control system should be integrated with the existing SCADA-EMS [1] system from TenneT, to allow the control center of TenneT to control the substation.

A mobile substation should contain all auxiliaries including, protection, control, metering, communication, and monitoring systems. The substation shall be safe, reliable, simple in design, flexible in operation, easy to maintain, and economical. The substation must be equipped with control, monitoring, and communication features that are integrated into an IEC 61850-compliant power automation system. The protection and control of the mobile system should seamlessly be integrate-able with the existing substation automation and system operation control to be able to take over a (part) of the substation.

5.2. Examples of mobile substations

Three examples of mobile substations will be discussed to get an overview of the mobile high-voltage substations which are used by transmission and distribution system operators during maintenance and as resilience solution during large outages.

5.2.1. Vattenfall 52/24 kV and 170/52/24 kV substation

The European utility Vattenfall developed two new types of mobile substations one of 52/24(12) kV and one of 170/52/24(12) kV. These mobile substations are used to quickly restore the supply of power to customers after faults in a substation [45]. The mobile substations can also be used as a temporary power supply during the maintenance of a substation. The mobile substations are easy to transport and quick to install. All equipment is housed in containers which makes fences unnecessary and equipment more reliable. The mobile substations are developed in cooperation with ABB Power Technologies.

52/24(12) kV substation [45]

The substation shown in Figure 5.1a is used to bypass distribution substations. It is built on one 17 m long trailer and has a total weight of 43 tonne. In Sweden, the trailer can be transported as normal road transport with no additional traffic permits and only has a maximum speed limit of 80 km/h. This allows the substation to be quickly transported to the location. Because it is already fully assembled it only needs to be connected to the grid which allows for quick setup within 8 hours.
Inside the trailer, as shown in Figure 5.1b a three-phase transformer of 6.5 MVA and a 24 kV reactor are present. For the connection to the original substation one single line connection of 52 kV and one incoming and two outgoing 24 kV, metal-clad switchgear bays are used. A single-line diagram showing the different components and their connections is given in Figure 5.2.
For disconnecting and protection 52 kV SF_6 circuit breakers are used for the high voltage side. Surge arresters to protect the equipment against incoming surges are located in the same bay as the circuit breakers. The current transformers which are used for the protection are mounted on the incoming and outgoing cables. On the secondary side of the transformer, the two outgoing and one incoming 24 kV feeders are protected using vacuum-type circuit breakers. A special oil pit is installed at the bottom of the trailer which is of sufficient size to handle oil spills from both the transformer and reactor. The mobile substation is connected to the existing substations high and low voltage connections using flexible cables. Shock detectors are mounted on the trailer to ensure that the electrical equipment does not sustain excessive vibrations during transport.

[1] SCADA: Supervisory Control and Data Acquisition, EMS: Energy Management Systems

(a) 52/24(12) kV mobile substation on a trailer [45]

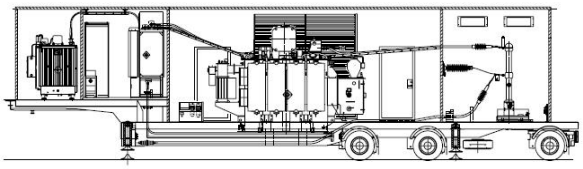

(b) 52/24(12) kV mobile substation on a trailer [45]

Figure 5.1

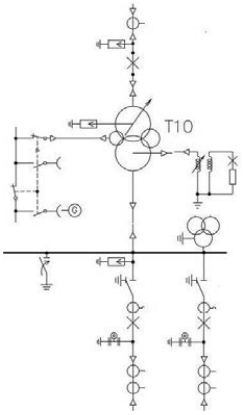

Figure 5.2: 52/24(12) kV mobile substation single line diagram [45]

170/52/24(12) kV substation [45]
The 170/52 kV mobile substation with a rating of 75 MVA [45] is much larger compared to the 52/24 kV (6.5 MVA) mobile substation. To be able to transport this substation over the road it is divided into several modules (Figure 5.3a). This also makes it possible to transport the substation through the air and over the sea. The three-phase power transformer is mounted on a trailer (Figure 5.3b). The other component and accessories are placed in containers. All sub-modules of the substation are completely enclosed which makes the use of fences to protect people from touching high-voltage parts obsolete. The installation time of this substation is higher compared to the 52/24 kV substation because now the individual parts need to be connected. Between the different modules, flexible cables are used. An overview and layout of the connected modules are given in Figure 5.3a.
A neutral reactor is incorporated in the design for compensation. Figure 5.4 shows a single-line diagram of the mobile substation.

The three-phase transformer is the largest and heaviest part of the substation and is thus mounted on a single trailer together with the prefabricated 170 kV cable on a motorized drum (Figure 5.3b). The transformer is designed for road transport over bad roads and adapted for air and sea transport. The gas-insulated switchgear is housed in a separate container and can be transported without reducing the SF_6 gas pressure. Shock detectors are mounted on the trailer and the containers to ensure that electrical equipment is not damaged during transport.

A separate container is used to house the control and protection equipment of the 170 kV switchgear. The 52 and 24 kV switchgear is controlled locally in the switchgear containers. The Alarms of all equipment are transferred to an alarm unit in the control container and to the central control center. The auxiliary power is supplied by the auxiliary winding of the transformer or from a local network. During installation, a diesel generator can be used.

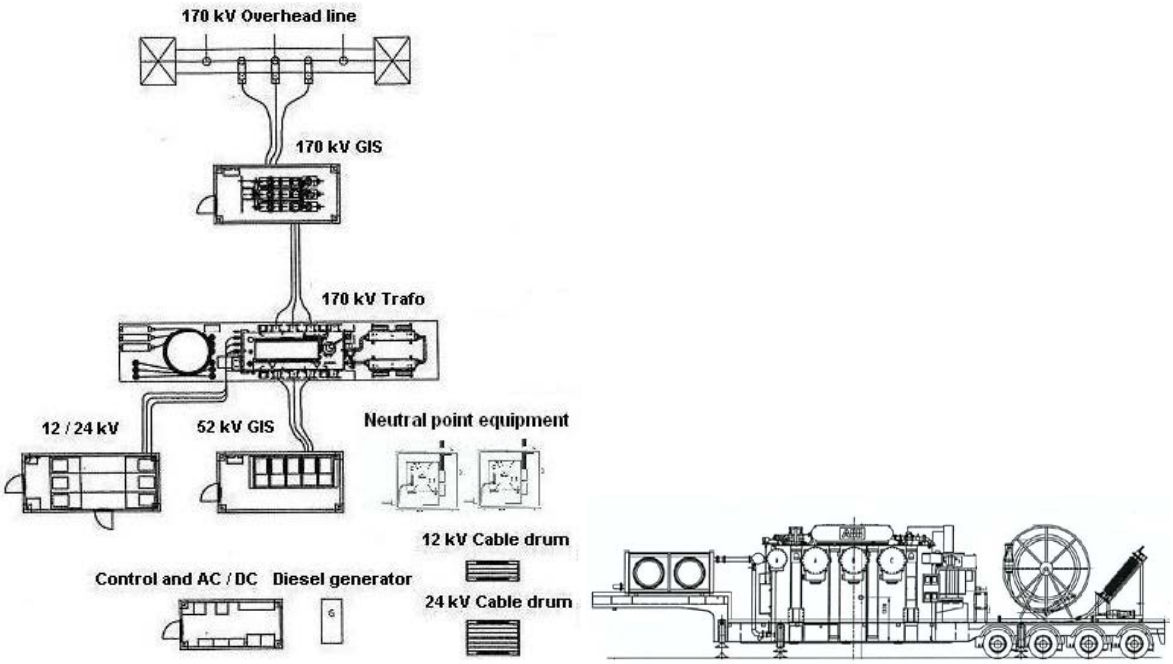

(a) 170/52/24(12) kV mobile substation on a trailer [45]

(b) 170/52/24(12) kV mobile substation on a trailer [45]

Figure 5.3: Vattenfall mobile substation

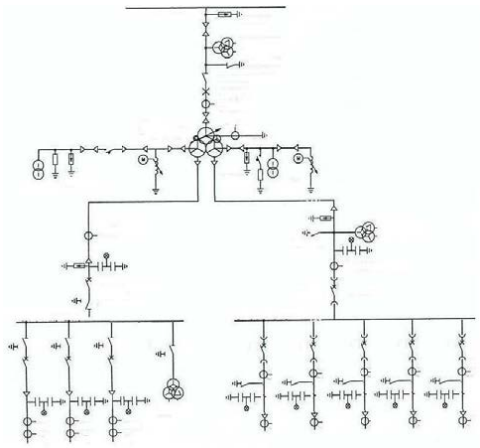

Figure 5.4: 170/52/24(12) kV mobile substation single line diagram [45]

5.2.2. Siemens 380/138/11 kV

A 380 kV 500 MVA mobile substation is designed by Siemens [25]. The substation is able to transform the main 380 kV to multiple lower voltages; 132, 115, and 110 kV. An example of a single line diagram of the substation is given in Figure 5.6 The substation consists of several modules which need to be interconnected on site (Figure 5.5):

- HV/MV switchgear
- three single-phase power transformers
- HV/MV cables
- Control
- Telecom
- Protection
- Monitoring
- Auxiliary power systems

When connected the modules form a complete high-voltage substation that can operate stand-alone and

can be used for emergency restoration of supply or during maintenance. The equipment is mounted on a base frame to protect it during transportation on rough roads. Three 167 MVA single-phase transformers are mounted on separate trailers. These 167 MVA transformers are probably still too heavy for road transport without special permits as will be discussed in Chapter 8.7.

Rotating bushings are used on the transformers and high-voltage switchgear modules, to be able to quickly install the substation on-site. The installation should take less than one week excluding civil works on-site. Not much information about the dimensions and weight of the substation is available, however, in section 7.1 the mobile transformers from Siemens are covered.

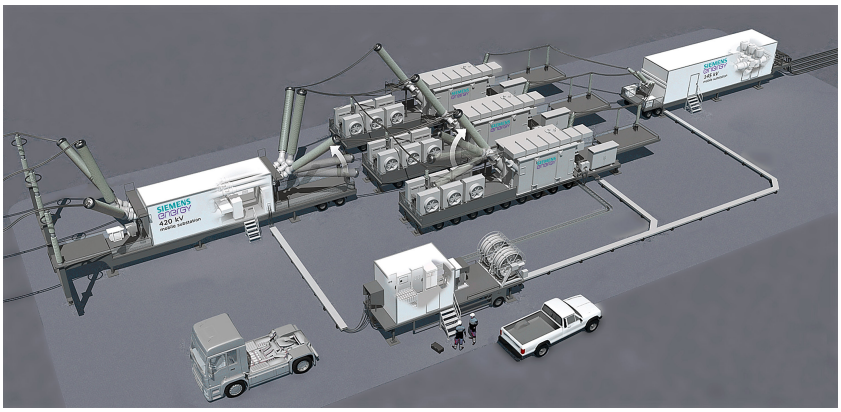

Figure 5.5: Mobile substation: 380/132-11 kV 500 MVA [25]

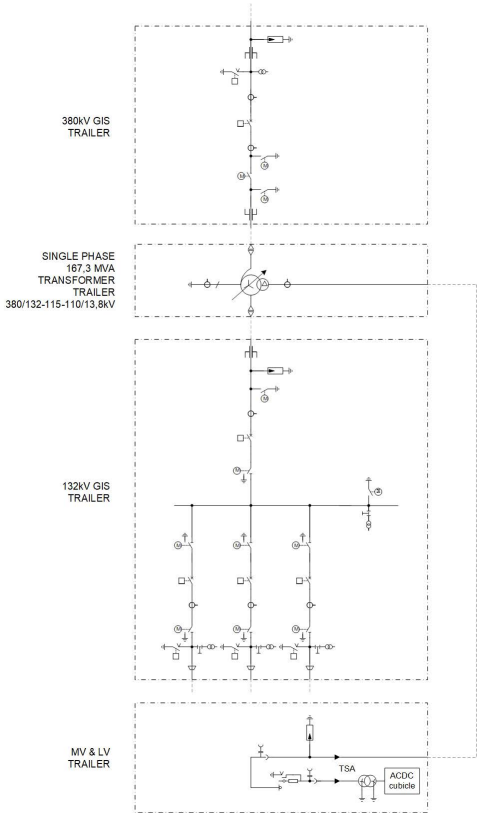

Figure 5.6: Example of a single-line diagram [25]

A summary of the main properties of the three mobile substations is given in Table 5.1. It should be noted that the mentioned substations have different voltage and MVA ratings. From the table, it can be concluded that for the higher voltage, 170 kV and above Gas Insulated Switchgear is used with SF_6 as insulating gas. For

the lower voltages vacuum circuit breakers and insulated cables are used.

The connection between different modules is different for the two modular substations, the Vattenfall 170/52 kV substation uses flexible cables between the modules and thus no bushings are required. While for the Siemens 380/132 kV substation air-insulated lines are used which are connected using rotating bushings.

The weight of both the Vattenfall substations is mentioned, the 52/24 kV system is allowed to be transported over the road in the Netherlands (Section A). However, the 170/52 kV substation exceeds the weight limitations of 50 tonne and special trailers and permits are required for transport. For the Siemens 380/132 kV substation the weight of the transformers is not mentioned. According to the brochure [25], the substation will be designed within the road specifications. However, when the three-single phase transformer configurations mentioned in Section 7.1 are analyzed it can be assumed that the three 167 MVA transformers will exceed the 50-tonne weight limit in the Netherlands.

In the next chapters, the design criteria for a mobile substation will be covered in more detail.

		Vattenfall 52/24(12) kV [45]	Swedish National Grid (Vattenfall) 170/52/24(12) kV [45]	Mobile substation: 380/132-11kV 500 MVA [25]
Manufacturer		ABB Power Technologies	ABB Power Technologies	Siemens
Open/enclosed		Completely enclosed	Different parts completely enclosed	Different parts completely enclosed
Voltage	Supported voltages [kV]	52/ 24(12)	170/52/24(12)	380 / 132, 115 & 110
Transformer	Single/three-phase	One three-phase	Three-phase, three-winding type with an equalizing winding.	Three Single phase units (167.3 MVA)
	Cooling	ONAF/ONAN	ONAF	-
	Power (rated) [MVA]	6.5/4	25/25/25/8.3	500
Protection	Switchgear	Metal-clad switchgear	GIS (SF6) (170 and 52 kV) Vacuum (24 kV)	GIS
Transport		single trailer	one trailer (Transformer) and several containers	six trailers
	L/W/H [m]	17/3.1/x	-	-
	Weight [tonne]	43	75.5 (only trailer with transformer)	-
Connections	HV	Flexible cables	Flexible cables	Rotating bushings
	LV	Flexible cables	Flexible cables	Bushings and cables
	Between substation parts	n.a	Prefabricated cables	AIS lines and bushings
Installation	Time	8 hours	2 days	< 1 week
Control			Local and remote	local and remote

Table 5.1: Mobile substations [45] [25]

5.3. Conclusion

From an electrical point of view, there is not much difference between a normal substation and a mobile substation. The mechanical layout and choice of equipment for a mobile substation however are different from that of a normal substation. There are limitations in the size, weight, and maneuverability of the substation

modules. The specific limitations on the size and weight of the trailers which carry the substation modules are mentioned in Appendix A. Special attention needs to be paid to the mechanical design of the components which need to be able to withstand frequent road transportation over bad road conditions.

As mentioned before the power transformer will be the heaviest component of the mobile substation. The MVA rating of the transformer is thus limited by the maximum size and weight specified in the road regulations. The design considerations of the mobile transformers will be covered in Part I.

The size of a mobile substation is limited by the available area in a substation location and road regulations. The size of a mobile substation will mainly be determined by the electrical clearances of the high-voltage parts of the substation. The electrical clearances and design considerations for compact and mobile substations will be covered in Part II.

I

Mobile power transformers

6

Introduction

The power transformer will be the heaviest component of the mobile substation [44]. The size and weight of the transformer are directly related to the MVA rating. The mobile substations should be transportable without special road permits. The maximum weight for road transport without a special permit in the Netherlands is limited to 50.000 kg for the tractor-semi-trailer combination as mentioned in Appendix A.

The goal is to have one design for a mobile substation with power transformers that can be used in all substations of TenneT. To be able to do this the following four different transformer ratios are required for the mobile substation;

- 380/220/50 kV 750/750/100 MVA (Autotransformers)
- 380/150/50 kV 500/500/167 MVA
- 380/110/50 kV 370/370/115 MVA
- 220/110/20 kV 370/370/105 MVA

The transformers with a ratio of 380/220/50 kV are autotransformers, these transformers are used to connect the 380 kV and 220 kV transport networks of TenneT. The three double wound transformers are used to deliver power from the 380 kV and 220 kV transport network to the 150 kV and 110 kV transport networks.

In this Section, there will be looked at different transformer designs to reduce the size and weight of the power transformer to be able to fit normal road regulations (Appendix A). At first, different mobile transformer designs are covered to give an overview of the state-of-the-art mobile transformers.

7

Background: Existing mobile power transformers

7.1. Siemens mobile transformers

Siemens designed three different sets of mobile transformers to be used as Resilience transformers (Figure 7.1a) [61]:

1. 335/136 kV, 300 MVA Autotransformer (Figure 7.1b)
2. 345/115 kV, 400 MVA autotransformer (Figure 7.2a)
3. 400/20.8 kV, 250 MVA (Figure 7.2a)

These transformers are stored and can be quickly transported to a substation when a critical fault occurs in a transformer. The transformers are optimized to be easily transported and due to the plug-and-play concept, they can be installed in a few days. Because these transformers are designed for road transport and quick installation they could also be used on mobile substations. However, the weight limit needs to be kept in mind.

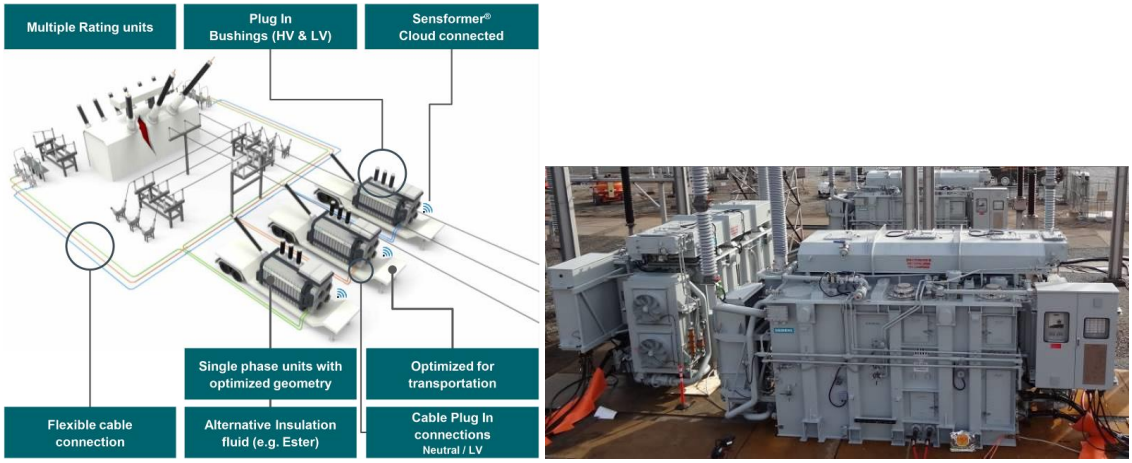

(a) Siemens Resilience Concept [61]

(b) 335/136 kV, 300 MVA Autotransformer [61]

Figure 7.1

Special high-temperature hybrid insulation with Nomex® solid aramid conductor insulation material and synthetic ester liquid (Midel® 7131) allows for a compact design [26]. Hybrid insulation uses high-temperature insulating materials in areas where the operating temperature is designed to be high (windings), in other areas conventional cellulose-based insulation is used [60] [74]. The Nomex® paper and pressboard

(a) Siemens 345/115 kV, 400 MVA Autotransformer[26]

(b) Siemens 400/20.8 kV, 250 MVA [26]

Figure 7.2

insulation can be operated above the temperature limits for cellulose and thermally upgraded cellulose paper [17]. The use of Nomex® pressboard and paper thus enables winding conductors with reduced cross-section and higher transformer winding temperatures [17]. The transformer can be lighter and more compact for the same power rating because it allows for higher temperatures. The synthetic ester liquid Midel® is fully biodegradable reducing environmental risks associated with transport and operation. Ester fluids have a higher thermal conductivity and slightly higher heat capacity than mineral oil which partly compensates for the reduced oil flow due to the higher viscosity of ester oil [53]. The ester transformer oil allows for a more compact transformer design because it can operate at higher temperatures and thus requires less oil [53][46].

Single-phase transformers are used to divide the transformer over multiple trailers to be able to have a higher total MVA rating and still be transportable. An efficient and high-capacity cooling system makes the smaller design for the transformers possible. The cooling system makes use of forced oil through predetermined paths between the windings due to which it is able to efficiently cool the transformer, this is called Oil Directed Air Forced (ODAF). When for the oil a medium is used with a flash-point higher than 300°C which are mostly natural esters this is called KDAF. The first two transformer sets are Autotransformers, this type of transformer requires less copper compared to a regular double-wound transformer [63] and can thus be made cheaper and more compact. A limitation of the autotransformer is that in contrast to the double wound transformer the primary and secondary windings of the autotransformer are not electrically and magnetically isolated [78] [3]. When an autotransformer is connected in a Y-Y configuration (which TenneT uses), there must be a common neutral between the high-voltage and low-voltage sides, which makes that the neutrals of the circuits cannot be isolated from each other. Thus it is not possible to ground one side of the transformer and keep the other side floating.

The transformers can be transported fluid-filled and the use of pluggable bushings and cable connections allow for a quick installation [26]. Due to the plug-in connections of the cables and bushings, the transformer does not need to be opened and thus no oil manipulation is required. In January 2017 it was successfully proven at a trial run that it took only 30 hours within 3 working days to install the 300 MVA transformer bank [58]. Due to the multi-ratio voltage rating of the transformers they can be used to replace different types of transformers [61]. However, for the multi-voltage ratio more windings are required and thus the transformers become heavier compared to transformers with only one voltage ratio. All accessories of the transformer banks are transported in specially designed standard containers.

		Siemens Auto-transformer Transmission Project Case I [61][26]	Siemens Auto-transformer Transmission Project Case II [61][26]	Generator step up GSU project Case III [61][26]
Manufacturer		Siemens	Siemens	Siemens
Voltage	Supported High voltage [kV]	335 @ 300 MVA & 136 @150MVA	345 & 230	400, 345, 230, 138 &115kV
	Supported Low Voltage [kV]	136 @ 300 MVA & 69 @150MVA	230 & 138 & 115	Delta: 34.5, 20, 18, 16, 14 & 12; Wye: 34.6, 31.2, 27.7, 24.3 & 20.8
	Voltage selection	OLTC voltage regulation(HV)	Switching links	Switching links
Transformer	Single/three-phase	Six single phase units (100MVA each)	Three single phase (133 MVA each)	three single phase (83.3 MVA each)
	Type	Autotransformer	Autotransformer	-
	Cooling	KDAF (synthetic ester)	ODAF	KDAF (synthetic ester)
	Power (rated) [MVA]	300 or 150	400	250
	Overloading capability	196% for 1 hour @30°C ambient	-	-
Connections Type	HV	Wye	Wye	Wye
	LV	Wye	Wye	Delta or Wye
	Tertiary	Delta	Delta	Delta
	Switching between configuration	DETC (De-Energized Tap-Changer)	Switching links	Switching links and connection box
Transport		6 trailers (transformers)	3 trailers (transformers)	3 trailers (transformers)
Weight [tonne]	fully assembled	98	75	97
	Without oil	60	56	61
	without oil,cooling and conservator	-	50	-
Connections	HV	plug-in bushing	plug-in bushing	345kV plug-in bushing
	LV	plug-in bushing or cable	plug-in bushing or cable	LV customer connection via oil/air bushing, LV interconnection via plug-in Cable connection
	Tertiary	plug-in cable	plug-in cable	plug-in cable
Installation	Time	30 hours within 3 days [58]	-	-

Table 7.1: Siemens mobile power transformer [61]

7.2. ABB Mobile Transformers

ABB developed mobile shell-type transformers as a solution for resiliency, which are designed to be transported on normal trucks and can withstand frequent transportation [2][4]. They have transformers for 345 kV, 400 kV, and 525 kV. The transformers are single-phase shell-type transformers which allows for a compact design due to the form fit tank (Figures 7.3a and 7.3b) [2][42]. A low height profile with a lay-down transport option is possible due to the shell-type design [4].

High-temperature hybrid insulation of DuPont™ Nomex® paper and pressboard is used instead of conventional cellulosic insulation. By using this hybrid insulation, winding conductors with a reduced cross-section can be used and higher winding temperatures are allowed [47]. Also, the lifetime is expected to be considerably longer compared to cellulose-based insulation due to the higher temperature limits of Nomex® [17]. This also increased the overload capacity and enhances the safety and reliability of the transformer.

According to R. Marek et al. [47] a 250 MVA, 400 kV transformer with a rated power that is 2 times that of a conventional insulated fast-deployable transformer of similar size has been built and tested in Spain (Table 7.2) [17]. The mobile transformers from ABB have an MVA to weight ratio of 3.58 MVA/tonne compared to standard substation transformers with a ratio of 1.77 MVA/tonne [17]. A comparison between a standard substation transformer and two fast deployable types of transformers from ABB is given in Table 7.2. This table shows that the MVA rating of the hybrid insulated transformer increased while the dimensions and weight decreased.

The transformers are able to transform a range of voltages making it possible to cover different substations, ABB calls these transformers polytransformers.

		Standard substation transformer	Conventional fast-deployable transformer	Hybrid insulation fast-deployable transformer
Rated Power	[MVA]	200	117	250
	p.u	1	0.6	1.25
Load losses	p.u	1	0.87	1.74
No load losses 100% exc.	p.u	1	0.6	0.77
Shipping weight	[tonne]	113	60	69.9
	p.u	1	0.53	0.62
Shipping dimensions	LxWxH [mm]	5650 x 3916 x 4585	6691 x 2713 x 3442	7488 x 2719 x 3245
	p.u	1x1x1	1.17x0.68x0.75	1.32x0.69x0.71
	Volume [m^3]	101	62	66
Overall dimensions	LxWxH [mm]	8915 x 7645 x 10659	8351 x 6250 x 3442	7488 x 2719 x 3245
	p.u	1x1x1	0.94x0.85x0.80	0.93x0.76x0.79
Ratio MVA/tonne		1.77	1.95	3.58
Ratio MVA/m^3		1.98	1.89	3.78

Table 7.2: comparison of the Key power, weight, and dimensional aspects of ABB transformers [17][47]

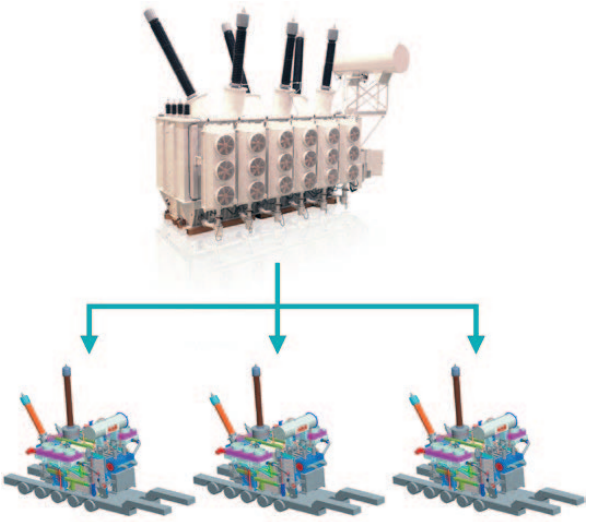

(a) ABB mobile transformers three-phase to single-phase [4]

(b) ABB mobile transformers single-phase in operation [4]

		ABB Shell speciality transformers (Standard insulation)	ABB Shell speciality transformers (Hybrid insulation)	ABB Shell speciality transformers (Contingency for wind generation)
Source		[4], [2]	[4], [2]	[4], [2]
Owner/ manufacturer		ABB / Hitachi Energy	ABB / Hitachi Energy	ABB / Hitachi Energy
frequency	Hz	50	50	50
Voltage	Supported High voltage [kV]	400 / 230-138 kV	400 / 230-138-110 kV	440/220 kV
Transformer	Single/three-phase	three single-phase polytransformer (117 MVA each)	three single-phase polytransformer (200 MVA each)	three single-phase polytransformer (150 MVA each)
	Type	Shell	Shell	Shell
	Cooling			
	Power (rated) [MVA]	350	600	450
Transport		3 trailers (transformers)	3 trailers (transformers)	3 trailers (transformers)
	L/W/H [m]	7/ 2.7/ 3.4	7.5/ 3/ 3.4	-
	Weight [tonne]	Total: 72.5 (shipping: 60)	Total: 90 (Shipping:70)	-
		Able to handle 5G of acceleration during transport		
Installation	Time	Days	Days	Days
Purpose		Fast recovery	Fast recovery	Fast recovery

Table 7.3: Mobile power transformers ABB [4], [2]

7.3. Conclusion

The details from the mobile transformers are summarised in Tables 7.1 and 7.3. From these mobile transformers, it is found that the transformers can be more compact when high-temperature insulation materials are used [74]. The transformer is also divided into three single-phase units to divide the load over multiple trailers [3]. shell-type and Autotransformers are used due to their compact and flexible design. The autotransformer cannot be connected in Y-Y configuration with isolated neutrals which makes it less suitable for bypassing TenneT substations. By allowing higher overloading of a transformer also smaller form-factor transformers can be used for the desired MVA rating. Different types of cooling can also be used to increase the MVA rating of the transformer. In the following chapters there will be looked at different transformer core types; core-type and shell-type.

8

Mobile power transformers

8.1. Introduction

This chapter will cover different transformer core types to determine which type is most suitable for a mobile power transformer to be able to fit the road regulations (Appendix A). When a three-phase transformer is too large and heavy for transport it can be divided into three single-phase transformers. The difference between a three-phase transformer and a bank of single-phase transformers will be covered. Multiple transformers could be used in parallel to have a high total MVA rating and still be transportable. The mobile substation also needs to be able to operate in parallel with existing transformers in the substation. Thus the parallel operation of power transformers will be covered in this chapter. The commissioning of a power transformer after transport will be covered, with the aim of bringing the transformer into service in a short amount of time. Finally, from the different transformer designs motioned in this chapter the design choices will be made for the mobile substations for TenneT.

8.2. Transformer types

There are two important types of core constructions possible for power transformers namely the core-type and shell-type, the difference between the core and shell-type will be discussed in this section.

The main difference between the core and shell-type is that for the core-type transformer the windings encircle the core whereas for the shell-type the core encloses the windings. Three-phase power transformers can be constructed in two ways: one three-phase transformer or three separate single-phase transformers. The majority of the three-phase power transformers are core-types [42] [3].

8.2.1. Literature: core-type

For the single-phase core-type transformer the windings encircle the core as shown in Figure 8.1a. The primary and secondary windings are on opposite core limbs. The core of a three-phase core-type transformer is usually made up of three limbs of stacked laminated iron slabs as shown in Figure 8.1b. For the three-phase transformer, each limb of the core carry's the primary and secondary windings of a phase, where the high voltage windings are placed over the low voltage windings. The high voltage windings are placed furthest from the core to reduce the amount of insulation required [42]. The coils in a core-type transformer have a cylindrical shape [12].

For the three-phase transformer the fluxes in the three core limbs are 120° apart, thus at any instant one of the three limbs acts as a return path for the magnetic flux of the other two limbs. For the large power transformers often five-limb core-type transformers are used, where there are two additional limbs on the sides to reduce leakage flux, minimize vibration, increase tank strength, and effectively use space inside the tank (Figure 8.2 [42]). Due to the extra side limbs, the sectional area of the yoke and the two side limbs can be 50% of that of the main limbs reducing the height of the transformer. However, these three-phase transformers are very large and for the 500 MVA rating, they can not be transported as normal road transport.

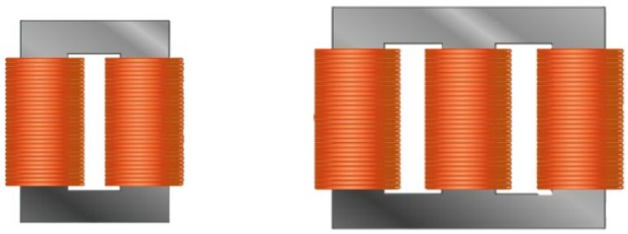

(a) Single-phase core-type transformer [64] (b) Three-phase core-type transformer [64]

Figure 8.1

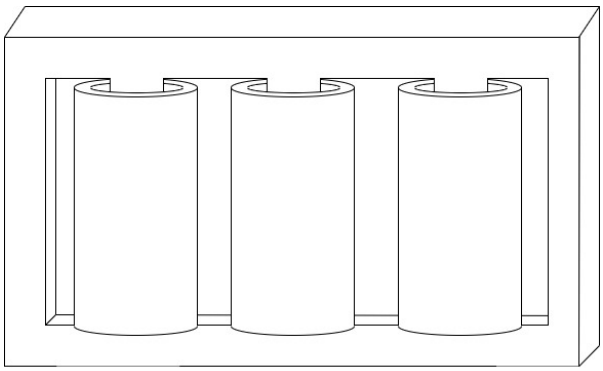

Figure 8.2: five-limb core-type transformer

8.2.2. Literature: shell-type

A less commonly used type of transformer is the shell-type, in this type of transformer the core surrounds the windings as shown in Figure 8.3a. A three-phase shell-type transformer can be constructed by stacking three single-phase shell-type transformers as shown in Figures 8.3b [42]. In this design, the core surrounds the windings on the three main limbs. The other two limbs act as a return path for the magnetic flux. Thus in the three-phase shell-type transformer, each phase has its own magnetic circuit and return path for the magnetic flux which makes the phases more independent compared to the core-type.

(a) Single-phase shell-type transformer [64] (b) Three-phase shell-type transformer [64]

Figure 8.3

The core encircles the windings and acts as a structural member. This reduces the amount of external clamping and bracing required and provides robustness to short-circuit and transportation and allows for compactness of design to match transportation restrictions [42].

The windings of a shell-type transformer are constructed from a number of pancake multi-turn coils, consisting of turns wound radial over one another from inside outwards and outside inwards alternately. The coils in a shell-type transformer are typically flat or oval-shaped [12]. The individual coils are connected in

series to form groups, these groups are connected in series to form packs [42].

The coils are stacked in alternating groups of HV and LV windings called an interleaved arrangement (Figure 8.4). Due to this interleaving, the short circuit forces for the HV and LV windings act in opposite directions, thus partially canceling each other. This increases the short-circuit withstandability of the transformer. When the capacity of a shell-type transformer is increased, the size of each coil is kept similar, but the amount of HV and LV coil groups is increased. This reduces the ampere-turns per winding group keeping the short circuit forces inside the transformer relatively constant [42].

An additional benefit of the use of coil groupings for the windings is the fact that it permits to achieve any impedance relationship between windings using various ampere-turns per coil group. This makes the shell-type transformer highly flexible to electrically match (impedance matching) existing units and thus the best option for the replacement of existing transformers [42]

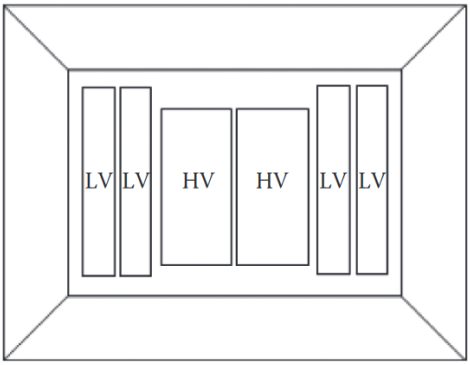

Figure 8.4: Interleaved arrangement of Pancake windings[42]

The main difference between core and shell-type apart from the core construction is the fact that it is much more difficult and expensive to assemble the shell-type. however, shell-type transformers are more compact and have better mechanical strength compared to core-type transformers [42]. Due to the form-fit construction of the transformer tank for the shell-type transformer, unnecessary oil volume is eliminated and according to López-Fernández [42], the oil volume is reduced by approximately 40% compared to a core-type transformer. A more in-depth comparison between the two transformer types is given in Table 8.1 where the properties which are important for the mobile transformer are marked in **bold**.

	core-type Transformer	**shell-type transformer**
Definition	The windings surround the core.	The core surrounds the windings.
Core cross Section	Square, cruciform, and three-stepped cross-section.	Rectangular cross-section.
Oil required (Cooling and insulation)	More	Less (40% due to form-fit tank to the core.[42])
Flux distribution	The flux is equally distributed on the side limbs of the core.	Central limb carry's the whole flux, the side limbs both carry half of the flux.
Winding type	Concentric cylindrical windings are used.	Sandwiched windings are used.
Magnetic circuit	one (single phase) (Two for a three-phase three limb)	Two (Single phase) (six for three-phase)
Losses	More losses due to higher flux leakage.	Lower losses due to lower flux leakage.
Mechanical Strength	Lower	High mechanical robustness and natural capability to withstand short-circuit events and transportation accelerations [42]
Size	Larger	Smaller, Due to the form-fit construction of the shell type transformer unnecessary oil volume in the transformer tank is eliminated. The oil volume of a shell type transformer is generally approximately 40% less than a comparable core type transformer [42].
Manufacturing	easy (more economical)	difficult (more labour intensive)
Power to weight	Lower	Higher [42]

Table 8.1: Difference between core and shell-type transformers [42]

8.3. Three-phase V.S Single-phase power transformers

Most power transformers used by TenneT are three-phase transformers, these are large and heavy which makes transportation difficult. A three-phase transformer can also be made by a bank of three single-phase transformers [78]. A single-phase transformer is considerably smaller and lighter compared to a three-phase transformer. The following pros and cons apply to a bank of three single-phase transformers [78][3]:

+ A single-phase transformer is smaller and lighter, which makes transportation easier.
+ Failure of one unit is less costly because only one single-phase unit needs to be repaired or replaced.
+ Only one spare single-phase transformer is required.
+ Either Y or Δ connections are possible with single-phase transformers connected in a bank because the neutral is brought outside the transformer.
- More expensive to build three single-phase transformers compared to one three-phase transformer.
- The bank of three single-phase transformers will be larger and heavier compared to a three-phase transformer.

For a mobile substation, it would be convenient in terms of size and weight to use single-phase transformers that can be transported on separate trucks. This will allow a high MVA rating while still being transportable. When three single-phase transformers are connected as a three-phase transformer bank it is extremely important that the impedances of the single-phase transformers are carefully matched, this will be discussed in Section 8.5

8.4. Parallel operation of power transformers

Power transformers can be connected in parallel and this is done for the following reasons [28]:

- A single transformer is not able to deliver the desired amount of power.
- As a redundancy measure, when one transformer malfunctions the power delivery can be continued.
- To be able to take one transformer out of service for maintenance without interrupting the power supply to customers.

When three single-phase transformers are still too large and/or heavy for road transportation it is possible to use multiple banks of single-phase transformers in parallel. The mobile substations will also need to be able to operate in parallel with existing transformers in the substation. To operate multiple transformers in parallel the following requirements are important:

- The transformers should be connected with the right polarity to prevent short circuits [3].
- The turn ratios should be equal to prevent circulating currents between the transformers [78][3].
- All transformers should have identical phase angle displacements, to prevent circulating currents [78].
- The percentage impedance (%Z) of the transformers should be nearly equal, to split the load current over the transformers in proportion of its MVA rating [78][3]. For a given voltage rating and %Z, the impedance (Z) of a transformer is inversely proportional to its MVA rating [78]. Thus when two transformers with the same %Z are put in parallel the load current will be split in proportion to the MVA rating of the transformers.

When a bank of three single-phase transformers needs to be connected in parallel to another bank of three single-phase transformers this can be done in two different arrangements. Two single-phase transformers can be put in parallel to form one large three-phase transformer bank as shown in Figure 8.5a. For this arrangement only one high-voltage switching bay is required, this reduces the costs of the mobile substation and can lower the installation time. However, when a fault occurs in one transformer all single-phase transformers are switched off and the capacity of the complete mobile substation will be lost.

The second possible arrangement is dividing the mobile substation into two banks of single-phase transformers as shown in Figure 8.5b. Now two high-voltage switching bays are required, which increases the investment cost and possibly increases the installation time because more connections need to be made to the substation. This setup will probably also require more space compared to the other arrangement due to the extra switching bays. However, with this arrangement, the redundancy is higher, because when now a fault occurs in one of the single-phase transformers only half of the mobile substation capacity will be lost. It is also possible to use one transformer bank of the mobile substation when only half of the mobile substation capacity is required.

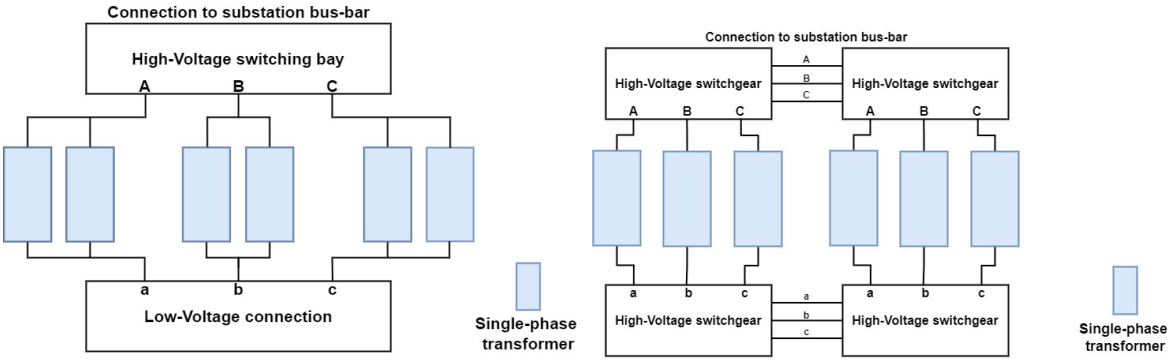

(a) Two single-phase transformers in parallel to form one transformer bank.

(b) Two parallel transformer banks.

Figure 8.5: A simplified representation of two different arrangements of a parallel connection of 6 single-phase transformers.

8.5. Impedance of transformer

Not all the flux which is generated by the primary winding is linked to the secondary winding of the transformer. It can thus be said that the transformer has leakage reactance (X) [3]. Together with the transformer resistance (R), this gives the impedance $\left(Z = \sqrt{(R^2 + X^2)}\right)$ of the transformer.

The percentage impedance (%Z) of a transformer is the voltage drop on full load current due to winding resistance (R) and leakage reactance (X) expressed as a percentage of the open-circuit voltage (E). Equation 8.1 gives the %Z as a function of the full-load current (I_{FL}) and open-circuit voltage (E) [3]. The %Z is determined as a percentage of the rated voltage which needs to be applied to the primary side of the transformer to cause the rated current to flow on the short-circuited secondary side of the transformer at the rated frequency [3].

$$\%Z = \frac{I_{FL}Z}{E} \cdot 100 \tag{8.1}$$

8.5.1. Transformer design: impedance

The magnitude of the leakage flux is related to the geometry and construction of the transformer [3]. The impedance can thus be varied by the design of the transformer. The reactance is a result of leakage flux thus the reactance can be lowered by reducing the leakage flux, which requires a larger transformer core [3]. Thus the size of a transformer can be reduced by accepting a higher reactance. A larger core cross-section and winding length will also reduce the reactance. Changing one parameter will also change the other parameter thus the transformer design is a trade-off between these parameters to get a particular reactance. By carefully designing a transformer almost all reactance values can be obtained, by adjustment of the physical dimensions [3]. However, when the dimensions of a transformer are restricted this becomes an issue for the impedance design of the transformer.

8.5.2. Impedance match for parallel operation

When transformers are operating in parallel it is important that their percentage impedances (%Z) do not deviate too much [3]. When two parallel operating transformers have equal percentage impedance the load current will be split over the transformers in proportion to their MVA rating [80]. When the impedances differ too much one transformer will carry relatively more load which could cause overloading, also this transformer will experience higher short circuit currents when a fault occurs. The mobile substation could be used to operate in parallel with existing transformers and thus the choice of percentage impedance of the mobile transformers should be in line with the impedance of existing transformers in the substation. If this is not possible resistance, reactance or both can be inserted in series with the primary or secondary circuits of the transformers to change the impedance and match to the parallel units. However, this would make installation much more complex and is thus not a desired solution.

8.5.3. Impedance matching for a bank of three single-phase transformers

When three single-phase transformers are connected as a three-phase transformer bank it is extremely important that the impedances of the single-phase transformers are carefully matched [78]. In addition to the rules for parallel operation which are mentioned in Section 8.4 the X/R ratios of the single-phase transformers should also be matched to keep the three-phase output voltages balanced.

8.5.4. Influence of transformer impedance on power system stability

The impedance of a power transformer has a major effect on the system fault current levels and voltage drop, and thus on the system stability. By specifying the minimum and maximum impedance of transformers it is possible to determine fault levels to meet values to suit the economic limitations of the switchgear and other connected equipment [3]. When a mobile substation is used to bypass an existing substation the impedance of the transformers may differ, causing different short circuit currents in the network. This will influence the protection system of the network.

Note that when two transformers are connected in parallel the combined impedance will be very much less compared to the impedance of the individual transformers (for two identical transformers in parallel the impedance will be half that of each individual unit) [3]. This results in an increase in the fault current levels.

For network stability calculations the short circuit current and the voltage drop in the network are important. The short circuit current (I_{sc}) can be calculated as follows;

$$I_{SC} = I_{Rated} * \frac{100}{\%Z} \tag{8.2}$$

Where $\%Z$ is the percentage impedance. When $\%Z$ of the transformer is lower, the short circuit current will be higher causing more stress on the insulation and higher mechanical stress. However, because of the lower $\%Z$ the voltage drop over the transformer will be lower which is positive for the voltage regulation in the network and lower losses will occur. Thus the transformer impedance should be chosen as a balance between the short circuit current and the voltage drop.

8.6. Commissioning of the transformer after transport

Standard power transformers are heavy and not designed to be transported on regular basis. For the mobile substations, the transformers will be road transported regularly thus special care must be taken for design and testing.

During transport, electronic shock recorders could be used to detect abnormal accelerations or vibrations on the equipment. When these sensors detect abnormal activity extra visual inspections and tests should be performed to make sure the device is in a healthy condition [11].
A frequently used test to identify damage due to transportation is the Frequency Response Analysis (FRA). During this test, the transfer function and change in voltage magnitude and phase angle of individual windings are measured by injection of low-voltage sinusoidal signals over a wide range of frequencies. These results could then be compared to previous benchmark tests, phase-to-phase comparisons, and comparisons of similar phases of an identical unit. The comparison to the benchmark test is the most meaningful [11]. Other tests which could be performed are [11];

- Core insulation resistance; to make sure not any unintentional ground has occurred during transport which would indicate damage to the core insulation.

- Leakage reactance; used to measure the short-circuit impedance. This additional test could be used when the FRA measurement shows some abnormalities. The leakage reactance test gives an indication of winding deformation or movement due to transport.

- Winding turn ratio (TTR): during this measurement, the ratio between the primary and secondary turns is measured at any tap position. When a difference or abnormality is measured this could indicate shorted turns or open circuits in the windings which could be caused during transport.

- Insulation power factor (tan δ); The power factor and capacitance between the various winding conductors, core, and tank are measured. The measurement can include the insulation liquid, bushings, and supports inside the tank. An increase in the power factor may indicate moisture content and contamination in the winding insulation.

- Winding insulation resistance; This measurement provides a measurement of the leakage current of the insulation. It gives a measure of the moisture content in the insulation and could also indicate disturbed or damaged ground insulation caused by shifting of the windings during transport.

Some mechanical tests also need to be performed for example:

- Pressure tests; this test is performed to make sure that there are no leakages developed in the transformer tank during transport.

- Dew point measurement; this measurement is used to determine the moisture content in the transformer. When the moisture in the transformer is high this reduces the breakdown strength of the paper-oil insulation and accelerates the aging of the cellulose insulation [23][16].

When the transformer is transported oil filled the dielectric strength of the oil will reduce due to vibrations, and a certain rest period is required after the trailer installation on-site [27]. Also shaking of the internal components of transformers will very likely have an adverse impact on the long-term performance and reliability of transformers [1].

When conventional transformers have been transported the above-mentioned checks and tests have to be performed on the transformer before it can be energized. The total installation, commissioning and testing can take up to 4 working weeks for large power transformers [61].

The goal of the mobile substations however is to be in operation as fast as possible. The Siemens resilience transformers from Section 7.1 are delivered to the site fully assembled and oil-filled and only the plug-in bushings need to be mounted. This results in the installation and commissioning time being much shorter. Siemens has proven that a 300 MVA transformer bank can be installed and put into service in 30 hours divided over 3 working days [58]. Siemens suggests that only the flowing test should be performed:

- Stored for a long time;
  - dissipation factor (tan δ) measurement
  - Transformer Turn Ratio (TTR) measurement
  - Insulation resistance measurement
- Stored for a short time (< 3 months);
  - Transformer Turn Ratio (TTR) measurement
- Optional: Frequency Response Analysis (FRA) after transportation.

8.7. Mobile power transformer for TenneT

In the previous sections, different types of transformers are discussed with a focus on size and weight. The mobile transformer's weight and size should stay within the road regulations from Appendix A. The transformers must also be able to withstand the influences of frequent road transportation and they should be fast deployable.

Most power transformers in the TenneT substations are core-type transformers (Section 2.2.4), thus when considering the experience of the crew, the core-type would be the preferred choice. However, the core-type transformers are heavier, larger, and less robust compared to shell-type transformers. The core-type also contains a larger amount of oil which imposes a larger threat to the environment when leakage occurs.

The shell-type transformer can be made more compact compared to the core-type transformer. The fact that the core surrounds the windings causes the transformer to be more resistant to the influences of transportation. Due to the form-fit tank, the core-type also requires less oil, and thus the impact on the environment is lower when a leak occurs. The fact that the impedance of the shell-type can be conveniently tuned by changing the ampere-turns makes this type of transformer the preferred choice for parallel operation with other transformers. A downside to the shell-type transformer is that it is more difficult to assemble and is thus more expensive in construction compared to the core-type. However, the shell-type transformer will be the most suitable core design for the TenneT mobile substations due to its robustness and compactness.

TenneT uses four different transformer ratings in its substations (Section 6), the 380/220 kV autotransformer has the highest power rating with a capacity of 750 MVA. There are only 7 of these transformers used in the grid and designing the mobile substation for this high rating would result in a very large power transformer. The second largest power transformers which are used by TenneT have a rating of 500 MVA. TenneT has approximately 52 transformers of this capacity in its substations. The majority of the transformers in the grid have a rating of 500 MVA, it is thus chosen to use 500 MVA as the minimal power rating for the mobile substation. To bypass a 380/220 kV autotransformer two of the 500 MVA mobile substations could be used in parallel. When a three-phase shell-type transformer of 500 MVA would be used this would be large and heavy.

From the different mobile transformers mentioned in Tables 7.1, 7.2, and 7.3 it is found that the average MVA/tonne of a mobile transformer is approximately 2.3 MVA/tonne when the oil is removed. Note that this is an average over a small number of transformers and thus is only an approximation. From this, it is found that a weight of 217 tonne can be expected for the 500 MVA transformer. This is too heavy for normal road

transport. The size and weight of the transformer can be reduced by using high-temperature hybrid insulation, forced cooling, and allowing higher temperatures and thus higher overloading capability. However, this still would result in a large and heavy transformer.

The first option to reduce the weight is to divide the three-phase transformer into three single-phase transformers of 500/3=166.7 MVA. This would then result in transformers with a weight of approximately 73 tonne which is still heavier than allowed for normal road transport in the Netherlands (max 50 tonne).
To reduce the size of the transformers further the single phases can be divided into two single-phase transformers of 167.7/2=83.33 MVA each. Thus six single-phase transformers with an approximate weight of 36 tonne would then be required. This is well below the maximum of 50 tonne however the weight of the trailer and truck should also be taken into account.

The size of the transformers can be determined with the rule of thumb of 2 MVA/m^3, this would result in a volume of 42 m^3. When this is compared to a 40-foot standard cargo container which has a volume of 64.6 m^3, it can be assumed that these units can be transported as normal road transport in terms of size.

The six single-phase transformers should be connected as two parallel banks of three single-phase transformers as shown in Figure 8.6. This configuration will give a high redundancy to the mobile substation, but the installation time will be longer. An additional benefit is that the mobile substation now also can be used with half its capacity (250 MVA) when this is desired. For example, when a 380/220 kV, 750 MVA autotransformer needs to be bypassed three 250 MVA mobile substations could be used in parallel to get a capacity of 750 MVA.

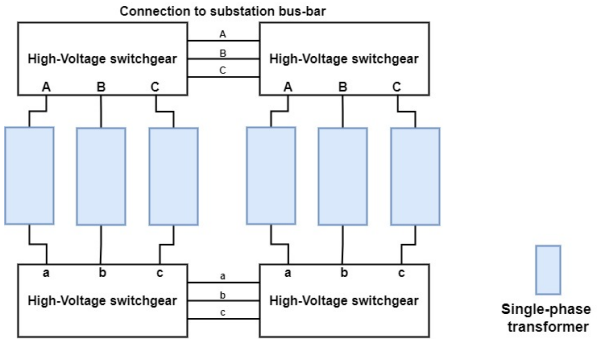

Figure 8.6: A simplified version of two parallel transformer banks.

The mobile transformer station should be compatible with all TenneT substations, thus different voltage ratings are required as mentioned in Section 2.2.4. The transformers in the mobile station should be able to cover all these voltages. This has a negative influence on the weight of the transformers because more windings will be required. It is also possible to design different mobile stations for every voltage rating however this is not a desired solution as it reduces flexibility and will increase costs.

The substation should be fast deployable, by using plug-in or wind-up bushings for the HV and LV connections the transformers do not exceed the maximum height during transport and are quick to install when they arrive at the substation location. The mobile substation can be connected to the incoming and outgoing lines of the substation by special cable terminations as in Figure 8.7.

Figure 8.7: Cable end terminals to connect the mobile substation to gantry structure, photo by TenneT.

8.8. Conclusion

The power transformer will be the largest and heaviest component of the mobile substation. For the mobile substation, a core-type and shell-type transformer core are considered, it is chosen to use a shell-type transformer because of its compact design and its resistance to the influences of transportation.

It is chosen to use six single-phase shell-type transformers, with an 83.33 MVA rating for a total capacity of 500 MVA. These transformers will have an approximate volume of 42 m^3 and a weight of 36 tonne, which is assumed to fit a normal dutch road size transport.

The six single-phase transformers should be connected as two parallel banks of three single-phase transformers (Figure 8.6). This configuration will give a high redundancy to the mobile substation, but the installation time will be longer and most likely more space will be required. An additional benefit is that the mobile substation now also can be used with half its capacity (250 MVA) when this is desired.

II

High voltage insulation distances

9

Introduction

The area inside and around a substation where the mobile substation should be diploid is limited, it is thus essential for a mobile substation to be as compact as possible. The mobile substation should also comply with road regulations to allow for road transport without special permits (Appendix A). The length of the bushings and the insulation distance between phases and ground and between opposite phases has a major influence on the size of a mobile substation when diploid and during transport [44]. To make a mobile substation as compact as possible the insulation distances should thus be as short as possible while still being safe and reliable.

In an air-insulated mobile substation, the smallest gaps are typically between equipment that may have large high-voltage electrodes (Figure 9.1a), for example, the combined current and voltage transformer.

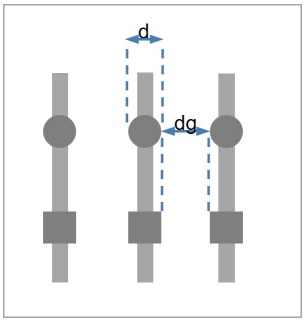

(a) Top-view of the distance between three phases in a substation with large components.

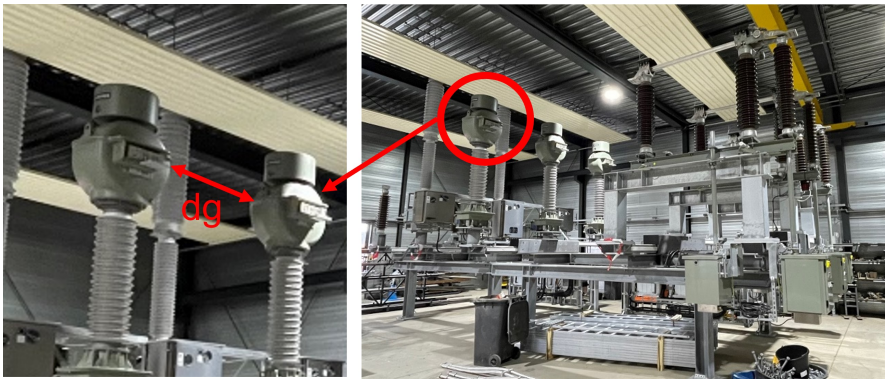

(b) Current-voltage measurement transformer on 150 kV TenneT skid with dg the smallest clearance in the skid.

Figure 9.1: 150 kV Skid from the Bay Replacement Project from TenneT. d = component diameter, dg = insulation distance

The main question for this part is:

How does the breakdown voltage between large electrodes with sharp points in compact air-insulated substations relate to gap length and are the minimal insulation distances as specified by the IEC 60071-1 [32] applicable to these compact substation?

The two different substation insulation methods: Air Insulated Substations (AIS) and Gas Insulated Substations (GIS) will be covered in Chapter 10. In Chapter 11 the principle of high voltage insulation coordination will be covered. Chapter 12 covers the minimal insulation distance in air as given by the IEC 60071-1 standard [32]. According to the standards, the Gap Factor approach can be used to find an approximation of the insulation distances for different electrode geometries, this method will be discussed in Chapter 13. To get more insight into the behavior of air insulation, the influence of overvoltage wave shape and electrode geometry on the breakdown in air will be covered in Section 14. Chapter 15 will cover an experiment to

provide more insight into the dielectric strength of a gap with large electrodes with sharp points in compact substations to verify if the standards can be applied to this situation.

10

Background: Mobile HV equipment

For the high-voltage insulation in a substation three options are available; an Air-insulated System, a Gas-insulated system, and a combination of the two. In this chapter, the difference between Air and Gas insulated substations will be covered. Also, the application of both insulation methods in a mobile substation will be covered.

10.1. Air-insulated substation

An Air-insulated substation (AIS) makes use of the dielectric strength of air to insulate the high voltage phases from each other and grounded parts. Most of TenneT substations are of air-insulated type. The clearances in an air-insulated substation consist of two components as specified by the NEN 3840 [52]:

- **Danger zone:** This distance is equal to the electrical clearance which is required to withstand the expected overvoltages in the system as specified by the IEC60071-1 [32]. It is forbidden for body parts and/or tools to enter this zone at any time.
- **Proximity zone:** The proximity zone comprises of the danger zone and an ergonomic component to ensure that workers outside the proximity zone cannot encourage the danger zone by reaching toward the energized components. It is allowed for body parts and/or tools to temporarily be in this zone when live work is performed by qualified personnel following specific working instructions.

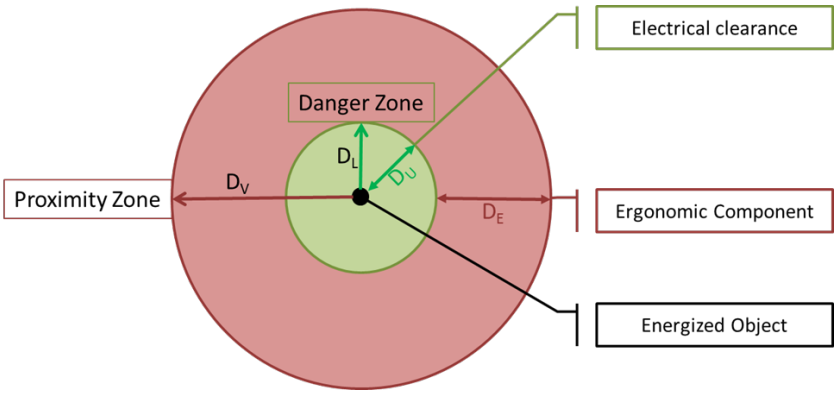

Figure 10.1: Components of the specified minimum air clearances according to NEN 3840 [52]

AIS is attractive because the investment costs for an air-insulated substation are considerably lower compared to a GIS [50]. Also, replacement and repair are easier and less expensive compared to GIS because components can be accessed independently. The main disadvantage of AIS is the fact that the insulation behavior is affected by environmental conditions. The AIS will require a large area in a substation compared to GIS because of the larger insulation distances in air.

10.2. Gas Insulated Substation

A Gas Insulated Substation (GIS) is a high-voltage substation in which the major part of the energized components are contained within an enclosed environment containing a dielectric gas as an insulating medium. The concept of gas-insulated substations was developed at the end of the sixties in Japan when there was a need for substations with a much smaller footprint. Because of this compactness, GIS technology is also attractive for the application to mobile substations.

The first systems used compressed air as an insulating medium. Later the compressed air was replaced with Sulphur Hexafluoride (SF_6) for better insulation and arc extinguishing purposes. The dielectric strength of SF_6 at atmospheric pressure is approximately three times higher compared to that of air [50] and SF_6 is about 100 times better in arc interrupting compared to air [15]. When the pressure is increased the dielectric strength of SF_6 increases due to the increased gas density. Typically the GIS uses a gas pressure of around 4 to 6 bar (0.4 to 0.6 MPa).

The required space or footprint of a GIS is only 10-25% of the required space for conventional air-insulated substations [50]. When the GIS uses high-pressure SF_6 only a few centimeters between the HV parts and the earthed parts are required making the system very compact and thus ideal for mobile systems in terms of size. By using GIS technology it is possible to design 230 kV mobile substations on trailers with a 2.5 m width [43].

However there are also some disadvantages to employing GIS systems, they are much more expensive compared to AIS [50], and the SF_6 is a very strong greenhouse gas [9].

Research is ongoing to address the climate concerns by finding alternative gases as insulating medium. Grid Solutions, a GE and Alstom joint venture, has identified a fluoronitrile-based gas mixture 'g3—green gas for grid' that could potentially be used instead of SF_6 and solve the greenhouse gas issue [34]. A mixture of C5-PFK or C4-PFN with CO_2 is also suggested as a possible alternative to SF_6 [62]. However, the above-mentioned alternative gasses are recently developed and have no proven long time track-record and thus the search for an alternative for SF_6 is still ongoing.

The GIS can be three-phase or single-phase enclosed meaning that either all phases are enclosed in one single housing or the three phases are in separate enclosures. The first GIS systems were three-phase enclosed. The current 220 kV and 380 kV GIS are single-phase enclosed because a three-phase enclosure becomes too large to be practical. For the 110 kV and 150 kV ratings, most GIS are three-phase enclosed (Figure 10.3).

There are special considerations when a GIS is applied to a mobile substation. The live parts inside the GIS are supported by support insulators that suspend the live parts from the grounded outer cylinders. These support insulators are normally not designed to handle frequent dynamic loads during transport, thus special attention is required for the design of these support insulators.

TenneT has substations with cable and line connections and thus the GIS needs to be able to be connected to the high voltage lines and cables. When it is directly connected to a high voltage line SF_6 air bushings are used (Figure 10.2). These bushings consist of a hollow insulating cylinder filled with pressurized SF_6. The outside of the cylinder can be exposed to atmospheric air. Inside the bushing, a metallic conductor is present which carries the current. The high voltage line can be bolted to the top of the bushing. The insulating cylinder is usually made of a composite consisting of a fiberglass epoxy cylinder with an external weather shed of silicone rubber. Because the high voltage line only needs to be bolted to the top of the insulator this connection has a short installation time.

When the GIS is connected to a high-voltage cable, cable terminations are used. The cable termination provides suitable electric field distribution at the end of the cable. The connection is made in the SF_6 gas thus no long termination is required compared to AIS systems. A convenient type of cable connection for the mobile substation would be the plug-in type of cable termination. For this termination, the GIS is equipped with a female plug-in termination in the factory. The cable is then terminated to a male plug termination which can be plugged into the female side on-site. By using the plug-in terminations the GIS can be factory sealed and the cables can be connected quickly on-site, reducing the installation time. A joint working group of Cigré suggests the implementation of standardized plug-in connections for high voltage (below 145 kV) GIS systems [49].

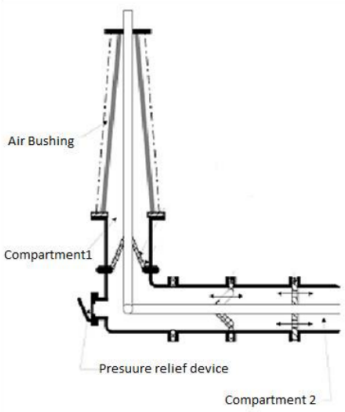

Figure 10.2: Schematic of GIS to Air bushing [33]

10.3. Mobile AIS used by TenneT

TenneT has developed compact and transportable air-insulated substations (110 and 150 kV) which are used for their bay replacement project as mentioned in Section 3.3.2. Special skids are developed which can be assembled in a factory and then transported to a substation where they can be slid into location and are connected together. The skids are designed to be compact to allow for transportation by road and to reduce the footprint in a substation. The mobile skids are comparable to a mobile air-insulated substation because they are both optimized to be as compact and mobile as possible. The skids are designed and are being manufactured at the time of writing this thesis. The insulation design is based on the standard insulation distances as given by the IEC 60071-1 [32].

10.4. Mobile GIS used by TenneT

TenneT already uses mobile GIS units which can be used on the 110 kV and 150 kV networks (Figures 10.3a and 10.3b). These mobile units are used as temporary substations during maintenance, as temporary solutions after calamity, and as segments of a larger GIS installation. They consist of 4 bays and have dimensions of less than 13x3.5 m. The units are mounted on transportable skids and can be transported on normal road-size trucks.

These modules were standardized to a double bus bar with one coupling bay as shown in Figure 10.4. The GIS is connected to the other bays in the substation by cables connecting to the main bus bars. Plug-in cable connections are used to improve the speed of connecting during installation.

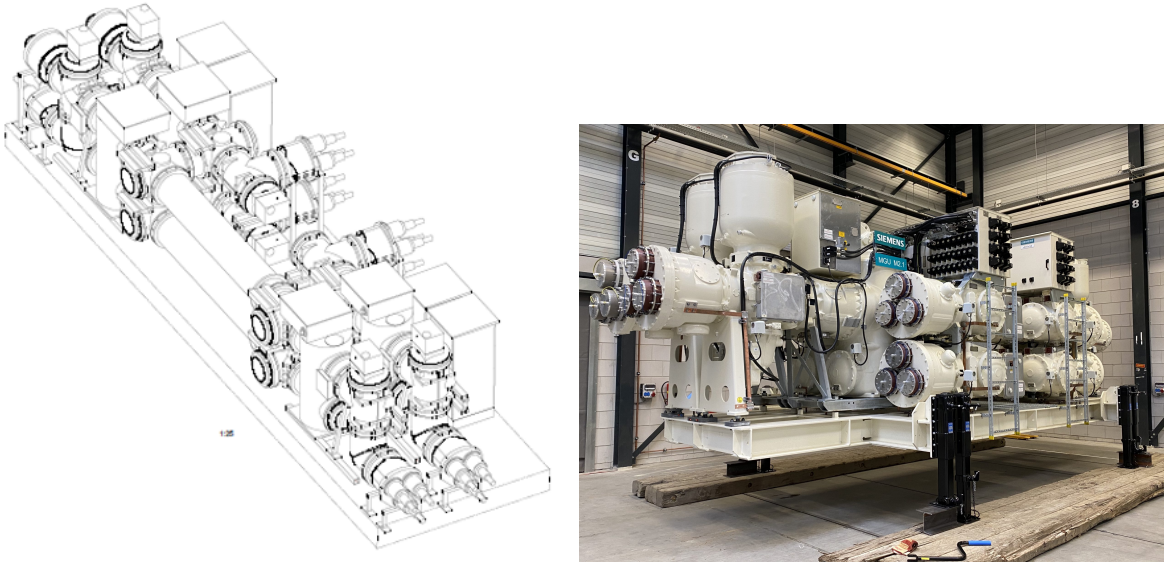

(a) Technical drawing of mobile GIS skid from TenneT (170kV)

(b) Picture of mobile GIS skid from TenneT (170kV)

Figure 10.3: Four bay double bus-bar mobile GIS skid from TenneT 170 kV

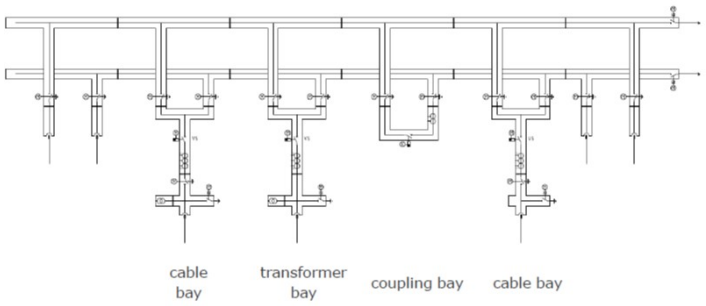

Figure 10.4: Four bay double bus-bar configuration as standardized by TenneT for the mobile GIS [40]

10.5. Conclusion

Both GIS and AIS could be used for a mobile substation, the GIS is more compact but much more expensive and as long as SF_6 is utilized as insulating gas it also possesses a great risk to the environment. According to the policy of TenneT GIS should only be used when AIS is not possible. Thus there is a need for developing a viable compact air-insulated mobile substation concept.

In the following chapters, the insulation coordination for air-insulated substations will be covered. Thereafter it will be discussed if the minimal insulation distances as specified by the IEC 60071-1 [21] are applicable to a compact substation containing large electrodes with sharp points.

11

Background: Insulation coordination

Insulation coordination is the balancing between the cost of insulation and the reliability of the system. It involves the proper choice of insulation level and includes overvoltage protection equipment such as spark gaps and surge arresters [38]. When breakdown is inevitable it should take place in a preferred location where it will cause the least harm. For example, when a high overvoltage occurs and breakdown is inevitable it should occur in the spark gap instead of touching the line insulator, and rather in the surge arrester than the expensive power transformer.

During the insulation coordination process, the dielectric strength of equipment is selected in relation to the operating voltages and transient overvoltages which can appear on the system for which the equipment is intended. In Sections 11.1 and 11.2 the overvoltages which can occur in the studied system and which overvoltages should be withstood by the equipment are discussed.

11.1. Overvoltages

To understand insulation coordination design it is first important to cover the different types of overvoltages for which the system needs to be designed. To aid substation designers and guarantee safety, the IEC has established a number of standardized insulation levels and specified a series of test requirements for the manufacturers and users. For the design of insulation construction and determination of test requirements three types of overvoltages are considered:

1. Lightning overvoltages (Fast-Front)
2. Switching overvoltages (Slow-Front)
3. A.C. overvoltages (Continuous and Temporary)

The high-voltage equipment must be dimensioned to withstand these elevated voltages. In the following sections the Lightning, switching, and temporary overvoltages will be covert. The IEC 60071-1 [32] also specified very fast overvoltages however these are typically only considered in GIS substations and will not be covered in this thesis.

11.1.1. Lightning overvoltages

It can be assumed that substations are effectively shielded by lightning rods against direct lighting hits, thus the lightning impulses will typically only reach the substation via the connected lines and cables [19]. Lightning can cause overvoltages on high-voltage lines in three different ways;

- **Direct hit:** When the lightning shielding of the overhead lines is insufficient a direct lightning hit to the phase conductor could occur, which results in a transient overvoltage that propagates along the affected phase conductor to the substation.
- **Backflash:** When lightning hits the transmission line earthing system, the lightning current flowing through the tower and earthing system, $(\omega L + R)$ increases the voltage between the energized phase conductors and the tower. When this voltage is high enough a flashover can occur over the insulators causing a fault and a transient overvoltage that propagates to the substation.

- **Induced voltage:** When lightning hits close to an overhead line it can induce a voltage on the phase conductors. This overvoltage is however generally below 300 kV and attenuates rapidly, these surges rarely reach the substation and are therefore ignored.

For testing purposes, a lightning surge should be represented by a standardized impulse, according to the IEC 60060-1 [30] as given by Equation 11.1.

$$U = \hat{U}(e^{-\frac{t}{\tau_1}} - e^{-\frac{t}{\tau_2}}) \tag{11.1}$$

where $\tau_1 = 68\ \mu s$ and $\tau_2 = 0.4\ \mu s$ which gives a wave with 1.2 μs front time (T_1) and 50μs tail time (T_2) as shown in Figure 11.1 [38].

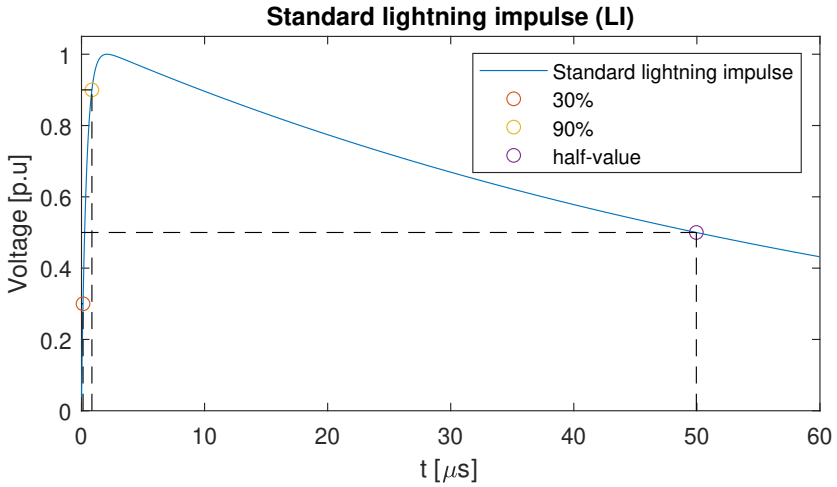

Figure 11.1: Standard 1.2/250 μs lightning impulse according to IEC60060-1 [30]

11.1.2. Switching overvoltages

Another cause of overvoltages are switching operations which can cause transient overvoltages in the network some examples of switching operations are [38]:

- Fault clearing
- Disconnecting unloaded transformers
- Disconnecting unloaded lines
- Connecting unloaded lines
- Non-simultaneous switching

The switching impulses are oscillating transients with frequencies between some hundreds to some thousands of Hertz, for which an average of 1000 Hz may be used [38]. For testing the IEC standard switching impulse is defined (Figure 11.2). In the standard switching impulse, the beginning of the oscillation is represented by a front of 250 μs as shown in Figure 11.2. The attenuation of the transient is represented by a half value after 2500 μs [37]. In most cases, the oscillation is represented by a unipolar impulse so that the same impulse generator can be used as for the lightning impulse.

11.1.3. A.C. overvoltages

The 50 Hz operating voltage can also attain a Temporary Overvoltage (TOV) due to the following reasons;

- When a large load is disconnected, the resistive and reactive voltage drop disappears and a temporary overvoltage occurs this is called load rejection. The overvoltage disappears when the operating value is restored by the control system.
- The capacitance of an unloaded cable together with a transformer or generator inductance can cause overvoltages.
- When a ground fault occurs in a network an overvoltage will occur until the fault is cleared. For example with a non-earthed neutral, a voltage of $\sqrt{3}$ times the operating value will occur.

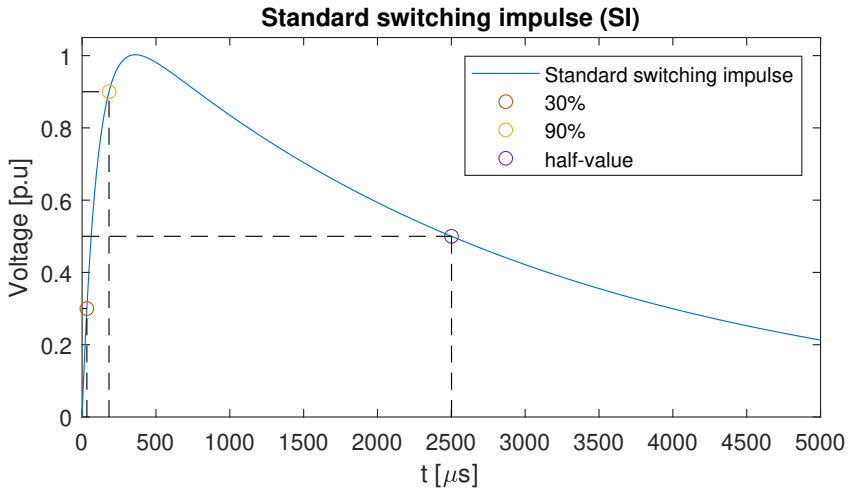

Figure 11.2: Standard 250/2500 μs switching impulse according to IEC 60060-1 [30]

When it is not possible to avoid the occurrence of TOV's the high-voltage equipment should be able to withstand these elevated voltages. For testing, a voltage amplitude should be used with an RMS value equal to the assumed maximum of the temporary overvoltage divided by $\sqrt{2}$ according to IEC 60060-1 [30].

11.2. Overvoltage amplitudes

To determine the minimal insulation distance for a mobile substation it is required to specify the maximum overvoltage amplitude which the insulation should be able to withstand. The IEC 60071-1 [32] specified standard rated withstand voltages for testing based on expected overvoltages which are associated with the standard highest voltage for equipment. It is the responsibility of the user to ensure that the overvoltages in the system do not exceed the capability of the equipment as referenced to the test withstand voltages.

For non-self restoring insulation e.g. transformer insulation the withstand voltages specified by the IEC 60071-1 are specified as the conventional withstand voltages, which means that the number of disruptive discharges which are tolerated at this test voltage is zero [32]. Thus the withstand probability is equal to $P_{withstand}$=100% [29]. For self-restoring insulation such as air-insulation, the withstand voltages specified by the IEC 60071-1 are the statistical withstand voltages [32]. This means that the withstand probability is equal to $P_{withstand}$=90% [29].

TenneT owns substations at five different voltage levels, Table 11.1 gives the standard rated overvoltage withstand levels in accordance with the IEC60071-1 [32] as applied to TenneT air-insulated substations. The high-voltage equipment and clearances should be designed to be able to withstand these voltages.

For the different nominal voltages (U_n) and the corresponding maximum voltages (U_m), the standard rated withstand voltages are specified. The standard rated temporary overvoltage (PFWV, Power Frequency Withstand Voltage) is the sinusoidal voltage with a frequency between 48 Hz and 62 Hz, and a duration of 60 s which the equipment should be able to withstand. The standard rated switching impulse withstand voltage (SIWV) is the maximum impulse voltage having a time to peak of 250 µs and a time to half-value of 2500 µs which should be withstood by the equipment. The standard rated lightning impulse withstand voltage (LIWV) is the impulse voltage having a front time of 1,2 µs and a time to half-value of 50 µs which the equipment must be able to withstand.

For the 110 up to 220 kV levels only the withstand for lighting overvoltages and short-duration power-frequency overvoltages are specified in the IEC 60071-1 standard. It is assumed that the standard rated short-duration power frequency or the standard rated lightning impulse withstand voltage should cover the required switching impulse withstand voltages [32]. Only for equipment with highest voltages for equipment (U_m) of 300 kV and above switching overvoltages are considered.

From Table 11.1 which shows the insulation levels used in the TenneT substations, it can be found that for

voltages above 110 kV there are multiple withstand voltage levels. TenneT specified in its standard (TBD.014.1 Isolatiecoordinatie [67]) that standard the highest insulation level should be used which are the **Bold** values in the table. According to this same standard a lower insulation level may be used when for example the price or size of a component can be lowered substantially, this is only allowed when this does not compromise the network performance and safety. For example, transformers that are well protected by surge arresters may have the lower insulation level specified when this substantially reduces the costs of the transformer.

Nominal voltage of system U_n	Highest voltage for equipment U_m	PFWV	SIWV	LIWV
[kV$_{rmsp-p}$]	[kV$_{rmsp-p}$]	[kV$_{rmsp-p}$]	[kV$_{peakp-e}$]	[kV$_{peakp-e}$]
50	72.5	**140**	n.a	**325**
110	123	185	n.a	450
		230	n.a	**550**
150	170	230	n.a	550
		275	n.a	650
		325	n.a	**750**
220	245	275	n.a	650
		325	n.a	750
		360	n.a	850
		395	n.a	950
		460	n.a	**1050**
380	420	n.a	850	1050
				1175
		n.a	950	
				1300
		n.a	**1050**	
				1425

Table 11.1: Insulation Voltages for TenneT substations as in the Nota Isolatiecoördinatie in accordance with IEC60071-1 [19]

12

Background: Insulation distances

To avoid flashover below the rated impulse withstand levels mentioned in Table 11.1 a minimal clearance between live parts and earth and between live parts of different phases is required. At standard reference atmospheric conditions, the switching and lighting impulse withstand voltages in air of a component shall be equal to or greater than the rated standard switching and lighting impulses which are mentioned in Table 11.1.

The IEC specified the minimum clearances in air for a rod-structure (Figure 12.1a) and a conductor-structure gap (Figure 12.1b), this is based on a conservative approach and taking into account historical practices of utilities. The clearances for a rod-structure and a conductor-structure gap under lightning overvoltages for the relevant voltage levels of TenneT are summarized in Table 12.1 [19]. According to the IEC for phase-to-earth insulation the minimum clearance for conductor-structure and rod-structure is applicable. For phase-to-phase, the minimum clearance for rod-structure should be used. Table 12.2 gives the minimal phase-to-earth insulation distances for switching overvoltages for the same gap configurations.

It should be noted that these clearances are intended only for the insulation coordination requirements and not for human safety requirements. To satisfy the latter requirement larger clearances may be needed as mentioned in section 10.1.

(a) Rod-Structure gap configuration

(b) Conductor-Structure gap configuration

Figure 12.1

There are some exceptions possible for the clearances in Tables 12.1 and 12.2. The clearance may be lower when it has been proven by tests on actual similar configurations that the standard rated impulse withstand voltages are met. Taking into account the relevant environmental conditions which can create irregularities on the surface of the electrodes, such as rain or pollution. The minimal clearances thus do not apply to equipment insulation that has a mandatory impulse type test included in their specification, since a mandatory minimal clearance might unnecessarily constrain the design of equipment, increase its cost, and impede progress. A lower clearance may also be used when it has been proven by operating experience that the overvoltages are lower than those expected in the selection of the standard rated withstand voltages, or that the gap configuration is more favorable than that assumed for the recommended clearances [32].

The IEC only specifies clearances for the rod-structure and conductor structure but not all clearances may be approximated by these configurations, especially in the case of compact substations where equipment, with large high-voltage electrodes, may be installed close together.

Nominal voltage of system U_n	Highest voltage for equipment U_m	Standard rated LIWV	Minimum clearance	
			Rod-structure	Conductor-structure
[kV$_{rmsf-f}$]	[kV$_{rmsf-f}$]	[kV$_{peakf-a}$]	[mm]	[mm]
50	72.5	**325**	630	-
110	123	**550**	1100	-
150	170	650	1300	-
		750	1500	-
220	245	850	1700	1600
		950	1900	1700
		1050	2100	1900
380	420	1175	2350	2200
		1300	2600	2400
		1425	2850	2600

Table 12.1: Minimum clearances for standard-rated lightning impulse withstand voltages in TenneT substations according to IEC60071-1: Table A.1 [32][19]

Nominal voltage of system U_n	Highest voltage for equipment U_m	Standard rated SIWV	Minimum phase-to-earth clearance	
			Rod-structure	Conductor-structure
[kV$_{rmsf-f}$]	[kV$_{rmsf-f}$]	[kV$_{peakf-a}$]	[mm]	[mm]
380	420	850	2400	1800
		950	2900	2200
		1050	3400	**2600**

Table 12.2: Minimum clearances for standard-rated switching impulse withstand voltages in TenneT substations according to IEC60071-1: Table A.2 [32]

12.1. Conclusion

The IEC 60071-1 [32] only specified the insulation distance for the rod-structure and conductor-structure electrode configurations. These are chosen because they are expected to represent the worst-case configuration in substations, the insulation distances are thus intentionally conservative. However, not all components in a substation can be considered as a rod-structure or conductor-structure, especially in the case of a compact substation with large energized components close together. Thus to determine the minimal insulation distance in a compact substation, the breakdown distance for different electrode configurations must be determined. In the following chapter, a method will be discussed which is used by the IEC 60071-2 [31] to approximate the insulation distance for different electrode configurations.

13

Gap Factor approach

As mentioned in the previous chapter the minimal insulation distances given by the IEC 60071-1 [32] in Tables 12.1 and 12.2 are only defined for a rod-structure and a conductor-structure gap configuration. However, not all components in a substation can be considered as a rod-structure or conductor-structure, especially in the case of a compact substation with large energized components close together. Thus it is desired to determine the insulating behavior of different gap configurations. It is possible to perform breakdown tests on these gap configurations and determine the 50% breakdown voltage (U_{50}) this is the voltage at which in 50% of the voltage applications breakdown occurs. When it is difficult or not possible to determine the U_{50} for a particular electrode configuration it is possible to estimate the U_{50} by calculations. The Gap Factor approach can be used to do these calculations.

In 1966 L. Paris [54] proposed the Gap Factor approach which later on was also incorporated in the IEC 60071-2 standard [31]. The Gap Factor K_g is the ratio between the 50% breakdown voltage of an air gap and the positive polarity 50% breakdown voltage of a rod-plane gap (Figure 13.1), for identical gap distance and voltage shape (Equation 13.1) [31]. The positively stressed rod-plane gap has the lowest minimal breakdown voltage of all common gap configurations and is thus used as a reference [54].

$$K_g = \frac{U^{50}_{K_g}}{U^{50}_{Rod-Plane}} \tag{13.1}$$

Figure 13.1: Rod-Plane gap

To use the Gap Factor first the U_{50} of the rod-plane gap is required. This could be determined by measurements on a rod-plane gap or by calculation. Different equations are proposed to determine the breakdown voltage for a positively stressed rod-plane gap these will be discussed in the next sections (13.1 and 13.2). The equations are all defined at standard atmospheric conditions which correspond to the air pressure at sea level, altitude corrections should be made for different conditions [30]. It should be noted that significant discrepancies occur for gap lengths less than 1 m where the accuracy of the equations in Sections 13.1 and 13.2 is questionable [31].

13.1. Slow-front overvoltages

Under slow-front surges like switching impulses the breakdown voltage of air insulation is lower compared to the fast-front surges with the same polarity as discussed in Section 14.2. Numerous switching impulse tests have been performed on different gap lengths to characterize the U_{50} for the critical time to crest and standard switching impulse. From these measurements, Kishizima et al. [35] proposed Equation 13.2 for the breakdown strength ($U_{50,rod-plane\_sf}$) in kV for a rod-plane gap at positive-polarity critical time-to-crest overvoltages as a function of the gap length d in m. The equation is valid for a gap length up to 25 m. This equation was adopted in the IEC standards [31].

$$U_{50,rod-plane\_sf} = 1080ln(0.46d+1) \qquad [kVcrest, m] \tag{13.2}$$

For the standard positive 250/2500 μs switching impulse as in Figure 11.2, the IEC standard uses Equation 13.3 which is derived by L. Paris from measurements on rod-plane gaps with lengths between 2 m and 6 m, with d in m and U in kV [31][54].

$$U_{50,rod-plane\_sf} = 500d^{0.6} \qquad [kV, m] \quad for \quad T_{crest} = 250\mu s \tag{13.3}$$

Gallet and Leroy [21] propose Equation 13.4 for positive switching impulse with critical time-to-crest, derived from indoor tests from 1 m up to 30 m.

$$U_{50,rod-plane\_sf} = \frac{3400}{1+\frac{8}{d}} \qquad [kV] \tag{13.4}$$

From a series of outdoor tests, Pigini et al [56] proved that Equation 13.4 is valid up to 15 m and proposed Equation 13.5 for positive switching impulse with critical time-to-crest on gap spacings with a range between 13 - 30 m.

$$U_{50,rod-plane\_sf} = 1400 + 55 * d \qquad [kV] \tag{13.5}$$

For impulses with negative polarity and critical time-to-crest Equation 13.6 for rod-plane gaps is proposed by Pigini et al [56] for the breakdown voltage, on gaps between 0 - 15 m.

$$U_{50,rod-plane\_sf} = 1180 * d^{0.45} \qquad [kV] \tag{13.6}$$

13.2. Fast-front overvoltages

For fast-front overvoltages, the breakdown voltage of a rod-plane gap for positive polarity is much lower compared to negative polarity, this will be discussed in Chapter 14.
For standard lightning impulses, the IEC standard uses Equation 13.7 to approximate the breakdown voltage for a positive polarity rod-plane gap with gap lengths between 1 m and 10 m. Cigre [66] suggests Equation 13.8 which is valid between 2 to 5 m, this equation is only slightly different from Equation 13.7.

$$U_{50,Rod-Plane\_ff} = 530d \qquad [kVcrest, m] \tag{13.7}$$

$$U_{50,Rod-Plane\_ff} = 525d \qquad [kVcrest, m] \tag{13.8}$$

13.3. Gap Factor

The Gap factors which can be found in literature [66][55] are based on the positive polarity switching impulse strength of a rod-plane gap. This is because the gap configuration has a larger influence on the breakdown strength under switching impulse than it does under lighting impulse [71]. The Gap Factor for slow front impulses and thus for switching impulses is denoted as K_{g_sf} [51]. The K_{g_sf} for different gaps are given in Table 13.1.

The breakdown voltage for different electrode configurations can be found by multiplying the $U_{50,Rod-Plane\_sf}$ from the equations in Section 13.1 by the Gap Factors for slow front overvoltages (K_{g_sf}) as in Equation 13.9. The Gap Factors which are mentioned in Table 13.1 are determined for the slow-front overvoltages and are not directly usable for the fast-front overvoltages (Section 13.3.4).

$$U^{50}_{K_{g\_sf}} = K_{g\_sf} * U^{50}_{Rod-Plane\_sf} \tag{13.9}$$

For actual substations, it is not always possible to simplify the electrode configurations to simple geometries and give a general Gap Factor value. For the Conductor - Lower structure, Conductor - Lateral structure, and Horizontal Rod - Rod from Table 13.1 which are common gap configurations in substations more detailed equations are given in Sections 13.3.1 13.3.2 and 13.3.3, to get a more accurate Gap Factor value.

13.3.1. Conductor-Lower structure

For the Conductor-Lower structure from Table 13.1 the detailed equation for the Gap Factor is given by Equation 13.10 [29][66]. If W/S ≤ 0.2, A = 0 otherwise A = 1. This equation is applicable in the range: d = 2 to 10m, S/d = 0 to inf and H_1/H = 0 to 1.

$$K_{g\_sf} = 1.15 + 0.81\left(\frac{H_1}{H}\right)^{1.167} + 0.02\left(\frac{H_1}{S}\right) - A\left[1.209\left(\frac{H_1}{H}\right)^{1.167} + 0.03\left(\frac{H_1}{S}\right)\right]\left(0.67 - e^{-\frac{2W}{S}}\right) \tag{13.10}$$

13.3.2. Conductor - Lateral structure

The more detailed equation for the Conductor - Lateral structure from Table 13.1 is given by Equation 13.11 [29][66]. The equation is applicable for: S = 2 to 10 m, W/S = 0.1 to 1.0, and H/S = 2 to 10.

$$K_{g\_sf} = 1.45 + 0.024\left(\frac{H}{S} - 6\right) + 0.35\left(e^{-\frac{8W}{S}} - 0.2\right) \tag{13.11}$$

13.3.3. Horizontal Rod - Rod

The Horizontal Rod - Rod gap configuration is a complex arrangement, it consists of two Gap Factors; K_{g_1} (Equation 13.12) for the Rod-Rod gap S_1 and K_{g_2} (Equation 13.13) for the Rod-Structure gap [29][66]. Where A = 0 if $W/S_2 \leq 0.2$ and otherwise A = 1. The equation is applicable for K_{g_1} if S_1 = 2 to 10 m and $S_1 < S_2$ and S_1/H = 0.1 to 0.8. For Gap Factor K_{g_2} the equation is applicable if $S_1 > S_2$, S_2 2 to 10 m and W/S_2 = 0 to inf.

$$K_{g1\_sf} = 1.35 - 0.1\frac{H_1}{H} - \left(\frac{S_1}{H} - 0.5\right) \tag{13.12}$$

$$K_{g2\_sf} = 1 + 0.6\frac{H_1}{H} - 1.093A\frac{H_1}{H}\left(0.549 - e^{-\frac{3W}{S_2}}\right) \tag{13.13}$$

13.3.4. Gap Factor for fast front overvoltages

From experimental results, it is found that the breakdown gradient of a general air gap for positive polarity in per unit of the breakdown gradient of a rod-plane air gap increases linearly with the switching impulse Gap Factor for positive impulse voltages [31]. A Gap Factor K^+_{ff} for fast-front lightning impulses with positive polarity is approximated by Equation 13.14 as a function of the positive switching impulse Gap Factor (K_{g_sf}) [31].

$$K^+_{g\_ff} = 0.74 + 0.26K_{g\_sf} \tag{13.14}$$

Gap Factors		$\mathbf{K}_{g\_sf}$
Rod - Plane		1.00
Rod - Rod	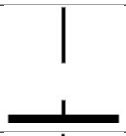	1.30 - 1.40
Rod - Structure	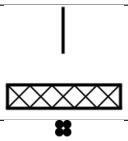	1.05
Conductor - Structure	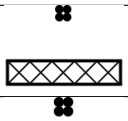	1.30
Conductor - Plane	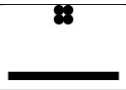	1.1 - 1.15
Conductor - Rod	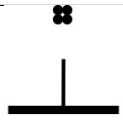	1.65 - 1.90
Protrusions	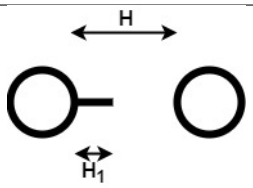	$k_0 = e^{\pm 0.7 \frac{H_1}{H}}$ k≥0 + sing for protrusion form the positive electrode - sign for protrusion from the negative electrode
Conductor - Lower structure	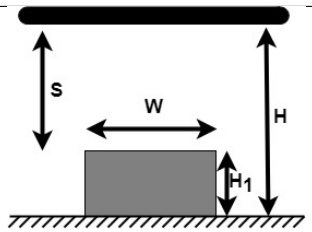	1.30 (Equation 13.10)
Conductor - Lateral structure	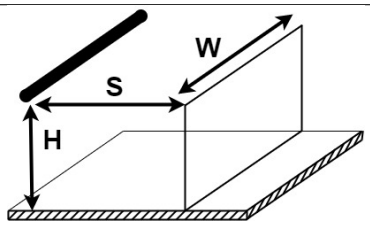	1.35 (Equation 13.11)
Horizontal Rod - Rod	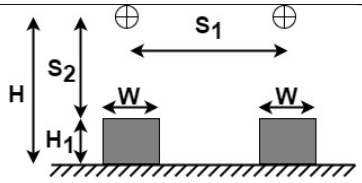	1.30 (Equations 13.12 and 13.13)

Table 13.1: Gap Factors for some common configurations [29][55]

13.3.5. Gap Factor for Phase-to-Phase configuration

The previously mentioned Gap Factors are for phase-to-ground configurations in which only one electrode is energized. For a phase-to-phase gap configuration, both electrodes are energized, one with positive polarity (U+), and one with negative polarity (U-). The voltage between the two phases depends on the amplitude of the two voltages and the time displacement Δt between their respective crests [48]. A ratio $\alpha = \frac{U^-}{U^+ + U^-}$ is thus required to determine a Gap Factor.

Gap Factors for α=0.33 and α=0.5 are shown in Table 13.2 and are validated up to D=8 m. Note that α=0.33 gives a lower Gap Factor and thus a lower breakdown voltage compared to α=0.5. This is because the breakdown voltage for positive and negative voltages are not equal and thus the worst case is when U+=2U-.

Electrodes	Gap Factors	
	α=0.5	α=0.33
Rod-rod	1.62	1.52
Conductor-conductor	1.62	1.52
Supported busbars	1.50	1.40

Table 13.2: Gap Factors for phase-to-phase insulation in Equation 13.4 for height up to 8 m [71]

13.4. Shortcomings of the Gap Factor approach

The breakdown strength of a gap is related to the electric-field distribution in the gap. However, according to the original definition the Gap Factor value K_g is not based on an electric-field computation but on a visual impression of the gap [71]. For practical reasons, only a few typical families of gap configurations are chosen each with its own Gap Factor. For other gap configurations, the Gap Factor from the best matching standard gap must be used. Also within these families, the effect of the dimensions of the energized electrode is not considered [71]. For short gap lengths, the Gap Factor is not defined because the equations for breakdown voltages from Sections 13.1 and 13.2 are only defined for gaps larger than 1-2 meters. Thus for short gap lengths and large electrodes, the gap factor approach is not applicable.

The insulation distances in a mobile substation for voltages between 110 and 150 kV will be lower than 2 m according to the IEC 60071-1 standard as shown in Table 12.1. The smallest gaps are typically between equipment that may have large high-voltage electrodes (Figure 13.2), for example, the combined current and voltage transformer (Figure 9.1b). It is therefore, questionable if the Gap Factor approach can be applied to these compact substation configurations.

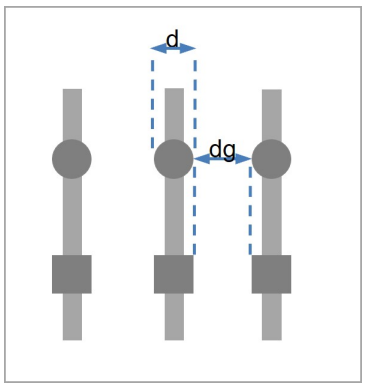

Figure 13.2: Illustration of the distance between three phases in a substation with large components. d = component diameter, dg = insulation distance

It should be pointed out that the empirical methods which are used for the Gap Factor determination simply indicate the relation between the influencing parameters and the 50% breakdown voltage [71]. While the breakdown in air depends on a number of successive stages which are all differently influenced by these parameters, thus the relations found are generally poor and difficult to generalize. It is thus important to

understand the parameters influencing the breakdown strength of large air gaps so that one can identify when the gap factor approach is applicable.

13.5. Conclusion

The minimal insulation distances given by the IEC 60071-1 [32] in Tables 11.1 and 11.2 are only defined for a rod-structure and a conductor-structure gap configuration. However, not all components in a substation can be considered as a rod-structure or conductor-structure, especially in the case of a compact substation with large energized components close together. To determine the insulation distance for different electrode configurations the U_{50} of these gaps should be determined. When it is difficult or not possible to determine the U_{50} for a particular electrode configuration by testing, it is possible to estimate the U_{50} by calculations using the Gap Factor. However, the Gap Factor is only specified for a few standard gap configurations which do not always match actual substation configurations. The Gap Factor is also not defined for gaps below 1 m and does not consider the electrode size. It is, therefore, questionable if the gap factor approach can be applied to compact substations with large electrode configurations.

The following chapter will cover the influence of overvoltage wave shape and electrode geometry on breakdown behavior of air.

14

Background: Breakdown in Air

14.1. Introduction

The insulation behavior of air depends on a number of factors; the type and polarity of the applied voltage, electric field distribution, gap length, and gas conditions. These parameters can be divided into three categories based on their influence on the strength of air insulation [66];

- **Decisive influence:** The insulation distance, the shape of the electrode, and the ratio between positive and negative electrodes in phase-to-phase configurations ($\alpha = \frac{U^-}{U^+ + U^-}$, Section 13.3.5) have a decisive influence on the insulation strength of air.
- **Significant influence:** The impulse shape has a significant influence on the insulation strength. When for the switching impulse; rise and fall time, are varied the breakdown voltage passes through a minimum value, the crest time at which this minimum occurs is called the critical time to crest.
- **Lower influence:** The pre-stressing of the air gap has a less significant influence and is neglected in the first approximation of the air gap strength.

The electrical discharge in air develops in successive phases which can be either well distinguished or partly superimposed depending on the type of applied voltage and the electrode geometry. The successive steps which can be distinguished are [66];

1. **Corona/streamer phase:**
   Thin ionized filaments called streamers are formed in the region of high electric field in the proximity of the electrode.
2. **Leader phase:**
   A leader channel is formed which is more highly ionized compared to the streamer, it propagates with leader corona developing from its tip. The leader can either reach the opposite electrode or stop depending on the value and shape of the applied voltage and gap length.
3. **Final Jump:**
   Once either the streamer or leader has reached the opposite electrode the final jump can take place. The leader channel elongates at increasing velocity and bridges the whole gap. The channel becomes highly ionized and the electrodes become short-circuited.

Which stages are present in the breakdown development depends on the overvoltage shape, for the slow front overvoltages such as the switching overvoltage all three stages are present [66] [71]. With other types of overvoltages, some stages may be absent. For lightning overvoltages, no significant leader phase can be present due to the short impulse time compared to the long leader phase [66][71]. The mechanism of breakdown in air is explained in more detail in Appendix B.

The characteristics of the first corona/streamer phase and leader phase are different for the different voltage polarities, this causes the breakdown voltage amplitude to be different for positive and negative polarity [66]. For almost all electrode geometries the breakdown voltage is lower for positive polarity compared to negative polarity overvoltages.

14.2. Influence of wave shape and electrode geometry

The breakdown mechanism with the three successive stages as mentioned in the previous section clearly describes the process which occurs for overvoltages of sufficiently long duration of front such as the switching overvoltage. For overvoltages with reduced time to crest such as lightning overvoltages, some stages may overlap or may be absent [66][71].

Lightning overvoltages have a very short time to crest and a very short tail, which are much shorter than the time of the continuous leader phase. Thus there is no time for a substantial leader to form. To achieve breakdown the voltage needs to be much higher and very long streamers will be formed, which are able to completely bridge the gap and cause complete breakdown [66].

The switching overvoltage may lead to the lowest dielectric strength of air insulation which is essentially due to the role played by the leader phase [71]. Due to this important leader phase, the breakdown voltage at switching overvoltage is very sensitive to a number of influencing factors such as the electrode size and geometry and impulse shape [66]. In the following sections, these influencing factors will be discussed in more detail.

14.2.1. Critical time to crest

The breakdown voltage under slow front impulses such as the switching impulse depends on the impulse shape, and mainly on the time to crest. When the tail duration of the impulse is kept constant and the front duration is varied this dependence is shown by L. Thione [71] in Figure 14.1 for a rod-plane gap of 4 m and a positive impulse voltage. In this figure a minimum for the breakdown voltage can be found, the time-to-crest (T_{cr}) for this minimum is called the critical time-to-crest ($T_{critical}$).

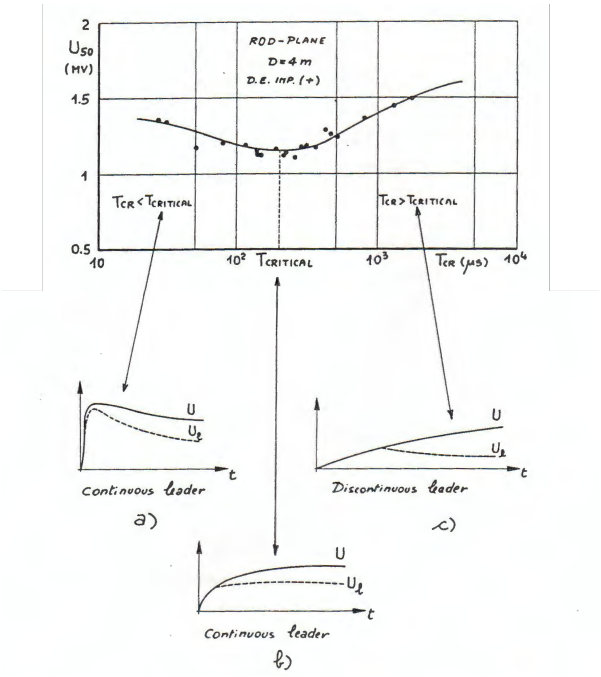

Figure 14.1: Influence of the time-to-crest of a rod-plane gap under positive switching impulse on breakdown strength [71].

Because the electrode which is used for the measurement in Figure 14.1 is small (a rod) leader discharge

will take place, three different discharge developments can be distinguished depending on the time to crest of the applied voltage.

- **T_{cr}<T_{crit}:**
  Because the front of the impulse voltage is short only a short leader is formed and breakdown occurs on the tail of the impulse voltage. During the increase of the voltage the potential of the leader tip increases, during the tail of the impulse this voltage decreases which impedes the propagation of the leader. Due to the short leader, a higher crest voltage is required to get breakdown.

- **T_{cr}=T_{crit}:**
  The time to crest is equal to the critical time to crest thus the breakdown will now take place at the crest of the voltage impulse. During propagation the potential of the leader tip remains almost constant, this means that the leader develops under the most favorable conditions and thus this gives the lowest breakdown voltage.

- **T_{cr}>T_{crit}:**
  The rate of increase of the voltage is too slow to compensate for the increase of the voltage drop on the leader during propagation which causes the leader to be discontinuous and its potential to slightly decrease during propagation. Thus breakdown will take place on the front of the impulse and higher crest voltages are required for breakdown.

From this, it can thus be concluded that the breakdown voltage for switching impulses will be lower compared to lighting impulses with the same polarity. Because the time to crest of a switching impulse is closer to the critical time to crest.

Note that according to the above considerations the dependence of the breakdown voltage on time-to-crest is related to the existence of a leader phase [71]. When electrodes of a larger radius relative to the gap length are used the electric field in the gap will be more uniform and thus the breakdown occurs directly without the need for the leader phase as will be discussed in Section 14.2.2. This causes the influence of the time-to-crest to be negligible for large electrodes and the U-curve to be almost flat [71].

For negative impulse voltage also a critical time-to-crest exists however the critical time-to-crest for negative polarity is shorter than for positive polarity [66], due to the higher mean leader velocity at negative impulse voltage.

14.2.2. Influence of geometry

The size of the electrode has an influence on the breakdown voltage of air under switching impulse. Figure 14.2 shows the variation between the corona-inception voltage U_i, the leader inception voltage U_l, and the breakdown voltage U_B, for a 4 m long sphere-plane gap, as a function of the sphere radius R with positive polarity switching impulses [71].
Breakdown can only occur when the electric field is strong enough to initiate corona. For a larger electrode radius, the surface electric field becomes lower for the same applied voltage and the voltage needs to be increased to cause sufficient field strength to initiate corona.
From Figure 14.2 it can be seen that the breakdown voltage is constant below a certain radius, this radius is called the critical radius (R_C) which is for this gap configuration approximately 0.2 m. This critical radius depends on the gap length and sphere size. When the radius becomes large in this case R= 0.9 m it can be seen from the figure that the breakdown voltage and the leader and corona interception voltage become equal, this is denoted as the radius R^*. Three different zones can be distinguished in Figure 14.2;

- **A: $0 < R \leq R_C$ (Small electrodes)**
  In this part the leader inception voltage is constant with the radius and much higher compared to the corona-inception voltage (U_l>U_i). The breakdown voltage is much higher than the leader inception voltage. At lower voltage corona will occur, when the voltage is sufficiently high leader propagation will occur and typical leader discharge will take place.
  Because all three discharge stages are present the scatter in breakdown voltage will be large.

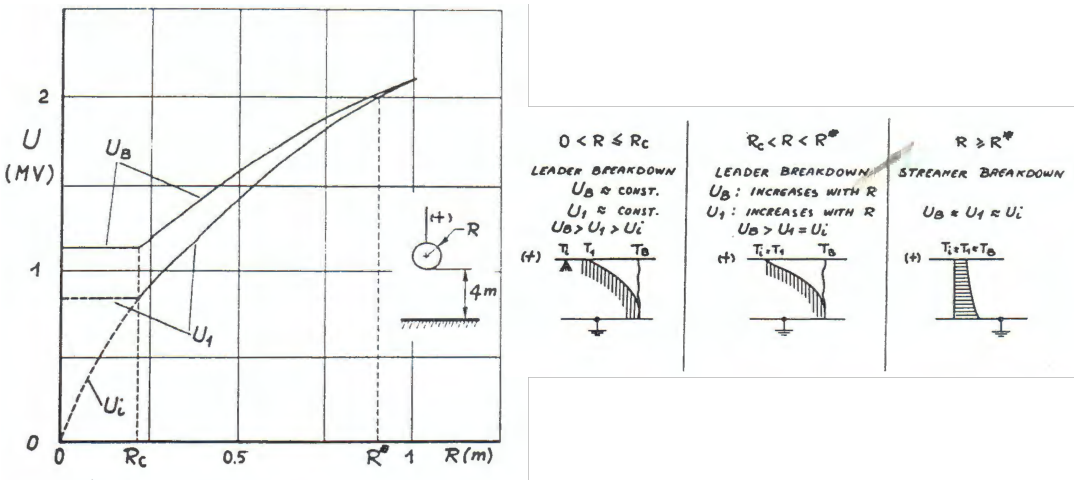

Figure 14.2: Influence of the radius of a spherical electrode under positive switching impulse on breakdown strength for 4m gap. with: U_i the corona-inception voltage, U_l the leader inception voltage, and U_B the breakdown voltage. [71]

- **B: R_C < R≤ < R^* (Large electrodes)**
  From the figure it can be seen that the corona-inception voltage and the leader-inception voltage are equal, thus the leader will form and start to propagate as soon as corona starts. The corona-inception voltage increases when the electrode radius increases this causes the leader-inception voltage to also increase. The discharge is still a leader discharge however, the leader length when the final jump takes place decreases with increasing electrode radius.
  For this area the scatter in breakdown voltage will be smaller because the length of the leader will decrease.

- **C: R≥ R^* (Extremely large electrodes)**
  For extremely large electrodes it is found that the breakdown voltage, corona-inception voltage, and leader-inception voltage are almost equal. When corona occurs streamers are formed which are long enough to bridge the whole gap, thus streamer breakdown will take place.
  Because the breakdown now only consists of the corona and final jump phases the scatter in breakdown voltage is reduced even further.

From Figure 14.2 it is clearly observed that the breakdown voltage of air increases with increasing electrode radius, which is due to the more homogeneous electric field and thus the lower field enhancement at large electrodes.

Figure 14.3 gives the 50% breakdown voltage (U_{50}) for different gap lengths as a function of the electrode radius. This figure clearly indicates the critical radius (blue dashed line) as previously discussed and shows the relation to the gap length. It can be observed that for increasing gap lengths the critical radius increases.

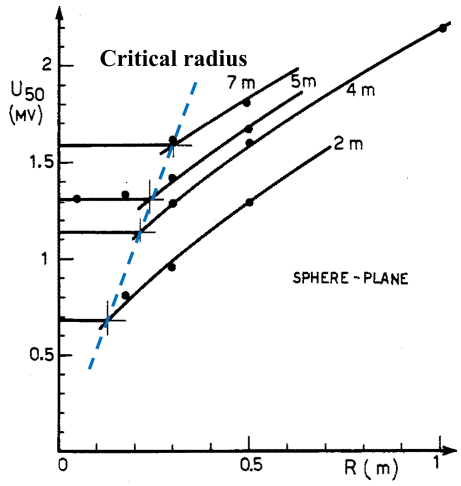

Figure 14.3: Influence of the radius of a spherical electrode under positive voltage on breakdown strength for different gap spacing. [7].

14.3. Conclusion

The insulation behavior of air depends on a number of factors; the type and polarity of the applied voltage, electric field distribution, gap length, and gas conditions. Especially for switching impulses, the electric field distribution and thus the electrode size are of great influence on the breakdown voltage. From Figures 14.2 and 14.3 it is clearly observed that the breakdown voltage of air increases with increasing electrode radius, which is due to the more homogeneous electric field and thus the lower field enhancement at large electrodes.

The IEC 60071-1 standard [32] gives minimal insulation distances for a rod-structure and conductor-structure and the Gap Factor method can be used to get an approximation of the insulation distances for other gap configurations. However, these do not take the electrode size into account. It is found that the electrode size is of great influence on the breakdown voltage and therefore it is questionable if the IEC 60071-1 tables and Gap Factor approach can be applied to compact substations with large electrode configurations.

In the following chapter an experiment will be described which is used to determine if the standard insulation distances do apply for compact substations with large electrodes.

15

Experiment: Insulation distance in compact substations

15.1. Introduction

The insulation distance between phases and ground and between opposite phases has a major influence on the size of a mobile substation when diploid and during transport [44]. To achieve a compact substation it is required to keep these distances as short as possible while still being safe and reliable.

TenneT has already developed compact and transportable air-insulated substations for 110 and 150 kV which are used for their Bay Replacement Program (BRP) as mentioned in Section 3.3.2. The substations contain a number of bays which comprise of transportable and preassembled sub-modules which are joined together as the bay is slid into place. The sub-modules, or skids, are built as compactly as possible (in comparison to existing bays), while still complying with the applicable safety and insulation standards.

The skids are designed to be compact to allow for transportation by road and to reduce the footprint in a substation. These design goals also apply to the mobile substation thus in this chapter the BRP skids will be used as a case study for the design of the insulation distances in compact air-insulated mobile substations. The mobile substation should have a nominal voltage of 380 kV on the high-voltage side. However, the BRP skids used as a case study in this experiment are designed for a nominal voltage of 110 and 150 kV, thus for this experiment, 150 kV will be considered as the nominal voltage.

In case the minimum clearances in a substation can not be tested, they are specified by the IEC 60071 standard [32] as discussed in Chapter 12. However, the electrode configurations on which the clearance tables are based may not be applicable to the compact substation configuration. The gap configurations in the standard are a rod-structure and a conductor-structure, which may not be representative of the large HV electrodes present on, for example, instrument transformers. Furthermore, the Gap Factor approach which according to the IEC 60071-2 standard [31] can be used to get an approximation of the insulation distance as is covered in Chapter 13 is only specified for a few standard electrode geometries. These standard geometries do not cater for the large electrodes associated with some equipment. Finally, the standards only consider the electrode geometry and gap length, not the electrode size, which is influencing the breakdown voltage as discussed in Chapter 14.

The combined current-voltage measurement transformers (CVT) (Figure 15.1) that are used in the BRP skids have a diameter of 75 cm and are thus relatively large electrodes which also forms the smallest clearance (dg) between phases in the bay. The insulation distances in the BRP skids are designed according to the IEC standard insulation distances which do not take the electrode size into account. Concerns have arisen if these standard insulation distances can be used for large electrodes in compact substations.

When air insulation is used for the mobile substation the same concerns as for the BRP insulation will apply to the mobile substation. There is a need to verify that the chosen clearances will be sufficient to withstand the anticipated overvoltage stresses. To address this issue, the experiment covered in this chapter aims to provide more insight into the dielectric strength of large electrodes with sharp points in compact substations and to verify if the insulation distances from the standards can be applied to this situation.

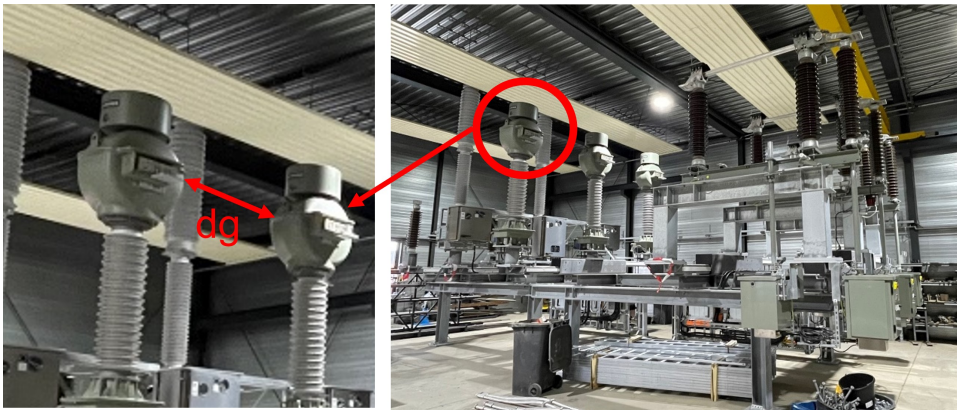

Figure 15.1: Current-voltage measurement transformer on 150 kV TenneT skid with dg the smallest clearance in the skid.

All types of overvoltages mentioned in Section 11.1 can occur in a substation. However, from experience, it is found that certain types of overvoltages are of more critical importance in certain voltage ranges. At present, the BRP skids are designed for 110 and 150 kV, and for these voltage levels only the withstand for lighting overvoltages and short-duration power-frequency overvoltages are specified in the IEC 60071-1 standard [32]. It is assumed that the standard rated short-duration power frequency or the standard rated lightning impulse withstand voltage should cover the required switching impulse withstand voltages. Thus for this experiment, only lightning overvoltages are considered.

15.2. Method

The goal of the experiment is to determine the dielectric behavior of large electrodes with small protrusions in a compact substation. For this experiment three different electrode configurations are used; a rod-rod gap, a sphere-sphere gap, and a gap with large spheres with small protrusions. The 50% breakdown voltage (U_{50}) for different gap lengths of these electrode configurations is determined in this experiment.

15.2.1. Electrode configurations

Three electrode configurations as shown in Figure 15.5 are designed to determine the U_{50} of these configurations.

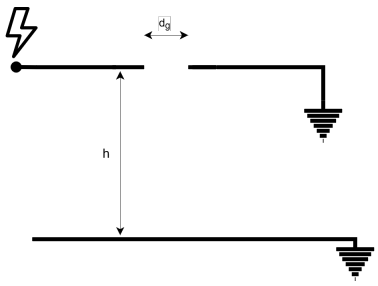

Figure 15.2: Rod-Rod test setup

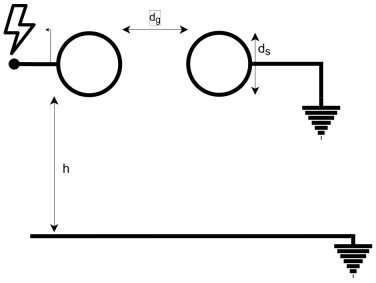

Figure 15.3: Sphere-Sphere test setup

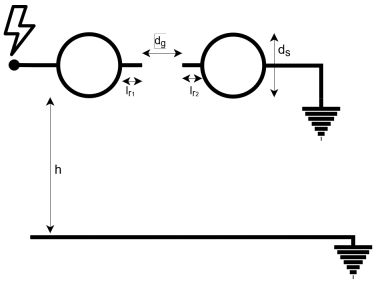

Figure 15.4: Combined configuration test setup

Figure 15.5

The first electrode configuration which is tested is a symmetric rod-rod gap as shown in figure 15.2, one of the rods is connected to the impulse generator while the other one is connected to ground. Special cylindrical rod tips with a blunt tip and a diameter of 1 cm are made for this test setup (Figure 15.7).
It is expected that this setup will have the lowest breakdown voltage due to the field enhancement at the tips of the rods. This setup is used to represent the extreme case where the breakdown is initiated by a non-uniform field.

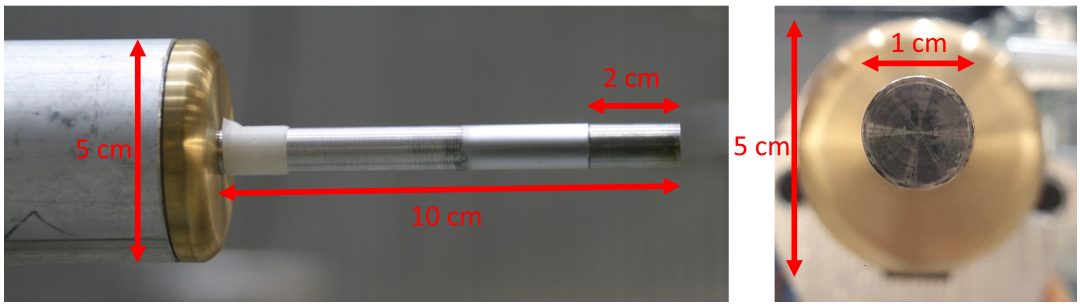

Figure 15.6: Tip of Rod-Rod configuration.

Figure 15.7: Tips that are used for the Rod-Rod setup, with labels for the earthed side and the high voltage side.

The second configuration is a sphere-sphere gap as shown in Figures 15.3 and 15.8. The spheres have a diameter of 50 cm to approximate the size of the CVTs (75 cm) which are used in the substations. The spheres have no sharp points or protrusions. This setup is used to represent a large smooth electrode. It is expected that the sphere-sphere gap will have the highest breakdown strength.

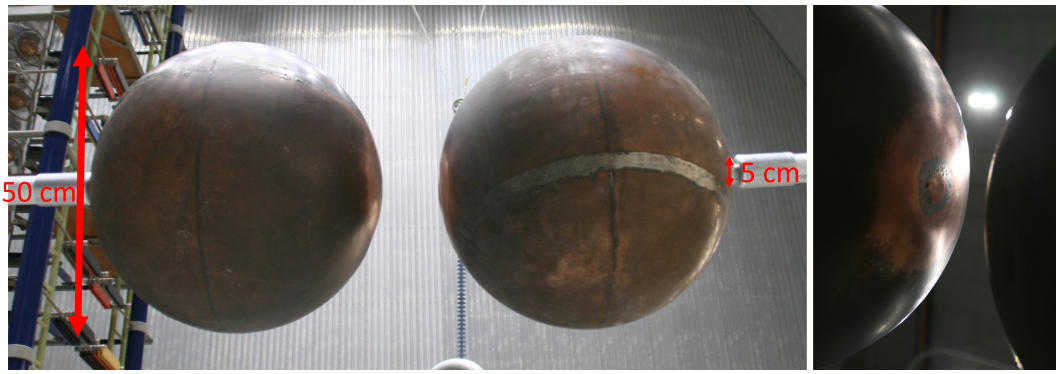

Figure 15.8: Sphere-Sphere gap with a sphere diameter of 50 cm

The third setup is a combination of the other two setups, a sphere-sphere configuration is used however now there are protrusions of 1 cm by 1 cm mounted on the spheres as shown in Figures 15.4 and 15.9. This setup should represent the CVTs as used in the substations (Figure 15.1), where the protrusions represent the rim of the CVTs. The same spheres are used as in the sphere-sphere configuration. The gap length (d_g) for this setup is defined between the protrusions as in Figure 15.4.

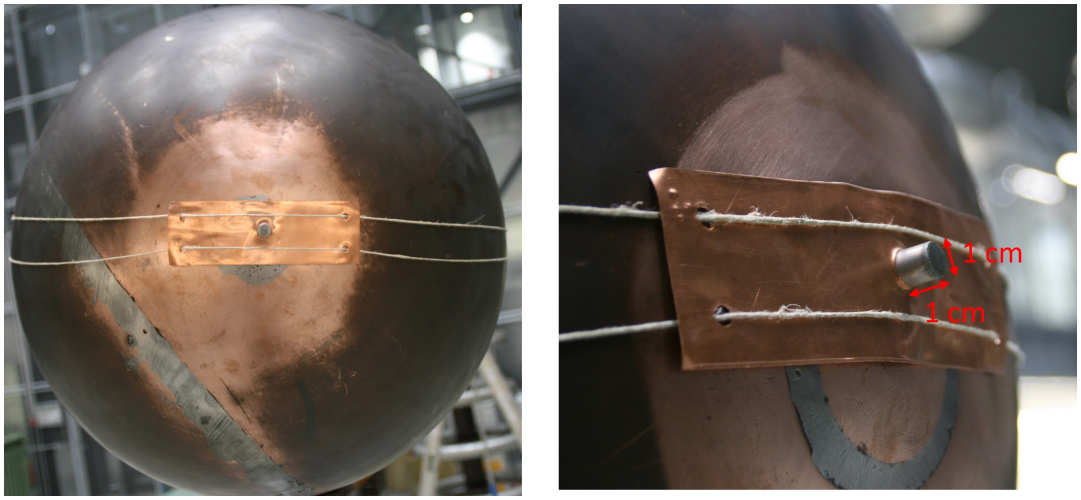

Figure 15.9: Protrusion of 1 by 1 cm mounted on 50 cm Sphere

15.2.2. Test setup

The setup as shown in Figure 15.10 is used for the experiments. A 1.20 m long aluminium tube with a diameter of 5 cm is mounted on a 2.65 m high insulator which can be moved on wheels. The length of the tube and height of the insulators are chosen to reduce the influence of the ground and the insulators on the electric field between the electrodes and prevent discharge to surrounding objects [39]. Different electrodes can be mounted on these aluminium tubes. The electrode on the right in Figure 15.10 is connected to the high-voltage impulse generator, and the electrode on the left is directly connected to ground.

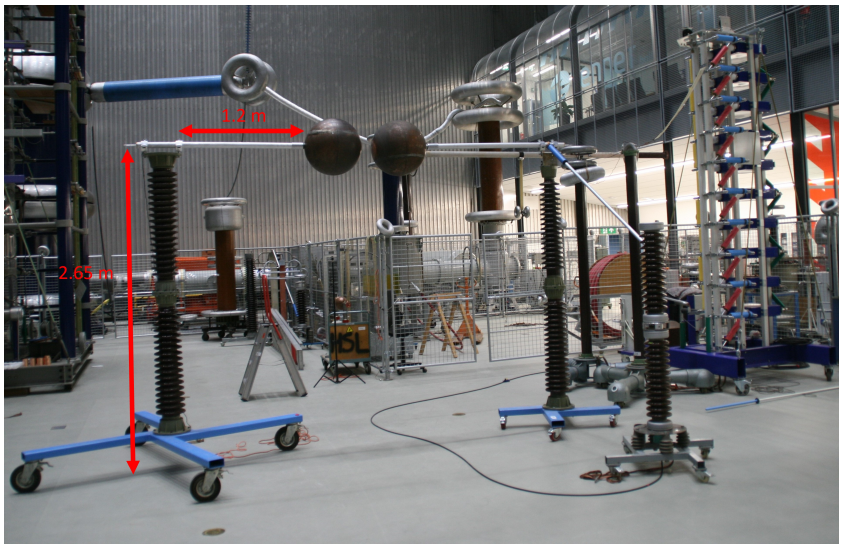

Figure 15.10: High voltage test setup with Sphere-Sphere electrodes

15.2.3. Marx generator

The breakdown tests are performed at the TU-Delft Electrical Sustainable Power Lab (ESP Lab). The standard lightning impulse is used according to the IEC 60060-1 [30]. Lightning impulses (LI) up to 430 kV are applied. The impulses are generated using a multi-stage Marx impulse generator (HAEFELY HIPOTRONICS: SGS 1000-50) with a maximum voltage of 1000 kV. The working principle of a Marx generator is explained in detail in Appendix C.

The values as mentioned in Figure 15.11 with n=10 stages are used in the Marx generator to generate the desired LI impulses. In Figure 15.12 the standard wave from IEC 60060-1, the calculated wave from the equations in Appendix C, and the measured wave are shown. From this figure it can be seen that the calculated wave closely resembles the standard wave, the measured wave deviates a little from the standard wave but complies with the tolerances from the standards; ±30% of the front time and less than ±5% for the overshoot. The expected efficiency of the impulse generator is 99.8% (Equation C.6), and the measured efficiency is 97%. The resistor of 100 Ω is added to the circuit as a damping resistance. A capacitive voltage divider is used to measure the voltage wave. The charging resistors R_c have a value of 4.8kΩ which is much larger than R_f and will thus not influence the output of the generator.

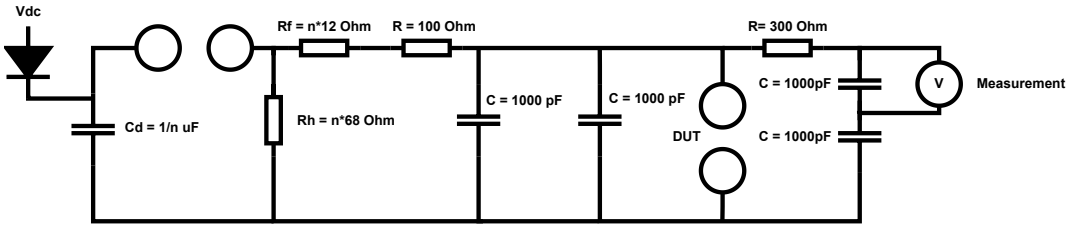

Figure 15.11: Equivalent circuit of the Marx generator used for this experiment, n=number of stages

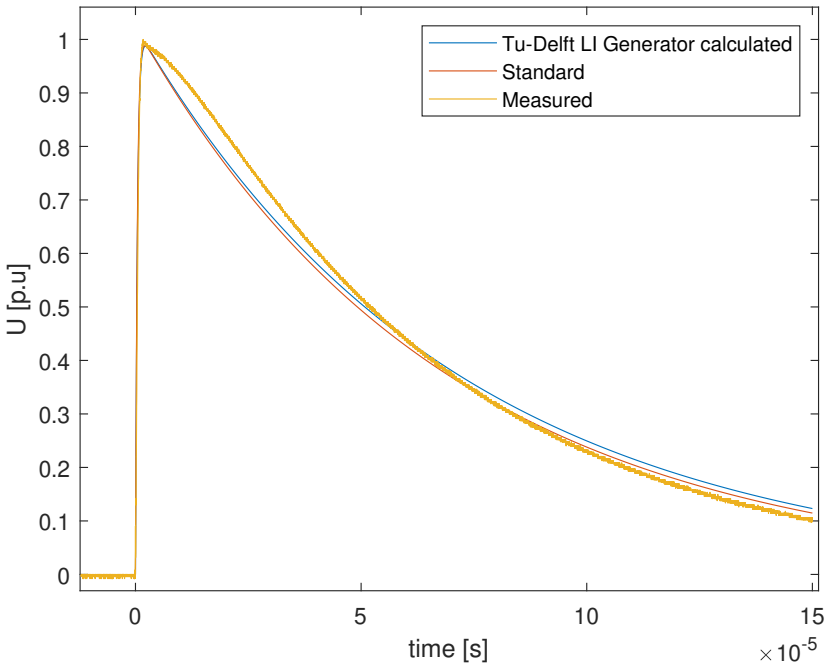

Figure 15.12: Lighting wave, standard, calculated and measured

From Figure 15.13a the rise time and time to half of the measured lighting wave are calculated to verify the settings of the LI impulse generator. The calculated rise time is 1.24 μs which is only a difference of 3.3% from the required 1.2 μs and thus lies inside the specified 30% tolerance. The time to half is 52 μs and thus with a difference of only 4% of the required 50 μs also inside the tolerance of 20%. In Figure 15.13b two

measured lightning impulses are shown, one with a breakdown and one with no breakdown, from the wave with a breakdown it can be seen that breakdown occurred on the tail.

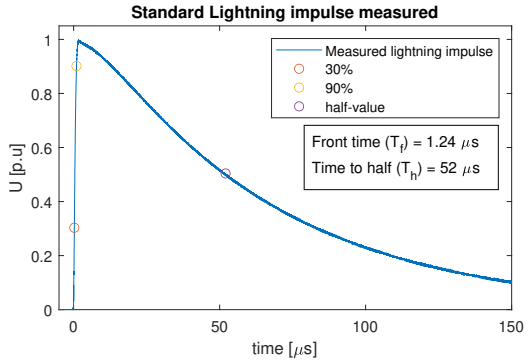

(a) Measured lightning impulse, with time to half and time to breakdown

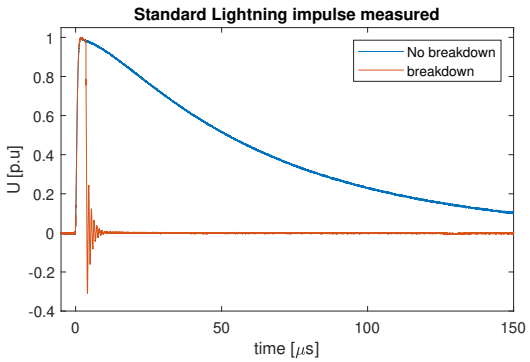

(b) Measured lightning impulse, with and without breakdown

Figure 15.13

15.3. Test Procedure

There are three methods that can be used to determine the U_{50} according to the IEC 60060-1 standard for this experiment two of these will be considered; the multiple-level method and the up-and-down method [30].

For the multiple-level test, a number of m different voltage levels are applied to the test object, with a difference between adjacent voltage levels being $\Delta U = U_{i+1}\text{-}U_i$ (i=1,2,...m). For all these voltage levels n_i impulses are applied. The number of disruptive discharges (k_i) which occur at each voltage level is recorded. For each voltage level (U_i) the discharge probability P_i can be estimated as the fraction of breakdowns observed $f_i = k_i / n_i$. This estimate gives a first approximation of the discharge probability function of the insulation [6]. A sufficiently long time Δt between two impulse applications should be used to guarantee independence between them. Values for $m \geq 5$, $n_i \geq 10$ for all i=1,2,...m and ΔU = (0.01 to 0.06)U_{50} should be used according to the IEC standard. Note that the U_{50} is not known thus for the choice of ΔU the expected U_{50} should be used. This method will give a good estimation of the U_{50} and U_{10} voltages and the standard deviation, however, this is a time-consuming method due to the number of impulses required.

For the second method, the up-and-down test m groups of n equal voltage stresses are applied at voltage levels U_i (i=1,2,...i). Depending on the result of the previous group of stresses the voltage level for the succeeding group is increased or decreased by a small amount ΔU. To find the U_{50} n is set to 1 and the procedure is as follows; The voltage level is increased by ΔU if a withstand occurs, otherwise, it is decreased by the same amount. This process will iterate to an average which is the U_{50} value. The test should start at a voltage close to the expected U_{50}. It is recommended to use at least 15 test impulse applications ($m \geq 15$) and ΔU = (0.01 to 0.03)U_{50}. It is again important to take a sufficiently long time Δt between two impulse applications to assure independence between measurements. The up-and-down method can be used for the same type of insulation as the multiple-level method. However, it is recommended only if one value for U_p is of interest, for example, U_{50} [6]. From this method, the breakdown probability can also be approximated by the discharge frequency $f_i = k_i / n_i$. This method gives a reasonable estimate of the U_{50} but not of the standard deviation however it is a much faster method because fewer impulse applications are required. Because time was limited in the High-Voltage laboratory it was decided to determine the U_{50} of the gap configurations for this experiment according to the up-and-down method.

The measurement is performed in two steps;

Step 1: Initialization

Before the Up-and-Down method can be used first a starting value for the U_{50} needs to be determined in the initialization phase. A guess of the U_{50} voltage is made based on literature and results from previous measurements. This voltage is used for the first impulse application. When breakdown occurs, the voltage is reduced by a large step; for example, 20% of the first application. If no breakdown occurs

at this new setting the voltage is increased by 10% of the previous setting. This is repeated until the steps become smaller than the minimum step size; ΔU = (0.01 to 0.03)U_{50}. The applied voltages during the larger steps are measured and noted however they are not used for the determination of the U_{50}. In Figure 15.14 this first step is shown with the impulses i=-7 to i=0, it can be seen that first three large steps are made, then some smaller steps are done to get to a new breakdown.

Step 2: Up-and-down method

Now the up-down method is used and the data is recorded as shown in Figure 15.14 starting with pulse i=1. After 20 impulse applications with a constant ΔU which lies in the range of (0.01 to 0.03)$U_{50,expected}$ the measurement is finished, and the U_{50} can be determined as explained in the following sections.

Figure 15.14 shows as an example the results of an up-and-down measurement for a 50 cm Rod-Rod gap configuration. The results of this measurement are also given in Table 15.1, the average charging voltage is 330 kV, note that this is not the U_{50}. The voltage measured with the capacitive divider will be lower as the charging voltage is reduced by the efficiency of the generator. The measured voltage needs to be referred to the standard atmospheric conditions, this will be covered in the next section.

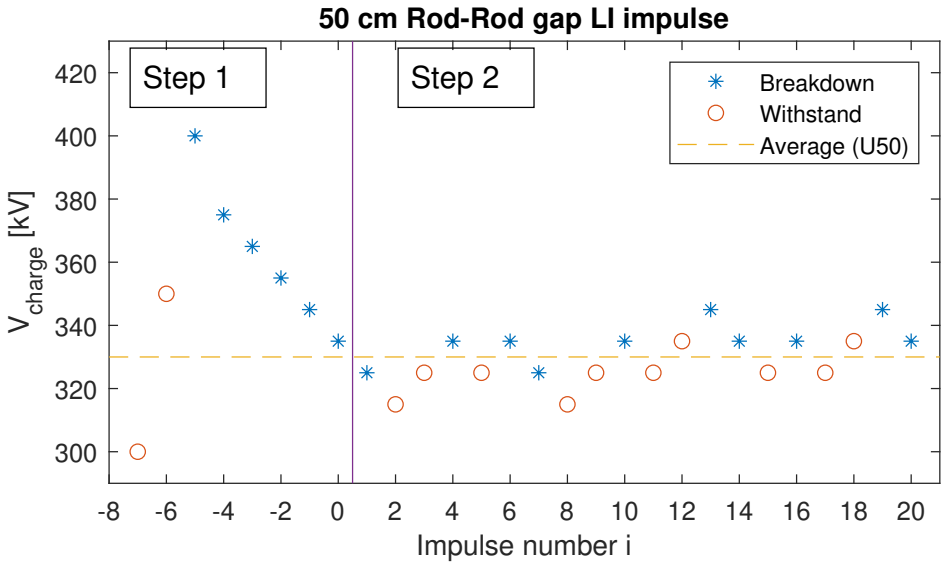

Figure 15.14: Results from the Up-and-down method for a 50 cm Rod-Rod gap with positive LI impulse

V_{charge} [kV]	Number of pulses: n	Number of breakdowns: k	Breakdown frequency: f
315	2	0	0.00
325	8	2	0.25
335	8	6	0.75
345	2	2	1.00
Total	20	10	

Table 15.1: Results from the Up-and-down method for a 50 cm Rod-Rod gap with positive LI impulse ΔU= 10 kV

15.4. Atmospheric correction factors

The atmospheric conditions have an influence on the breakdown behavior of high-voltage air insulation. The IEC 60060-1 [30] specified reference atmospheric conditions to which test results should be related. In the following section, the measurement data from the performed test will be converted to the value which would have been obtained at reference atmospheric conditions, to be able to compare the results to the standard insulation distances from the IEC600 71-1 [32].

The standard reference atmospheric conditions as specified by IEC 60060-1 [30] are:

- Temperature: T_0 = 20° C
- absolute air pressure: P_0 = 1013 hPa
- Absolute humidity: h_0 = 11 g/m^3

Equation 15.1 [30] is used to calculate the absolute humidity from the relative humidity R.

$$h = \frac{6.11 \cdot R \cdot e^{\frac{17.6 \cdot t}{243+t}}}{0.4615 \cdot (273+t)} \tag{15.1}$$

Equation 15.2 [30] gives the air density δ as a function of the reference and measured temperature and pressure.

$$\delta = \frac{p}{p_0} \cdot \frac{273+t_0}{273+t} \tag{15.2}$$

The breakdown process is affected by the humidity, and the type of test voltage, Equation 15.3 [30] gives a parameter K which is related to SI and LI impulse voltages.

$$k = 1 + 0.010 \cdot \left(\frac{h}{\delta} - 11\right) \qquad \text{for} \quad 1g/m^3 < h/\delta < 20g/m^3 \tag{15.3}$$

Two correction components: m and w need to be determined for this first a parameter g is calculated according to Equation 15.4 [30]. With U_{50} the measured or estimated 50 % breakdown voltage at the actual atmospheric conditions in kV (peak) and L the minimum discharge path. From the g value now an m and w can be found in Table 15.2.

$$g = \frac{U_{50}}{500 \cdot L \cdot \delta \cdot k} \tag{15.4}$$

g	m	w
<0.2	0	0
0.2 - 1.0	g(g - 0.2)/0.8	g(g - 0.2)/0.8
1.0 - 1.2	1.0	1.0
1.2 - 2.0	1.0	(2.2 - g)(2.0 - g)/0.8
>2.0	1.0	0

Table 15.2: Air density and humidity correction exponents m and w according to IEC60060-1 [30].

From the above-found parameters, an air density correction factor k_1 (Equation 15.5) and a humidity correction factor k_2 (Equation 15.6) can be determined. Together these two factors give the atmospheric correction factor K_t (Equation 15.7). Equation 15.8 is used to convert the measured voltages to the voltages at reference conditions.

$$k_1 = \delta^m \tag{15.5}$$

$$k_2 = k^w \tag{15.6}$$

$$K_t = k_1 \cdot k_2 \tag{15.7}$$

$$V_{corrected} = \frac{V_{measured}}{K_t} \tag{15.8}$$

15.5. Statistical analysis

When a test voltage is applied to a test object it can either withstand this voltage or a breakdown could occur. These events occur randomly, even if before each test the greatest care has been taken to ensure that all conditions are the same. Thus the reaction of the insulation to the test voltage can be described only in terms of probability and must be analyzed statistically [6]. For this analysis, it is assumed that there is a certain discharge probability P(U) which depends on the characteristics of the test voltage. From tests with the same voltage shape and different peak values denoted with U, a discharge probability can be determined which ranges from zero to one. For most insulation types the discharge probability increases with an increasing peak voltage as shown with line A in Figure 15.15. However, in some cases more than one discharge mechanism is effective and for a particular voltage range, the discharge probability may even be decreasing with voltage for example due to dependence on the steepness of the wavefront (Figure 15.15:B) [6]. The steepens changes when the crest value is changed due to the constant rise time. For the slower wavefront leader discharge takes place, when the steepens increases streamer discharge will occur.

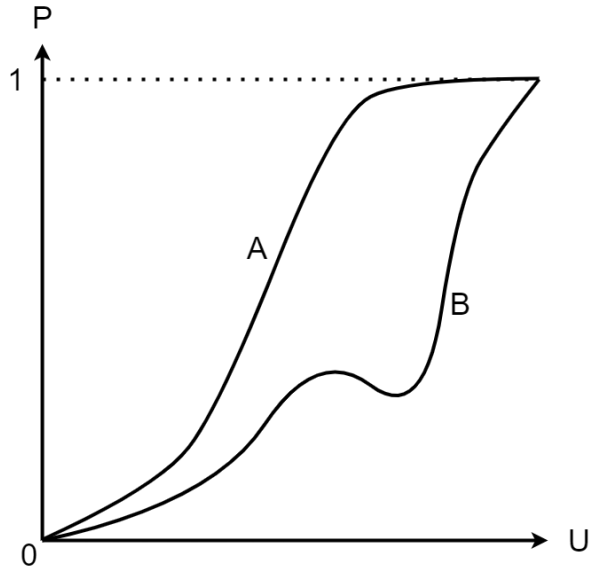

Figure 15.15: Shape of breakdown probability.
A: Commonly encountered shape where P monotonously increases with peak voltage U.
B: The shape of a particular dependence of the breakdown mechanism on the steepness of the wavefront.

A number of theoretical distributions can be applied to fit to the measurement data for example the normal, Gumbel, and Weibull distributions [79]. The cumulative normal distribution function is often used to relate the breakdown voltage to breakdown probability in air insulation [6] [5]. The normal distribution is also called the Gaussian distribution. The cumulative normal distribution is given in Equation 15.9.

$$P = \frac{1}{\sqrt{2\pi Z}} \int_{-\infty}^{X} \left(e^{-\frac{(y-U_{50})^2}{Z^2}} \right) dy \tag{15.9}$$

The U_{50} is the scale parameter that is equal to the mean value, the mode, and the median. The Z is equivalent to the standard deviation and is defined as $Z=U_{50}-U_{16}$. This mathematical expression can only be used if it has a sufficient good fitting to the measurement data. Note that there is neither physical nor statistical support for the use of the Gaussian distribution and it is only used because it gives the best fit to the measurement data [6].

15.5.1. Maximum likelihood method

The next step is to find the U_{50} and Z values which give the best fit to the flashover probabilities determined during the test. For this, the maximum likelihood method (MLM) will be used. The MLM is a method to estimate the parameters of an assumed distribution, in this case, the normal distribution, given some observed data; the measurement data. This is done by maximizing a likelihood function so that under the assumed

statistical model the observed data is most probable. The MLM has the advantage that no assumptions have to be made as is required [5].

The measurement data consist of m voltage levels (U_i, (i=1,2..,m)), with n_i pulses which give k_i breakdowns at the ith voltage level U_i. The probability to get precise k_i breakdowns out of n_i impulse applications when P_i is the true breakdown probability is given by Equation 15.10, which is a binomial distribution. Where P_i is the normal distribution at U_i (Equation 15.9). In other words, the binomial distribution as given in Equation 15.10 gives the likelihood that the normal distribution represents the measurements, the better the normal distribution approaches the measurements the higher F will be.

$$F(k_i, n_i, p_i) = \left(\frac{n_i!}{k_i!(n_i - k_i)!} \right) p^{k_i} (1 - p_i)^{n_i - k_i} \tag{15.10}$$

It is assumed that the events are statically independent and thus the probability of getting exactly k_m breakdowns in n_m voltage applications is the product of the different probabilities as represented in Equation 15.11.

$$L = \prod_{i=1}^{m} F(k_i, n_i, p_i) \tag{15.11}$$

Since F is nonnegative, and since it is easier to deal with a summation instead of a product, the logarithm of F is used as in Equation 15.12.

$$L_{log} = log \left(\sum_{i=1}^{m} F(k_i, n_i, p_i) \right) \tag{15.12}$$

The cumulative normal distribution P_i is a function of two statistical parameters, U_{50} and Z. By maximizing the likelihood function with respect to the U_{50} and Z value using a computer software tool such as Python, Matlab, or excel the most likely U_{50} and Z values are found. At the start of the maximization an initial guess for U_{50} and Z is made, and the likelihood is calculated. From here on the optimization algorithm optimizes U_{50} and Z to the most likely solution. As an initial guess the following values are used:

$$< U_{50} >= \frac{1}{m} \sum_{i=1}^{m} V_i \tag{15.13}$$

$$< Z >= 0.03 V_{50} \tag{15.14}$$

From the example of the 50 cm rod-rod gap with positive LI impulse in Section 15.3 the results mentioned in Table 15.3 are found. When L_{log} is maximized, U_{50} is found to be 320.5 kV, with a standard deviation Z of 6.2 kV which is equivalent to 1.9%. Figure 15.16 shows the fitted normal distribution and the breakdown frequency (k_i/n_i). From this figure, it can be seen that the fitted normal distribution closely resembles the measurement data.

Charging voltage	Measured peak voltage	Voltage converted to ambient conditions	Number of pulses	Number of breakdowns	Breakdown frequency	Normal	Optimization: binomial (log)
V_{charge} [kV]	V_{peak} [kV]	$V_{converted}$ [kV]	n	k	f		
315.0	303.6	306.7	2	0	0.00	0.013	-0.027
325.0	312.7	316.0	8	2	0.25	0.236	-1.171
335.0	321.5	324.9	8	6	0.75	0.763	-1.170
345.0	331.8	335.2	2	2	1.00	0.991	-0.017
Total			20	10			-2.385

Table 15.3: Results from the Up-and-down method for a 50 cm Rod-Rod gap with positive LI impulse ΔU= 10 kV

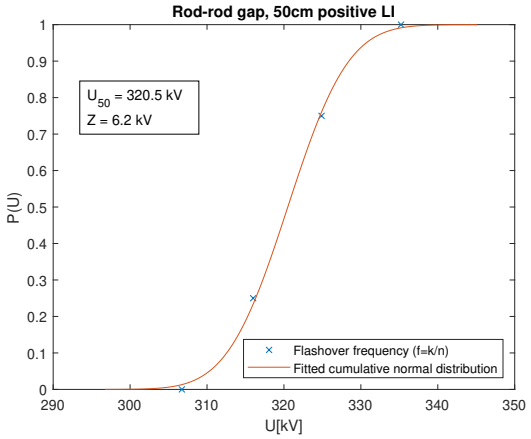

Figure 15.16: Fitted normal distribution for a 50 cm rod-rod gap with positive lightning impulse

15.6. Test results

To be able to compare the different electrode configurations as mentioned in Section 15.2.2, for each electrode configuration measurements are performed for a number of different gap lengths. The gap lengths are chosen such that the voltage ranges for the three setups are all between 150 and 400 kV. This voltage range is chosen because it makes it possible to compare the different electrode configurations. The maximum voltage is limited by the measurement range of the used voltage divider.

A picture is taken from the gap every time an impulse is applied, to verify in case of a breakdown that it occurred between the expected points in the gap. An example of such a photo is given in Figure 15.17. An overlay of eight pictures of breakdowns with a positive lightning pulse on a rod-rod gap of 50 cm is shown in Figure 15.18. The photographs are assessed manually and it can be seen that all paths are different but they all start and end at the points of the rods. From the pictures which are taken it is found that all breakdowns occurred between the expected points in the gap.

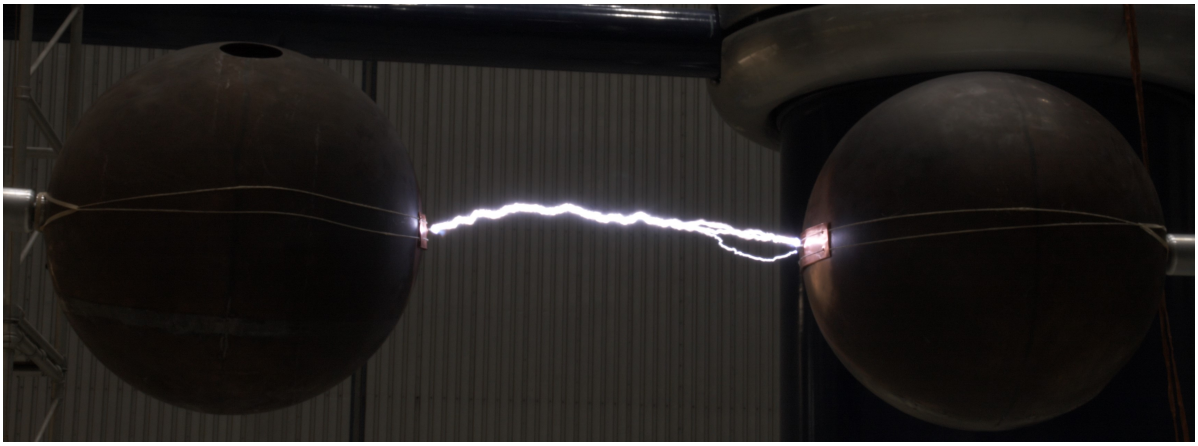

Figure 15.17: Photo from a breakdown in a 50 cm Sphere-Sphere gap with a 1 by 1 cm protrusion on both spheres.

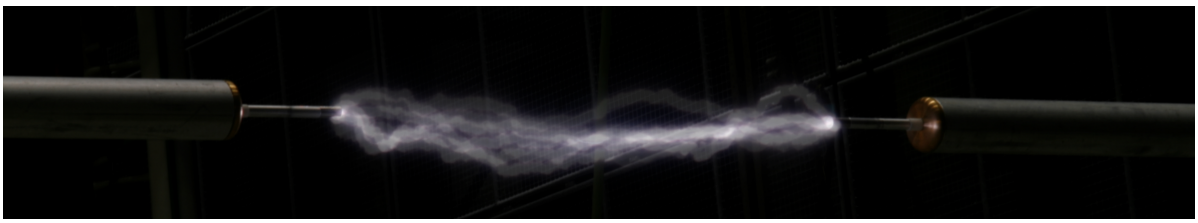

Figure 15.18: Combination of 8 breakdowns between a 50 cm rod-rod gap

During the measurements in the HV lab, a digital "UNI-T UT330C" data logger is used to continuously measure the Temperature, absolute air pressure, and relative humidity. For every measurement (one gap length of an electrode configuration), an average over the test duration (1 hour) of these values is used to convert the measurement data to the reference conditions.

15.7. Determined breakdown strengths of gap configurations

15.7.1. Sphere-Sphere gap

The U_{50} for the sphere-sphere gap is determined for three gap lengths; 7.1, 9.6, and 15.1 cm, the results are shown in Table 15.4. Only three different gap lengths are used because of the linear relation of the U_{50} and gap length for sphere-sphere gaps on these short distances due to the almost homogeneous electric field [39]. From Figure 15.19a it can be seen that for these short gaps the U_{50} values for positive and negative impulses are almost equal. The 95% confidence interval as shown with the vertical bars in the figures is small. The U_{50} per meter gap length is given in Figure 15.19b.

Sphere-sphere (diameter: 50 cm)					**Lighting impulse**		
Polarity (+/-)	Length [cm]	datum	temp [°C]	pressure [mbar]	humidity [%]	U_{50} [kV]	U_{50}/m [kV]
+	7,1	22-6-2022	22,7	1014,6	52,5	191,6	2699,2
+	9,6	22-6-2022	22,7	1014,6	52,5	249,7	2601,4
+	15,1	21-6-2022	22,1	1017,1	51,8	386,3	2558,3
-	7,1	22-6-2022	22,7	1014,6	52,5	191,5	2697,0
-	9,6	22-6-2022	22,7	1014,6	52,5	250,3	2607,3
-	15,1	21-6-2022	22,1	1017,1	51,8	373,4	2473,0

Table 15.4: Measurement results for the sphere-sphere gap (diameter: 50 cm)

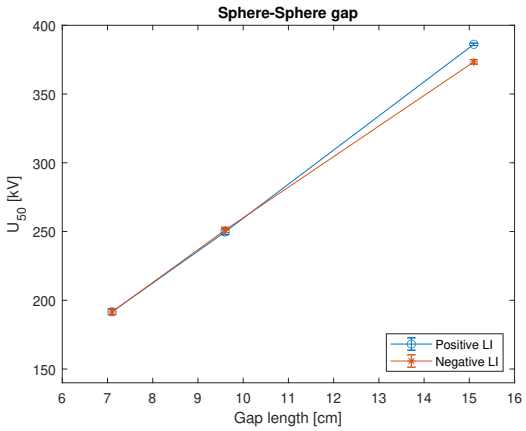

(a) Measurement results for a sphere-sphere gap (diameter: 50 cm), with 95% confidence intervals

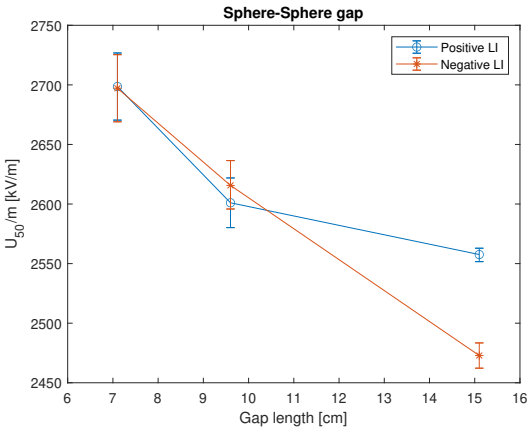

(b) Measurement results for a sphere-sphere gap (diameter: 50 cm), with 95% confidence intervals

Figure 15.19

15.7.2. Rod-Rod gap

For the rod-rod gap, the U_{50} for five different gap lengths and both positive and negative lighting impulse voltages are determined, and the results are shown in Table 15.5. The results are plotted in Figure 15.20a. In contrast to the sphere-sphere gap, a clear difference can be observed between the U_{50} for positive and negative impulse voltages, where the negative impulse results in a higher U_{50} for the larger gaps.

Rod-rod			**Lighting impulse**				
Polarity (+/-)	Length [cm]	datum	temp [°C]	pressure [mbar]	humidity [%]	U_{50} [kV]	U_{50}/m [kV]
+	20	20-6-2022	22,0	1018,0	45,0	183,4	917,1
+	25	21-6-2022	22,1	1017,1	51,8	195,6	782,6
+	30	21-6-2022	22,1	1017,1	51,8	208,5	695,0
+	40	20-6-2022	22,0	1018,0	45,0	261,0	652,5
+	50	21-6-2022	22,1	1017,1	51,8	320,5	640,9
-	20	21-6-2022	22,1	1017,1	51,8	171,4	857,2
-	25	21-6-2022	22,1	1017,1	51,8	227,7	910,9
-	30	21-6-2022	22,1	1017,1	51,8	291,0	970,0
-	40	20-6-2022	22,0	1018,0	45,0	373,6	934,1
-	50	21-6-2022	22,1	1017,1	51,8	413,1	826,2

Table 15.5: Measurement results for the rod-rod gap

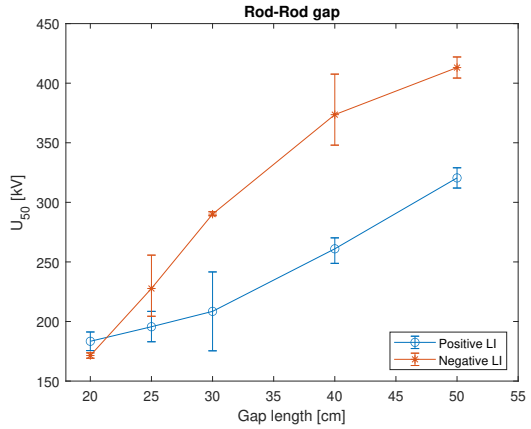

(a) Measurement results for Rod-Rod gap, with reference [24], with 95% confidence intervals

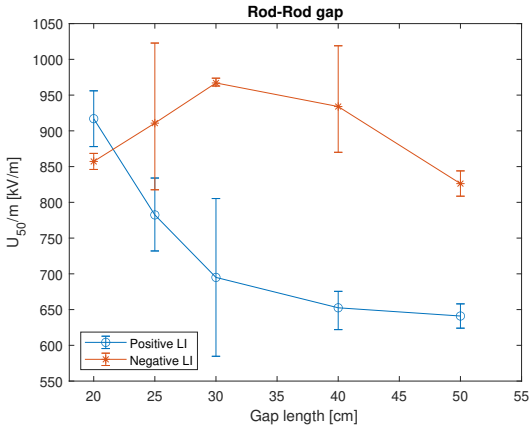

(b) Measurement results for Rod-Rod gap, with reference [24], with 95% confidence intervals

Figure 15.20

15.7.3. Spheres with protrusion

The last electrode geometry for which the U_{50} is determined are the spheres with a protrusion as shown in Figure 15.9. These electrodes should mimic the large CVTs which are used on the compact substations (Figure 15.1). The measurement results are shown in Table 15.6, and a graphical plot is shown in Figures 15.21a and 15.21b. From Figure 15.21a it can be concluded that for gaps with a length between 15 and 50 cm both for positive and negative impulse voltages the U_{50} as a function of gap length shows a linear trend. The U_{50} for a negative impulse voltage is higher compared to that for a positive lightning impulse.

Spheres with protrusion			**Lighting impulse**				
Polarity (+/-)	Length [cm]	datum	temp [°C]	pressure [mbar]	humidity [%]	U_{50} [kV]	U_{50}/m [kV]
+	15,34	22-6-2022	22,7	1014,6	52,5	153,0	997,1
+	20	23-6-2022	22,8	1012,1	58,5	177,6	887,9
+	25	23-6-2022	22,8	1012,1	58,5	183,6	734,6
+	30	23-6-2022	22,8	1012,1	58,5	210,7	702,2
+	40	23-6-2022	22,8	1012,1	58,5	261,6	654,1
+	50	22-6-2022	22,7	1014,6	52,5	312,1	624,3
-	15,34	22-6-2022	22,7	1014,6	52,5	151,0	984,2
-	20	23-6-2022	22,8	1012,1	58,5	186,3	931,6
-	25	23-6-2022	22,8	1012,1	58,5	228,1	912,5
-	30	23-6-2022	22,8	1012,1	58,5	258,4	861,3
-	40	23-6-2022	22,8	1012,1	58,5	327,3	818,4
-	50	23-6-2022	22,8	1012,1	58,5	394,0	788,0

Table 15.6: Measurement results for the Sphere-Sphere gap (diameter: 50cm) with 1x1cm cylindrical protrusions

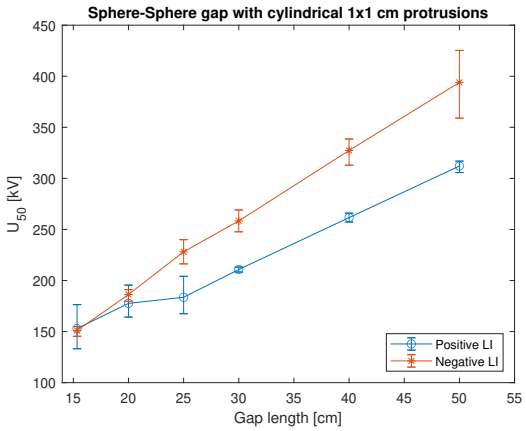

(a) Measurement results for Sphere-Sphere gap (diameter: 50cm) with 1x1cm cylindrical protrusions, with 95% confidence intervals

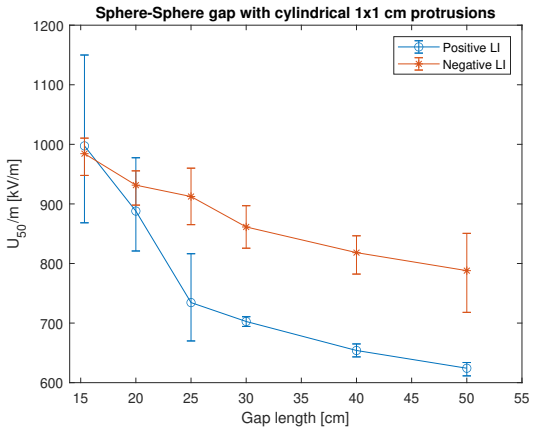

(b) Measurement results for Sphere-Sphere gap (diameter: 50cm) with 1x1cm cylindrical protrusions, with 95% confidence intervals

Figure 15.21

15.8. Discussion

The goal of the experiment is to determine how the U_{50} of a large electrode with a small protrusion is related to the gap length and how this can be compared to other electrode geometries.

The electrodes used in this experiment were not perfectly identical, the spheres for example have some dents and have been repaired before. The protrusions on the spheres for the sphere with protrusion configuration from Section 15.7.3 are mounted on the spheres with a copper plate (Figure 15.9), this copper plate has sharp edges and has not a 100% connection with the spheres. However, from the photos taken of every breakdown, it is found that all breakdowns started and ended at the point of the protrusions, and thus it is assumed that these sharp points did not have a considerable influence on the breakdown behavior.

Sphere-Sphere gap

From Figure 15.22a it can be seen that for the sphere-sphere gap with these short gaps the positive and negative U_{50} amplitudes are almost equal and comply with the reference data from the literature [39]. The small difference between the positive and negative U_{50} at 15.1 cm can be caused by some measurement uncertainty or due to the fact that the two spheres are not perfectly identical. However, it is only a small difference and is still close to the reference data [39].

Rod-Rod gap

For the rod-rod gap, the positive and negative U_{50} from literature [24] are plotted in Figure 15.22b to validate the measurement results. It can be seen that the determined values are close to the reference data and the same difference between positive and negative impulse voltage can be observed. The differences between the measurements and the reference data are caused by the fact that for the reference data 3.18 cm square rod electrodes are used [24], while for the measurements 1 cm diameter round electrode tips are used (Figure 15.7).

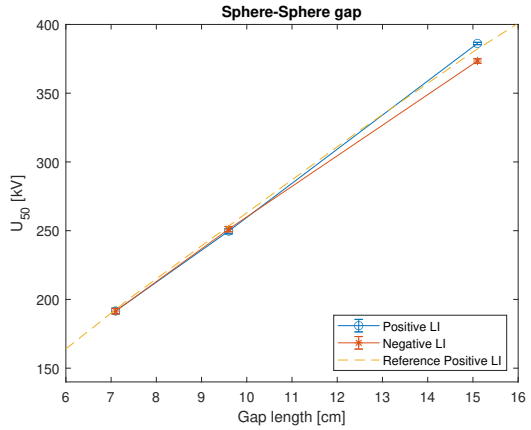

(a) Measurement results for a sphere-sphere gap, with a sphere diameter of 50 cm, with reference [39], with 95% confidence intervals

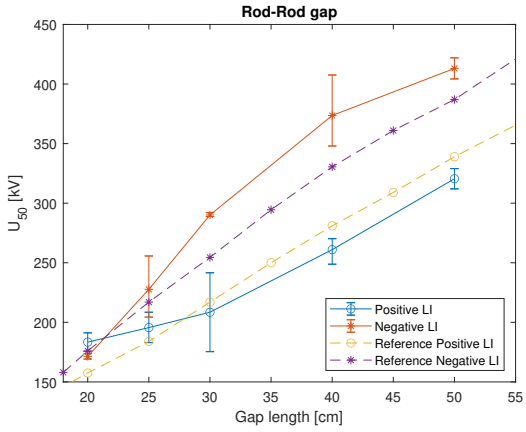

(b) Measurement results for Rod-Rod gap, with reference [24], with 95% confidence intervals

Figure 15.22

In Figure 15.23a the measurement results for the three different electrode configurations are shown in one figure. From this figure, it can be seen that the sphere-sphere gaps have a much higher breakdown voltage compared to the rod-rod gap and the spheres with protrusions which have quite similar breakdown voltages.

In the ideal case the horizontal rod-rod gap and the spheres with protrusions, when tested in isolation would be symmetrical gaps. In a symmetrical gap, the electric field strength is equal at the positive and negative electrode and breakdown develops at the same applied voltage irrespective of the polarity applied. Thus the breakdown voltage would be the same for positive and negative lightning impulses. However, in practical test setups, nearby ground planes and a non-symmetrical lead setup introduce asymmetry in the electric fields at the electrodes which result in a difference between the positive and negative breakdown voltages. Applying a negative impulse to the electrode that has the highest electric field will therefore result in a higher breakdown voltage than when a positive polarity impulse is applied. This can also be found from our results

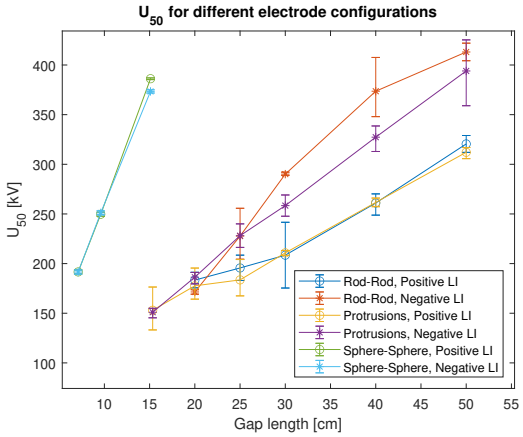

(a) Measurement results for the three different electrode geometries, with 95% confidence intervals

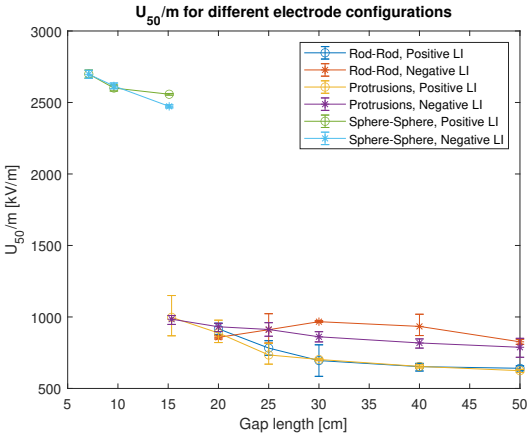

(b) Measurement results for the three different electrode geometries, with 95% confidence intervals

Figure 15.23

in Figure 15.24a, where for positive and negative impulse voltages a large difference in breakdown voltage is found, up to 100 kV for the 50 cm gaps. When the gap distance is small compared to the overall electrode size, the electric field in the gap tends to be more symmetrical. This is also shown in Figure 15.24a, where it can be seen that for the 15 and 20 cm gaps the positive and negative impulses resulted in similar breakdown voltages. This asymmetry should be verified by electric-field calculations in a future study.

From Figure 15.24a it can be seen that for the positive lightning impulse the breakdown voltages for the rod-rod gap and the spheres with protrusions are almost identical. Only small differences can be observed, however, they lay within each other's 95% confidence interval.

In the same figure, it is shown that for the negative lightning impulse the U_{50} of the spheres with protrusions even lies below that of the rod-rod gap. It was expected that the rod-rod gap would result in a lower breakdown voltage compared to the large spheres with small protrusions. The lower breakdown voltage for the spheres with protrusions could possibly be explained by the fact that the presence of the spheres tends to make the electric field in the gap more symmetrical, as it is a large electrode that will dominate the electric field more than the ground plane and the perpendicular running earth lead. Due to this symmetry breakdown will develop from both sides of the gap and thus positive and negative breakdown strengths will be closer together. Because positive breakdown starts at a lower voltage the breakdown voltage is lower. This should be verified by electric-field calculations in a future study.

From the above observations, it can be concluded that for large electrodes with a small protrusion the insulation distance is greatly reduced compared to a sphere-sphere gap configuration and that it behaves more like a rod-rod gap.

An important question is if the insulation distances mentioned in the IEC 60071-1 [32] can be used to determine the insulation distances for compact substations with large high-voltage electrodes. In Table 12.1, the withstand voltages are given for different insulation distances. The withstand voltage is specified as the 90% withstand probability which is equivalent to the U_{10} voltage. To compare the standard to the determined U_{50} the U_{10} needs to be converted to U_{50}. Equation 15.15 gives the relation between the U_{50} and the U_{10}. The recommended standard deviation from the IEC 60071-2 [31] is 3% for lightning impulses and the standard deviation is given by Equation 15.16. Equation 15.17 gives the U_{50} values for the gap lengths in Table 12.1.

$$U_{10} = U_{50} - 1.3Z \quad [kV] \tag{15.15}$$

$$Z = 0.03 \cdot U_{50} \qquad \text{For lightning impulses} \tag{15.16}$$

$$U_{50} = \frac{U_{10}}{1 - 1.3 \cdot 0.03} \quad [kV] \tag{15.17}$$

The calculated U_{50} values from Table 12.1 for the rod-structure gap are plotted in Figures 15.25a and 15.25b. It can be seen that the U_{50} for the large spheres with protrusions lies above the rod-structure U_{50} from the IEC

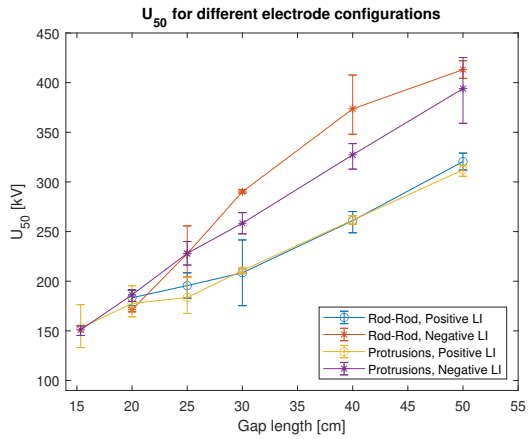

(a) Measurement results for the two different electrode geometries, with 95% confidence intervals

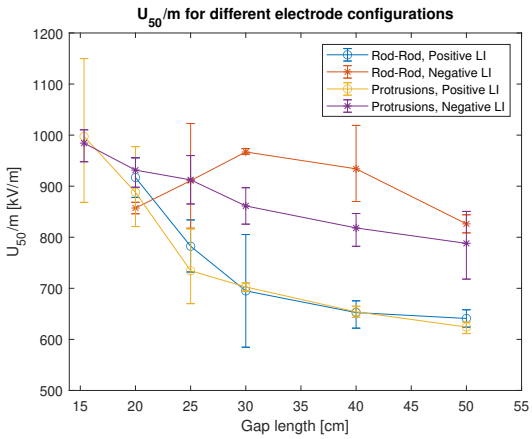

(b) Measurement results for the two different electrode geometries, with 95% confidence intervals

Figure 15.24

standard. Thus by using the standard values the insulation distances between large high-voltage components with small protrusions will be sufficient.

In the current design of the BRP skids, the insulation distance is determined according to the specified rod-structure gap from the IEC 60071-1 [32]. The large CVT's will probably form the shortest distance in the skid as shown in Figure 13.2. The determined U_{50} values for the spheres with protrusions which represent these CVT's lays above the U_{50} for the Rod-structure and thus it can be considered to even use shorter insulation distances in the mobile substations. However, it should then be shown by test on an actual skid that the insulation is indeed sufficient.

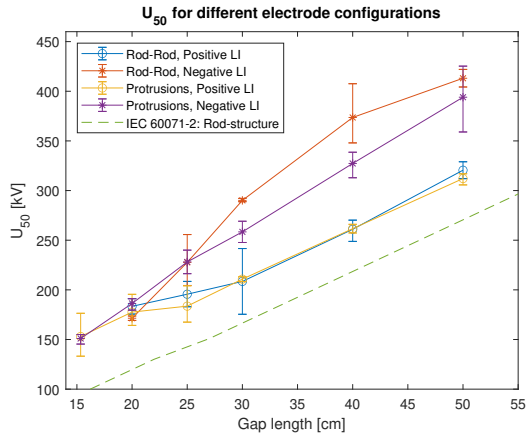

(a) Measurement results for the two different electrode geometries compared to the IEC60071-1 standard [32], with 95% confidence intervals

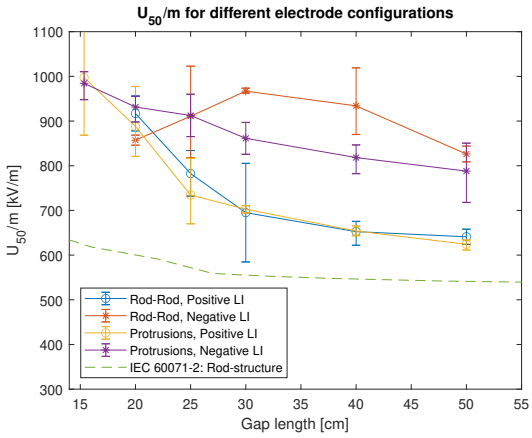

(b) Measurement results for the two different electrode geometries compared to the IEC60071-1 standard [32], with 95% confidence intervals

Figure 15.25

15.9. Future work

In a future study the experiment could be extended with the following points;

- The test should be extended to also cover gap lengths with a withstand voltage in the order of 750 kV which is the highest lightning overvoltage considered by the IEC 60071-1 [32] for a 150 kV substation, giving more insight into the actual insulation distances for a 150 kV substation.
- In this experiment the BRP skids with a nominal voltage of 150 kV are used as a case study. In a future study, there should also be looked at the possibility to use air-insulation for the 220 and 380 kV in the mobile substations.
- Tests should also be performed to characterize the strength of the gap under switching impulses. Switching impulses are typically not considered for systems with a nominal voltage of 110 and 150 kV. However from literature, it is known that switching impulses will result in lower U_{50} values, and also the electrode geometries are of a larger influence on the breakdown voltage with switching impulse due to the leader discharge [71].
- For the tests performed as part of this thesis, a test setup is used to mimic the large CVTs in a compact substation. To prove that the determined breakdown distances also apply in an actual substation the breakdown voltages of an actual mobile skid should be tested. When the BRP skids from TenneT are used for this test it is possible to test the U_{50} for different gap lengths because the different phases can be moved closer to each other in the skid. From these tests, it would be possible to determine exactly how compact a substation can be made.
- In the experiment it is found that in a gap which is assumed to be symmetrical there is a difference between the positive and negative breakdown voltages when the gap length becomes larger. Electric-field calculations should be performed for the rod-rod gap and the spheres with protrusions to investigate the reason for the different breakdown voltages.
- For the experiment a sphere with protrusion is used to mimic the large CVT's from the compact substation. The breakdown strength of the actual CVT geometry should be tested to determine if this configuration is a good representation of the CVT.

15.10. Conclusion

The goal of the experiment is to provide more insight into the dielectric strength of large electrodes with sharp points in compact substations and to verify if the standard insulation distances can be applied to this situation. It is determined how the U_{50} of a large electrode with a small protrusion is related to the gap length and how this can be compared to other electrode geometries.

The breakdown voltage of three electrode configurations is determined; a sphere-sphere gap, rod-rod gap, and a sphere-sphere gap with 1x1 cm protrusions. It is found that the sphere-sphere gaps have a much higher breakdown voltage compared to the other two gaps. The rod-rod gap and the spheres with protrusions have similar breakdown voltages. From this observation, it is concluded that even for large electrodes with a small protrusion the insulation distance is greatly reduced compared to a sphere-sphere configuration and that it behaves more like a rod-rod gap.

When the U_{50} values from the IEC 60071-1 [32] for the rod-structure gap are compared to the determined breakdown voltages for the spheres with protrusions it is found that the U_{50} for the large spheres with protrusions lies above the rod-structure U_{50} from the IEC standard. Thus by using the standard values to determine the insulation distances between large high voltage components in a mobile substation the insulation will be sufficient.

In the current design of the BRP skids, the insulation distance is determined according to the specified rod-structure gap from the IEC 60071-1 [32]. The large CVT's will probably form the shortest distance in the skid (Figure 13.2). Because the determined U_{50} values for the sphere with protrusions lay above the U_{50} for the Rod-structure it can be considered to even use shorter insulation distances in the mobile substations. When shorter insulation distances can be used the substation can be made more compact. However, it should then be shown by test on an actual skid that the insulation is indeed sufficient.

16

Conclusion

The energy transition requires massive expansion and reinforcement of the transmission grid. Extending and reinforcing the grid is a challenge because it requires additional planned outages which must be planned alongside regular maintenance, replacement, and repair. The high utilization of the Dutch grid makes this planning problem even more difficult.

This master thesis investigated the important design aspects for a mobile high-voltage substation to (partly) bypass a TenneT substation during maintenance, replacement, and expansion projects to reduce/prevent planned outages, this objective is partially met. The general conclusions are:

- When a mobile substation is used to bypass a 380 kV or 220 kV substation it would be possible to perform maintenance on multiple 380 kV or 220 kV substations at the same time. It would also make it easier to get planned outage (VNB) permits for projects in the 150 kV and 110 kV networks. This would increase the efficiency of maintenance replacement and expansion projects in the entire grid. (Chapter 4)
- In a case study it is found that TenneT can potentially save a few hundred million euros every year and reduce its CO_2 footprint when mobile substations are used. It is not determined what the investment and operational costs of the mobile substation will be and thus these savings are not net savings. (Chapter 4)

Specific conclusions

Part I: Mobile power transformers

- A shell-type transformer will be the most optimal transformer for a mobile substation because of its compact design and its high mechanical strength which makes it resistant to the influences of transportation. (Section 8.2)
- High-temperature hybrid insulation should be used to make the transformers more compact. (Section 7.2)
- Six single-phase shell-type transformers, with 83.33 MVA rating will be required to bypass a 500 MVA conventional substation transformer. The mobile transformers will have an approximate volume of 42 m^3 and a weight of 36 tonne (without oil). This would fit the dutch road size and weight limits. (Section 8.7)
- The six single-phase transformers should be connected as two parallel banks to create redundancy in the mobile substation (Figure 8.6). An additional benefit is that the mobile substation now also can be used with half its capacity (250 MVA) if this is desired. A downside to this configuration is the fact that it requires a longer installation time and most likely more space. (Section 8.4)

Part II: High voltage insulation distances

- For the mobile substation Gas-Insulated Switchgear (GIS) or Air-Insulated Switchgear (AIS) could be used, GIS is more compact but much more expensive and as long as SF_6 is used as insulating gas it also possesses a great risk for the environment. According to the policy of TenneT GIS should only be used when AIS is not possible and thus there is a need for developing a viable compact air-insulated mobile substation concept. (Chapter 10)

- The size of an air-insulated mobile substation when deployed will mainly be determined by the electrical clearances of the high-voltage parts. The specified insulation distances from the IEC 60071-1 standard for insulation coordination are based on a rod-structure and conductor-structure gap configuration which is possibly not representative of the large electrodes found in compact substations. (Section 11)
- It is also possible to estimate the insulation distance by calculations using the Gap Factor. However, the Gap Factor is only specified for a few standard gap configurations which do not always match actual substation configurations. The Gap Factor is also not defined for gaps below 1 m and does not consider the electrode size. It is, therefore, questionable if the gap factor approach can be applied to compact substations with large electrode configurations. (Chapter 13)

An experiment was performed to determine how the 50% breakdown voltage (U_{50}) of a gap with a large electrode with a small protrusion is related to the gap length and how this can be compared to other electrode geometries. Based on this experiment the following is concluded:

- For large spherical electrodes with a small protrusion such as a current-voltage measurement-transformer, the insulation distance is greatly reduced compared to a sphere-sphere configuration and it behaves more like a rod-rod gap. (Section 15.8)
- The determined U_{50} for the large spheres with protrusions lies above the rod-structure U_{50} from the IEC standard. Thus, by using the standard values to determine the insulation distances in a mobile substation the insulation will be sufficient. (Section 15.8)
- The large Current-Voltage-Transformers (CVTs) will form the shortest distance in the skid (Figure 13.2). The determined U_{50} values for the spheres with protrusions which represent these CVTs lie above the U_{50} for the Rod-structure from the IEC 60071-1 and thus it can be considered to even use shorter insulation distances in the mobile substations. However, it should then be shown by test on an actual skid that the insulation is indeed sufficient. (Section 15.8)

16.1. Recommendations

In this thesis, it is found that the use of a mobile substation could be a solution to reduce the required VNB time, the amount of critical resources, and redispatch costs during maintenance, replacement, and expansion projects in TenneT substations. In addition to the recommended future work for the experiment as mentioned in Section 15.9 the author recommends the following for TenneT:

- Investigate how many mobile substations are required to reduce the 80% of VNB.
- Investigate the investment and operational costs of a mobile substation to determine the actual savings.
- Investigate the precise savings in VNB time and costs when a mobile substation is used.
- Determine which substations should be bypassed to get the highest VNB reduction.
- In this thesis it is assumed that a 500 MVA mobile substation is required to bypass a TenneT substation during maintenance, replacement, and expansion projects. It is assumed that the full capacity of a substation needs to be bypassed to be N-1 redundant during maintenance. It should be investigated if it is possible to use a lower capacity mobile substation and still be N-1 during maintenance, this would allow a smaller mobile substation and would reduce the footprint and make the transport considerably easier.
- A mobile substation that is able to take over a complete station will require a rather large area, which in a lot of TenneT substations is not readily available. Temporary permits will be required to set up a mobile substation outside the substation area. In a future study, a more detailed mobile substation design has to be investigated to determine the required area for the mobile substation.
- TenneT has decided to only use Gas Insulated Substations (GIS) when Air Insulated Substations (AIS) are not possible. In a future study, it should be determined what the footprint of an AIS substation will be and if it is realistic to use AIS for the extra-high voltages (220 kV and 380 kV). A comparison should be made between AIS and GIS to determine if the disadvantages of GIS should be accepted and if GIS should be allowed for a mobile substation because GIS will be much more compact and thus more convenient for transport.

Bibliography

[1] Aadeghvaziri M. A., Allahverdi N. H., and Ashrafi A. Qualitative assessment of seismic response of internal components of power transformers. *13th World Conference on Earthquake Engineering*, 8 2004.

[2] ABB Ltd. Shell transformers Securing continuous supply through innovation and experience Power transformers. Technical report, ABB, Zurich, 2011.

[3] R. Arnold and M. Heathcote. *The J & P Transformer Book*. Elsevier, 1983. ISBN 9780408004947. doi: 10.1016/C2013-0-00832-8.

[4] S. A. Asea Brown Boveri. High Voltage mobile power transformers. Solving contingencies in Transmission and Distribution. Technical report, ABB, Cordoba, 2011. URL `https://www.hitachienergy.com/offering/product-and-system/transformers/power-transformers/shell-transformers`.

[5] Gordon W. Brown. Method of Maximum Likelihood Applied to the Analysis of Flashover Data. *IEEE Transactions on Power Apparatus and Systems*, PAS-88(12):1823–1830, 1969. ISSN 00189510. doi: 10.1109/TPAS.1969.292298.

[6] G. Carrara and W. Houschild. Statistical evaluation of dielectric test results. *Electra*, 133:109–130, 1990.

[7] G. Carrara and L. Thione. Switching surge strength of large air gaps: A physical approach. *IEEE Transactions on Power Apparatus and Systems*, 95(2):512–524, 1976. ISSN 00189510. doi: 10.1109/T-PAS.1976.32131.

[8] Centraal Bureau voor de Statistiek (CBS). Elektriciteitsproductie stijgt in 2020 naar recordhoogte, 6 2022. URL `https://www.cbs.nl/nl-nl/nieuws/2021/09/elektriciteitsproductie-stijgt-in-2020-naar-recordhoogte`.

[9] Inuk Cha, Seungmin Lee, Ju Dong Lee, Gang Woo Lee, and Yongwon Seo. Separation of SF6 from gas mixtures using gas hydrate formation. *Environmental Science and Technology*, 44(16):6117–6122, 8 2010. ISSN 0013936X. doi: 10.1021/es1004818.

[10] Lars Hofmann Christensen. Design, construction, and test of a passive optical prototype high voltage instrument transformer. *IEEE Transactions on Power Delivery*, 10(3):1332–1337, 1995. ISSN 19374208. doi: 10.1109/61.400913.

[11] Transformers Committee of the IEEE Power and Energy Society. IEEE Guide for the Transportation of Transformers and Reactors Rated 10 000 kVA or Higher Sponsored by the Transformers Committee IEEE Power and Energy Society. Technical report, IEEE, New York, 2 2013.

[12] Robert M. Del Vecchio, Bertrand Poulin, Pierre T. Feghali, Dilipkumar M. Shah, and Rajendra Ahuja. *Transformer Design Principles*. CRC Press, 12 2017. ISBN 9781315218342. doi: 10.1201/EBK1439805824.

[13] Digsilent. PowerFactory, 2022.

[14] Juan Dixon, Luis Morán, José Rodríguez, and Ricardo Domke. Reactive power compensation technologies: State-of-the-art review. *Proceedings of the IEEE*, 93(12):2144–2163, 2005. ISSN 00189219. doi: 10.1109/JPROC.2005.859937.

[15] P. E. Donald Parnell. An Introduction to Gas Insulated Electrical Substations Credit: 3 PDH. Technical report, Continuing Education and Development, Inc., Woodcliff Lake, 2003.

[16] Y. Du, M. Zahn, B.C. Lesieutre, A.V. Mamishev, and S.R. Lindgren. Moisture equilibrium in transformer paper-oil systems. *IEEE Electrical Insulation Magazine*, 15(1):11–20, 1 1999. ISSN 0883-7554. doi: 10.1109/57.744585.

[17] DuPont. ABB's first 250 MVA, 400 kV fast-deployable transformer uses DuPont™ Nomex® insulation for high output and compactness. Technical report, DuPont, 2014. URL www.nomexpaper.dupont.com.

[18] energiemarktinformatie.n. KWH prijzen Elektra APX, ENDEX, BELPEX grafiek | Informatie over de energiemarkt, 2022. URL https://www.energiemarktinformatie.nl/beurzen/elektra/#stockchart_dpb.

[19] C. S. Engelbrecht, P. L. J. Hessen, C. S. Stuurman, I. Tannemaat, and E. P. Evertz. Nota Isolatiecoördinatie voor 50, 110, 150, 220 en 380 kV elektriciteitsnetten Deel 2 - Technische onderbouwing. Technical report, DNV KEMA, Arnhem, 7 2013.

[20] ENTSO-E. Unavailability of Production and Generation Units, 2022. URL https://transparency.entsoe.eu/outage-domain/r2/unavailabilityOfProductionAndGenerationUnits/show.

[21] G. Gallet, G. Leroy, R. Lacey, and I. Kromer. General expression for positive switching impulse strength valid up to extra long air gaps. *IEEE Transactions on Power Apparatus and Systems*, 94(6):1989–1993, 1975. ISSN 00189510. doi: 10.1109/T-PAS.1975.32045.

[22] I. Gallimberti. The mechanism of the long spark formation. *Le Journal de Physique Colloques*, 40(C7): 7–193, 1979. ISSN 0449-1947.

[23] Belén García, Juan Carlos Burgos, Ángel Matías Alonso, and Javier Sanz. A moisture-in-oil model for power transformer monitoring - Part I: Theoretical foundation. *IEEE Transactions on Power Delivery*, 20 (2 II):1417–1422, 4 2005. ISSN 08858977. doi: 10.1109/TPWRD.2004.832366.

[24] G. Gela. Air gap sparkover and gap factors: Analysis of published data. Technical report, Electric Power Research Institute (EPRI), Lenox, 12 1994.

[25] MetaDesign GmbH. Siemens-Prefabricated Power Solutions - Brochure. Technical report, Siemens-energy, Erlangen, 2021.

[26] E. Gomez Hennig, K. Kaineder, R. Mayer, and E. Schweiger. *Bypassing GSU transformers in case of emergencies or maintenance*. Elsevier, 1970. ISBN 9780080160351. doi: 10.1016/C2013-0-02376-6.

[27] T. Grun. Equipment for on-site testing of HV insulation. In *11th International Symposium on High-Voltage Engineering (ISH 99)*, volume 1999, pages 5–240. IEE, 1999. ISBN 0 85296 719 5. doi: 10.1049/cp:19990930.

[28] Haibo Liu, Chengxiong Mao, Jiming Lu, and Dan Wang. Parallel operation of electronic power transformer and conventional transformer. In *2008 Third International Conference on Electric Utility Deregulation and Restructuring and Power Technologies*, pages 1802–1808. IEEE, 4 2008. ISBN 978-7-900714-13-8. doi: 10.1109/DRPT.2008.4523699.

[29] Andrew R. Hileman. *Insulation Coordination for Power Systems*. CRC Press, 10 2018. ISBN 9781315219509. doi: 10.1201/9781420052015.

[30] International Electrotechnical Commission (IEC). IEC 60060-1: High-voltage test techniques - Part 1: General definitions and test requirements, 2010.

[31] International Electrotechnical Commission (IEC). IEC 60071-2 Insulation co-ordination-Part 2: Application guidelines, 3 2018.

[32] International Electrotechnical Commission (IEC). IEC 60071-1 Insulation co-ordination-Part 1: Definitions, principles and rules, 8 2019.

[33] Shailesh R Joshi. SF 6 N 2 Mixtures for Application in EHV Gas Insulated Systems. *International Journal of Advanced Research in Electrical, Electronics and Instrumentation Engineering (An ISO*, 3297, 2007. doi: 10.15662/IJAREEIE.2016.0506107.

[34] Yannick Kieffel, Todd Irwin, Philippe Ponchon, and John Owens. Green Gas to Replace SF6 in Electrical Grids. *IEEE Power and Energy Magazine*, 14(2):32–39, 3 2016. ISSN 15407977. doi: 10.1109/MPE.2016.2542645.

[35] Isamu Kishizima, Kohsuke Matsumoto, and Yasuo Watanabe. New Facilities for Phase-to-Phase Switching Impulse Tests and Some Test Results. *IEEE Power Engineering Review*, PER-4(6):31–32, 1984. ISSN 02721724. doi: 10.1109/MPER.1984.5526086.

[36] Joni Klüss and William Larzelere. Reconfiguration of 3 MV Marx Generator into a Modern High Efficiency System. *Proceedings of the Nordic Insulation Symposium*, 25, 10 2017. ISSN 2535-3969. doi: 10.5324/nordis.v0i25.2372.

[37] F. H. Kreuger. *Industrial High Voltage: 1. Electric fields 2. Dielectrics 3. constructions*. Number v. 1 in Industrial High Voltage. Delft University Press, 1991. ISBN 9789062755615.

[38] F. H. Kreuger. *Industrial High Voltage: 4. Coordinating, 5. Testing, 6. Measuring*. Delft University Press, Delft, 12 1992.

[39] E. Kuffel, W. S. Zaengl, and J. Kuffel. *High voltage engineering : fundamentals*. Butterworth-Heinemann/Newnes, 2000. ISBN 0750636343.

[40] A. Lathouwers, P. Jansen, and E. Meulemeester. TenneT's giant leap to be able to replace 140 substations within next 10 year, while in service and coming from different lay-outs. Technical report, Cigre, Paris, 2020.

[41] Andre Lathouwers. TBD.013 Aanpak tb het verhelpen van storingen mede gembruikmakend van de strategische voorraad, 9 2018.

[42] X. M. López-Fernández, H. B. Ertan, and J. Turowski. *Transformers: Analysis, Design, and Measurement*. Taylor & Francis, 2012. ISBN 9781466508248.

[43] J. Lopez-Roldan, J. Alfasten, J. Declercq, R. Gijs, P. Mossoux, and M. Van Dyck. technical considerations regarding the design and installation of mobile substations. Technical report, Cigre, Paris, 2004.

[44] J. Lopez-Roldan, J. Enns, P. Guillaume, and C. Devriendt. Mobile substations: Application, engineering and structural dynamics. In *Proceedings of the IEEE Power Engineering Society Transmission and Distribution Conference*, pages 951–956, 2006. ISBN 0780391942. doi: 10.1109/TDC.2006.1668630.

[45] Willy Lord. Mobile Substations - Vatenfall (Sweden) (170/52/24(12) kV). Technical report, Vattenfall & ABB Power Technologies AB, Vienna, 5 2007.

[46] M & I Materials. MIDEL 7131 Synthetic Ester Transformer Fluid Fire safe and Biodegradable MIDEL ® SAFETY INSIDE - Brochure. Technical report, M&I Materials Ltd, Manchester, 2019.

[47] R. Marek, T. Prevost, and J. C. Duart. High Temperature Insulation Systems: An Option for Resilient Transformers. *Proceedings of the IEEE Power Engineering Society Transmission and Distribution Conference*, 2018-April, 8 2018. ISSN 21608563. doi: 10.1109/TDC.2018.8440478.

[48] C. Menemenlis, H. Anis, and G. Harbec. Phase-to-phase insulation Part II: Required clearances and coordination with phase-to-ground insulation. *IEEE Transactions on Power Apparatus and Systems*, 95 (2):651–659, 1976. ISSN 00189510. doi: 10.1109/T-PAS.1976.32147.

[49] Pierre Mirebeau. Feasibility of a Common, Dry Type Plug-in Interface for GIS and Power Cables above 52 kV. In *Accessories for HV and EHV Extruded Cables*, chapter 7, pages 317–368. CIGRE Green Books, 2021. doi: 10.1007/978-3-030-39466-0{_}7.

[50] Raj Nagarsheth and Sushant Singh. Study of gas insulated substation and its comparison with air insulated substation. *International Journal of Electrical Power and Energy Systems*, 55:481–485, 2014. ISSN 01420615. doi: 10.1016/j.ijepes.2013.09.012.

[51] NEN. NEN-EN 50341-1: Overhead electrical lines exceeding AC 1 kV-Part 1: General requirements-Common specifications. Technical report, NEN, 2013.

[52] Normcommissie 363623. NEN 3840+A3 (nl) Bedrijfsvoering van elektrische installaties-Hoogspanning. Technical report, NEN, 7 2019.

[53] Ernst Peter Pagger, Michael Muhr, Kevin Rapp, and Norasage Pattanadech. Alternative Insulating Fluids - Interpretation of Test Results. In *Proceedings of the 2020 International Conference on Diagnostics in Electrical Engineering, Diagnostika 2020*. Institute of Electrical and Electronics Engineers Inc., 9 2020. ISBN 9781728158792. doi: 10.1109/Diagnostika49114.2020.9214642.

[54] Luigi Paris. Influence of Air Gap Characteristics on Line-to-Ground Switching Surge Strength. *IEEE Transactions on Power Apparatus and Systems*, PAS-86(8):936–947, 8 1967. ISSN 0018-9510. doi: 10.1109/TPAS.1967.291917.

[55] Luigi Paris and Rosario Cortina. Switching and Lightning Impulse Discharge Characteristics of Large Air Gaps and Long Insulator Strings. *IEEE Transactions on Power Apparatus and Systems*, PAS-87(4):947–957, 1968. ISSN 00189510. doi: 10.1109/TPAS.1968.292069.

[56] A. Pigini, G. Rizzi, R. Brambilla, and E. Garbagnati. Switching impulse strength of very large air gaps. In *Third international symposium on high voltage engineering, Milan*, 1979.

[57] Akshaya Prabakar. The real challenges in transition to eco friendly power networks. Technical report, TenneT, 3 2022.

[58] Stefan Riegler, Ewald Schweiger, Christian Ettl, Martin Stössl, and Sanjay Bose. Recommendation of site commissioning tests for rapid recovery transformers with an installation time less than 30 hours. *Elektrotechnik und Informationstechnik*, 135(8):543–547, 12 2018. ISSN 0932383X. doi: 10.1007/s00502-018-0669-5.

[59] Rijksdienst voor het Wegverkeer. Wettelijke afmetingen ontheffingen | RDW, 2012. URL `https://www.rdw.nl/zakelijk/branches/transporteurs/incidentele-ontheffing/wettelijke-afmetingen-ontheffingen`.

[60] Tapan Kumar Saha and Prithwiraj Purkait. *Transformer Ageing : Monitoring and Estimation Techniques*. John Wiley & Sons, Incorporated, New York, SINGAPORE, 2017. ISBN 9781119239994.

[61] Ewald Schweiger, Christian Ettl, Eduardo Gomez Hennig, Stefan Riegler, Martin Stoessl, and Sanjay Bose. Resilience solutions for bypassing power transformers and recommendations of site commissioning tests. In *2019 IEEE Power & Energy Society General Meeting (PESGM)*, pages 1–5. IEEE, 8 2019. ISBN 978-1-7281-1981-6. doi: 10.1109/PESGM40551.2019.8973405.

[62] M. Seeger, R. Smeets, J. Yan, H. Ito, M. Claessens, E. Dullni, L. Falkingham, C. M. Franck, F. Gentils, W. Hartmann, Y Kieffel, S Jia, G Jones, J Mantilla, S Pawar, M Rabie, P Robin-Jouan, H Schellekens, J Spencer, T Uchii, X Lia, and S Yanabu. Recent development of SF6 alternative gases for switching applications. *ELECTRA (cigre)*, 2017.

[63] K. M. Smith. *Electrical Engineering Principles for Technicians*. Elsevier, 1970. ISBN 9780080160351. doi: 10.1016/C2013-0-02376-6.

[64] Spinningspark. Spinningspark, 2022. URL `https://en.wikipedia.org/wiki/User:Spinningspark`.

[65] StatLine. Elektriciteitsbalans; aanbod en verbruik, 7 2022. URL `https://opendata.cbs.nl/statline/#/CBS/nl/dataset/84575NED/table?ts=1657179936544`.

[66] Study Committee 33. Cigre Technical brochure No 72 - Guidelines for the evaluation of the dielectric strength of external insulation. Technical report, Cigre, 1992.

[67] Imre Tannemaat. TBD.014: TenneT Beleidsdocument Isolatiecoördinatie. Technical report, TenneT, 11 2019.

[68] TenneT. Maintenance strategy TenneT, 12 2021. URL `https://www.tennet.eu/our-key-tasks/transport-services/maintenance-strategy/`.

[69] TenneT. Scheduled maintenance TenneT, 12 2021. URL `https://www.tennet.eu/our-key-tasks/transport-services/scheduled-maintenance/`.

[70] TenneT. Transportcapaciteit TenneT, 2022. URL https://www.tennet.eu/nl/elektriciteitsmarkt/nederlandse-markt/transportcapaciteit/.

[71] L. Thione and K. Ragaller. The dielectric strength of large air insulation. In *Surges in High-Voltage Networks*. Plenum Press, 1980.

[72] Anton Tijdink, Hoffmann Mathias, Ruud Vrolijk, and Bob van Breukelen. Annual market update 2021 - TenneT. Technical report, TenneT, Arnhem, 4 2022.

[73] E. van Toor. *Technische onderdelen in het elektriciteitsnet*. TenneT, 2020.

[74] Jon Trout. new Technology Changing the Heart of Power Systems High Temperature Insulation Systems: An Option for Resilient Transformers Interview with. Technical report, FirstEnergy, 3 2019.

[75] Wetten.nl. Regeling - Regeling voertuigen - BWBR0025798, 2018. URL https://wetten.overheid.nl/BWBR0025798/2018-01-01#Hoofdstuk5_Afdeling18.

[76] Wetten.nl. Regeling - Elektriciteitswet 1998 - BWBR0009755 (Dutch), 12 2021. URL https://wetten.overheid.nl/BWBR0009755/2021-07-01#Hoofdstuk3_Paragraaf2_Artikel16.

[77] B. van Wezel. Elektriciteit in Nederland. Technical report, Centraal Bureau voor de Statistiek (CBS), 2015.

[78] J. Winders. *Power Transformers: Principles and Applications*. Power Engineering (Willis). Taylor & Francis, 2002. ISBN 9780824744434.

[79] S. Yakov. Statistical analysis of dielectric test results. Technical report, Cigre working group 15, 1991.

[80] Ed Zientek. Loading Considerations whenParalleling Transformers. Technical report, Schneider Electric, 2011.

A

Road Regulations

Every country has its regulations concerning the maximum dimensions and mass of road transport. In Europe central guidelines are in place to make sure all countries have the same regulations. Countries are however allowed to make regulations that exceed the European regulations. It is assumed that the mobile substation will be mounted on several trailers that can be transported using trucks. According to chapter 5 of "de regeling voertuigen 5.18.11 - 5.18.18" [75] the following regulations are in place in the Netherlands for trailers.

A.1. Dimensions

- semi-trailer (Figure A.1a)
  - length from kingpin to the rear of the truck (A) < 12.00 m
  - With < 2.55 m
  - Height < 4.00 m
- Combination tractor and semi-trailer (Figure A.1b)
  - length (A) < 16.50 m
  - With < 2.55 m
  - Height < 4.00 m
- Combination tractor and semi-trailer non-divisible load (Figure A.2)
  - length (A) < 22.00 m
  - front-crossing (B) < 4.30 m
  - rear-crossing (B) < 5.00 m
  - With < 3 m
  - Height < 4.00 m

From these regulations, it is found that for a semi-trailer the maximum length is 12 m and the width 2.55 m. When the mobile substation is considered to be a non-divisible load it may be bigger which gives some flexibility in the design of mobile substation components. The height of the trailers is always limited to 4 m considering the height of overpasses and tunnels in the Netherlands. The mentioned regulations are the standards for which no additional permits are required. However, there are possibilities to request special permits to allow some larger dimensions. For now, the goal is to dimension the trailers in such a way that no additional permits are required.

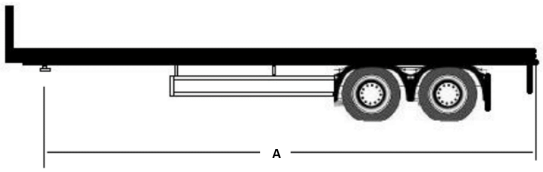

(a) The maximum length of semi-trailer in the Netherlands [59]

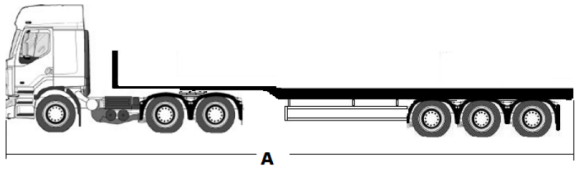

(b) The maximum length of tractor and semi-trailer combination in the Netherlands [59]

Figure A.1

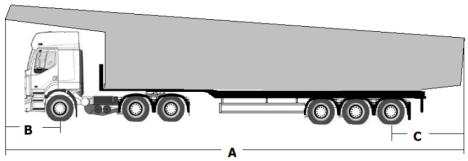

Figure A.2: The maximum length of truck and trailer combination in the Netherlands for non-divisible load [59]

A.2. Mass

Maximum total masses are specified in the road regulations for a tractor semi-trailer combination of 50.000 kg. Assuming that an unloaded tractor weighs approximately 8.000 kg, the weight of the trailer and substation component may have a mass of approximately 42.000 kg. A maximum weight per axle is also specified and differs between a divisible and non-divisible load, it is assumed that a double-double axle is used because this may carry the highest loads. The max loads are mentioned in Table A.1. The detailed design of the trailer and positioning of the axle should be determined together with the truck manufacturer.

	divisible load	non-divisible load
A < 1.00 m	13.000 kg total	16.000 kg total
1.00 m < A ≥ 1.30 m	17.000 kg total	12.000 kg per axle
1.300 m < A ≥ 1.80 m	21.000 kg total	16.000 kg per axle

Table A.1: Maximum axle load for the four-axle configuration from Figure A.3

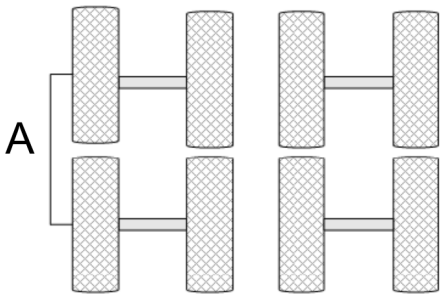

Figure A.3: Four axle configuration [59]

B

Background: Breakdown in Air

B.1. Introduction

The insulation behavior of air depends on a number of factors; the type and polarity of the applied voltage, electric field distribution, gap length, and gas conditions. These parameters can be divided into three categories based on their influence on the strength of air insulation [66];

- **Decisive influence:** The insulation distance, the shape of the electrode, and the ratio between positive and negative electrodes in phase-to-phase configurations ($\alpha = \frac{U^-}{U^+ + U^-}$, Section 13.3.5) have a decisive influence on the insulation strength in air.
- **Significant influence:** The impulse shape has a significant influence on the insulation strength. When for the switching impulse shape; rise and fall time, are varied the strength passes through a minimum value the crest time at which this minimum occurs is called the critical time to crest.
- **Lower influence:** The pre-stressing of the air gap has a less significant influence and is neglected in the first approximation of the air gap strength.

The electrical discharge in air develops in successive phases which can be either well distinguished or partly superimposed depending on the type of applied voltage and the electrode geometry. The successive steps which can be distinguished are [66];

1. **Corona/streamer phase:**
   Thin ionized filaments called streamers are formed in the region of high electric field in the proximity of the electrode.
2. **Leader phase:**
   A leader channel is formed which is more highly ionized compared to the streamer, it propagates with leader corona developing from its tip. The leader can either reach the opposite electrode or stop depending on the value and shape of the applied voltage and gap length.
3. **Final Jump:**
   Once either the streamer or leader has reached the opposite electrode the final jump can take place. The leader channel elongates at increasing velocity and bridges the whole gap. The channel becomes highly ionized and the electrodes become short-circuited.

Which stages are present in the breakdown development depends on the overvoltage shape, for the slow front overvoltages such as switching impulse all three stages are present[66] [71]. With other types of voltages, some stages may be absent, for lightning overvoltages no significant leader phase can be present due to the short impulse time compared to the long leader phase [66][71]. This will be covered in the following sections

The characteristics of the first corona/streamer phase and leader phase are different for the different voltage polarities, this causes the breakdown voltage amplitude to be different for positive and negative polarity [66]. For almost all electrode geometries the breakdown voltage is lower for positive polarity compared to

negative polarity. The rod-plane gap has the lowest breakdown voltage of the practical geometries because the electric field is enhanced on one side only causing high stresses on the gap at the rod.

B.2. breakdown with positive polarity

As discussed before the lowest breakdown strength of air is for a positive switching overvoltage on a rod-plane gap, this type of stress is used to explain the breakdown mechanism because the three stages of discharge development can be well distinguished[66]. Note that for the lightning overvoltage there is no significant leader formed, however, the corona/streamer and final jump phase are comparable to the breakdown development at switching overvoltages [71].

B.2.1. Corona/streamer phase:

In a gaseous dielectric, there are always free electrons present because gas molecules may be ionized by light, radioactive radiation, or cosmic radiation. These free electrons are accelerated in the direction of the electric field caused by the applied voltage. The accelerated free electrons will collide with the gas molecules. When the electron has gained sufficient speed due to the electric field an electron can be liberated from a gas atom by the collision, causing an additional free electron and leaving a positive gas atom behind. This is called Ionization. The new free electrons are created with a rate of α per unit length of path. When the electrons did not gain enough energy they are captured by neutral oxygen or water vapor molecules (electronegative gases) at a rate of η per unit length of path forming negative ions. When the collision between the gas molecules and the electron is inelastic the gas atom is excited by the collision to a higher energy state. After a short amount of time, the atom falls back to its original state and a photon is emitted [37]. Due to the collisions causing new free electrons an electron avalanche as shown in Figure B.1 is formed which has at its arrival at the electrode a number of electrons in the head given by Equation B.1[66].

$$n = e^{\int_a^b (\alpha-\eta)\,dx} \tag{B.1}$$

Where a and b are the starting and arrival points of the avalanche and (α-η) is the net ionization coefficient. The same number of positive ions is left in the gap.

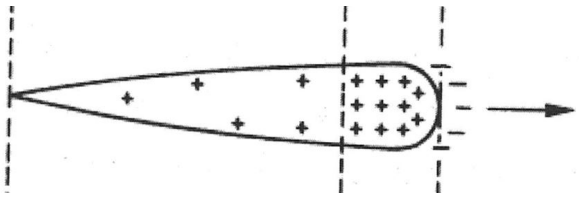

Figure B.1: Electron Avalanche [37]

Both α and η depend on the energy which the electrons gain between two collisions and on the number of collisions per unit length of path [66]. Thus they depend on gas density and electric field strength. Equation B.2 gives the energy (W) which is gained by an electron in a path l in the field direction between two collisions. E is the electric field and q is the electron charge. The path between two collisions (l) is inversely proportional to gas density and pressure.

$$W = Eql \qquad [J] \tag{B.2}$$

The avalanche will only grow when α-$\eta \geq 0$, in air at atmospheric pressure this occurs for field values higher than about 26 kV/cm [66].

The positive ions are also accelerated by the electric field and will move slower in the opposite direction, due to the large difference in mass the positive ions will move with a velocity in the order of 1 to 10 mm/μs while the electrons move with a velocity of 100 to 1000 mm/μs [37]. The positive ions are thus still at the spot where they were created while the electrons are vanished, creating a positive space charge concentrated at the tip of the avalanche.

When the head of the avalanche contains a sufficient number of ions it creates a large space charge which affects the electric field in the gap. It is assumed that this effect starts to influence the breakdown in air when the concentration of ions in the head of the avalanche reaches 10^8 ions (Equation B.1) [37].

When the avalanche reaches the anode all electrons are absorbed and a positive space charge remains, which greatly enhances the local electric field. This gives a field strength E_s of approximately 1 kV/mm at the head of the avalanche [37].
The original electric field due to the applied voltage is in the order of 3 kV/mm for breakdown in atmospheric air, thus the additional electric field due to the space charge gives a substantial field enhancement.

Due to the strong electric field more ionization takes place and the creation of photons is increased even more. These photons collide with gas molecules and at the high field strength, this leads to violent ionizations. New avalanches are started that move in the direction of the space charge. When they reach the positive space charge the avalanches are neutralized and leave a new positive charge in a more advanced position from the electrode. This process repeats and step by step the positive charge moves into the gap creating a partially ionized filament called a streamer as shown in Figure B.2 [37].

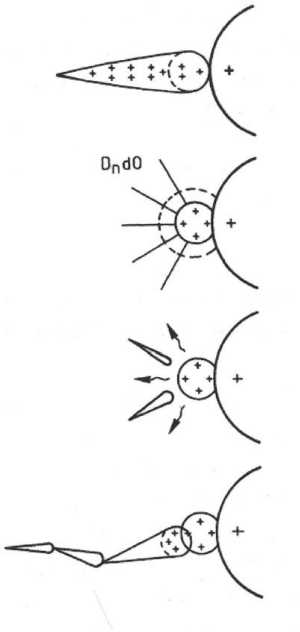

Figure B.2: Anode initiated streamer [37]

This growth of the streamer does not happen in a straight line but is tortuous like a lightning pattern and forms branches in larger gaps [37]. This is due to the stochastic nature of the processes. The field enhancement due to the space charge is not always in a direct path towards the opposite electrode. Also, the photons may cause two avalanches to be created at the same time and reach the streamer hat at the same time creating two branches. A streamer will have a stable propagation in a constant field of 4.5 to 5 kV/cm at atmospheric pressure, which is also the electric field along the filament [66].

The negative charge created by the ionization process flows along the streamers into the positive electrode leaving a net positive space charge behind, which alters the electric field distribution. Close to the electrode, the field strength is reduced while the field strength is increased at the tip of the streamer as shown in Figure B.3. If the applied voltage is not increased anymore the ionization processes will stop.

B.2.2. Leader phase

When the electric field is increased further the ionization process will restart after the first corona and a leader channel is formed from the corona stem [66]. The electric field can be increased due to three phenomena;

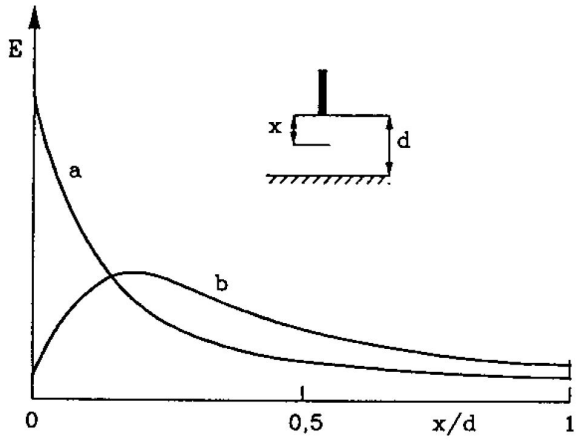

Figure B.3: Field distribution along a rod-plane gap before corona (a) and after corona (b) [66]

Increase of the applied voltage, diffusion of the space charge, and change in the characteristic of the stem.

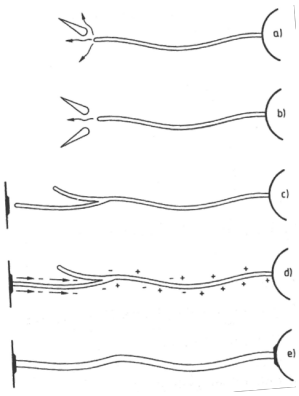

Figure B.4: Positive Leader growth [37]

The energy input due to the current flow in the stem is stored in vibrational energy of the gas molecules and then relaxed into thermal energy [22]. Due to the delayed increase in temperature thermal detachments of negative ions in the streamer takes place which increases its conductivity. The electrons which are released in the stem flow to the positive electrode causing a rapid increase of net positive space charge in the stem. The electric field around the stem is increased due to the increase in conductivity and space charge. This causes the restart of the ionization process and the inception of a second corona which will form a leader.

This process of propagation continues forming a leader (Figure B.4) which elongates with an almost constant velocity of the order of 1.5-2 cm/μs along a tortuous path that can be 10 to 30% longer than the gap length.

Note that for electrodes with a large radius the leader stage is sometimes absent because the streamers formed at corona-inception are long enough to immediately reach the opposite electrode [71].

B.2.3. Final jump

The final stage of breakdown in air is the final jump, this is when the streamer or leader corona reaches the opposite electrode (cathode). The leader velocity and current increase almost exponentially until the leader has reached the opposite electrode. Negative electrons and positive ions now move through the path of the leader and form a conductive plasma, and complete breakdown of the gap is obtained. The duration of the final jump stage is short in comparison to the stage of continuous leader propagation.

B.3. Breakdown with negative polarity

The breakdown voltage of air with negative polarity is higher compared to the same geometry and voltage shape with positive polarity. Because of the higher voltage and the higher complexity of the breakdown mechanism less study is performed on the breakdown for negative polarity impulse voltages. However, when for example a symmetrical electrode configuration (rod-rod gap) is studied the negative voltage breakdown mechanism is of interest. For breakdown with switching overvoltage the same three phases can be distinguished; corona/streamer, leader propagation, and final jump whereas for lightning overvoltage no significant leader phase is present [71].

B.3.1. Corona/streamer phase

When the applied voltage is sufficiently high and a free electron is present the first corona will occur as a burst of streamers developing from the negative electrode propagating towards the anode. Figure B.5 gives a schematic representation of the formation of a negative streamer in a nonuniform electric field. Close to the cathode, a free electron is present which is accelerated by the electric field in the direction of the anode causing an electrode avalanche. Because the electrons move much faster than the ions positive ions are left behind after the collisions between the gas molecules and the electrons. This causes an increase in the electric field on both sides of the avalanche.

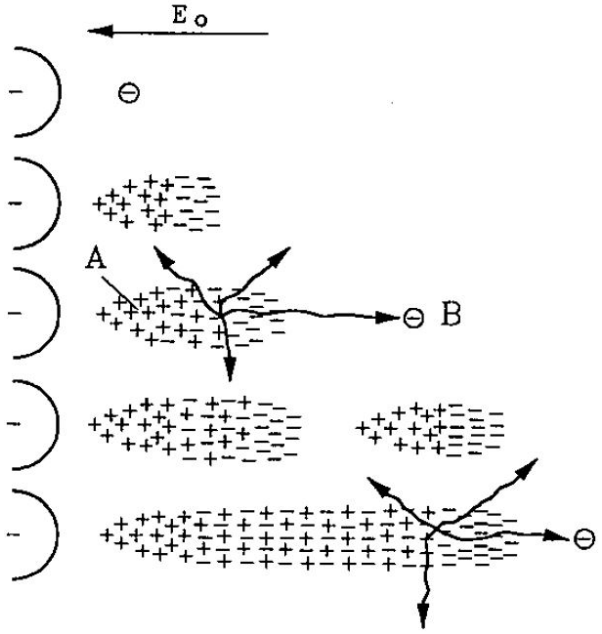

Figure B.5: Schematic representation of the negative streamer process [66].

When the avalanche has reached a sufficient size a streamer will develop in both directions. From point A in Figure B.5 a positive streamer develops in the cathode direction. A photoelectron is developed at point B in Figure B.5 which causes a secondary avalanche. When the secondary avalanche also reaches a sufficient size a positive streamer is formed between the primary and secondary avalanche. This phenomenon will repeat itself and a negative streamer grows towards the anode.

Due to the space charge at the tip of the streamer and the resulting increased electric field, the streamer can propagate in regions where the applied field is reduced leaving behind a partly ionized filament with an excess of negative charge. Due to the movement of negative ions resulting from electron attachment a positive charge is left at the cathode side which causes an increase of the electric field there. Electrons are emitted from the cathode due to photoionization and ion bombardment. Due to the arrival of positive ions at the cathode and the emission of electrons, the excess negative charge in the filament is caused.

The photoelectrons which start the secondary avalanches are produced at a certain distance from the tip of the streamer and are accelerated in a region where the field due to space charge is low. These electrons are manly accelerated due to the applied field, and thus the negative streamers will develop approximately along the field lines, have fewer ramifications, and with the same applied voltage a shorter length in comparison to positive streamers. In the region of the reduced field, the electron attachment is increased which reduces the possibility of collisional ionizations in the final part of the avalanche development [66].
The difference in breakdown voltage between negative and positive voltages is caused by the difference in the possibility of the propagation of ionization phenomena.

B.3.2. Leader phase

Similar to the positive breakdown mechanism also for the negative voltage a leader is formed after the first corona. The difference is that the leader now develops from the negative electrode. At a certain distance from the tip of the leader a luminous nucleus called the "space stem" is located, from this space stem positive and negative streamers are propagating in opposite directions. This process repeats itself elongating the leader with an equivalent displacement velocity towards the anode of approximately 10cm/μs. Due to this process, the direction of propagation is largely random and re-illuminations with large instantaneous elongations occur.

B.3.3. Final jump

When the space stem gets close to the anode, a positive leader channel is formed between the space stem and the electrode. The positive leader will propagate in the direction of the tip of the negative leader. Both leaders will accelerate and meet together to complete breakdown. When there are protrusions on the positive electrode there will be field enhancement which can facilitate an earlier formation of a positive leader.

B.4. Breakdown when both electrodes are energized

In practical situations, it often occurs that both electrodes are stressed with opposite polarity, as is often the case for rod-rod gaps. In this case, both discharge processes; positive and negative occur at the same time from the different electrodes propagating towards each other. When the applied voltage and thus electric field in the gap is sufficiently high the two streamers will meet in the gap and complete breakdown will take place.

C

Marx Generator

C.1. Single-stage impulse generator

The basics of an impulse generator will be covered in this appendix. The Marx generator from the Electrical Sustainable Power Lab from the TU Delft will be used as an example. Figure C.1 shows a single stage of the impulse generator. Discharge capacitor C_d is charged through a DC source with a maximum voltage of 100 kV. The capacitor C_l represents the load capacitance which is the combination of the capacitance of the test object, additional capacitance to alter the wave shape, and the capacitive voltage divider used for measurements. The discharge capacitor (C_d) must always be at least a factor 3 larger than the load capacitance (C_l) otherwise the efficiency of the generator will be too low. R_f is the front resistance which determines the front time of the impulse wave. R_h is the discharge resistance that determines the half-value. A sphere gap is used to trigger the impulse. The gap length of the sphere gap needs to be adjusted in tandem with the charging voltage to ensure the correct firing of the impulse generator.

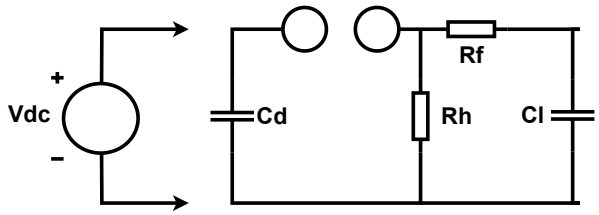

Figure C.1: Single-stage impulse generator

At first, C_d is charged by the DC source up to the desired voltage. At a certain moment, the breakdown of the sphere gap is self-ignited or triggered by a spark plug. The sphere gap is now conducting and C_d discharges itself through R_f into the load C_l. This causes a fast increase in the voltage on the load capacitor. The two capacitors are now in series which results in the time constant τ_2 (Equation C.1), in this equation R_h is neglected because of $R_h \gg R_f$.
At the same time but much slower ($R_h \gg R_f$) the two capacitors discharge through R_h, here the capacitors are in parallel which results in time constant τ_1 (Equation C.2). These two charge displacements cause the complete voltage wave which can be approximated by Equation C.3 which is also shown in Figure C.2 for a lighting impulse [36]. A more accurate representation as shown in Equation C.4 of the waveform can be found using the Laplace transform, the same time constants τ_1 and τ_2 apply [39] [36].

$$\tau_2 = R_f * \frac{C_d * C_l}{C_d + C_l} \tag{C.1}$$

$$\tau_1 = R_h * (C_d + Cl) \tag{C.2}$$

$$V_{out,t} = A(e^{-t/\tau_1} - e^{-t/\tau_2}) \tag{C.3}$$

$$V_{out,t} = \frac{V_{charge}}{R_f C_l} \frac{\tau_1 \tau_2}{\tau_1 - \tau_2} (e^{-t/\tau_1} - e^{-t/\tau_2}) \tag{C.4}$$

The time constants τ_1 and τ_2 are related to the front time (T_f) and the half-time (T_h) which are specified in the IEC 60060-1. For the lightning impulse (1.2/50 μs) wave T_f=2.96τ_2 and T_h=0.73τ_1 [38]. Thus by varying the R_f and R_h values the front and half-time of the impulse can be adjusted. For the Marx generator which is used for this experiment the R_f and R_h can easily be adjusted to obtain LI and SI impulses.

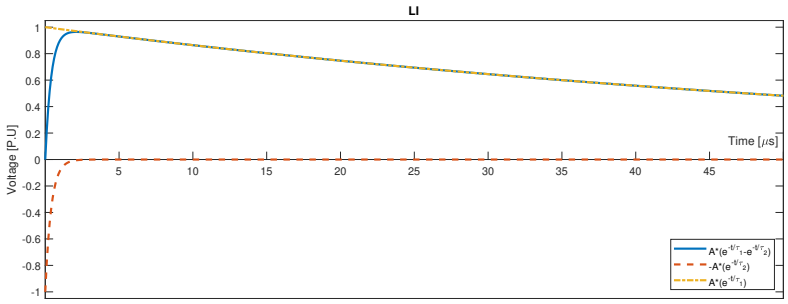

Figure C.2: Composition of standers lightning impulse

The Voltage which is charged on C_d is not 100% delivered to C_l but with a certain efficiency. For the lightning impulse with purely capacitive load the maximum voltage at the load $V_{out,max}$ is given by equation C.5 this results in efficiency as given in Equation C.6. To ensure sufficient efficiency it is important that $C_d \gg C_l$.

$$V_{out,max} = \frac{C_d}{C_d + C_l} * V_{charge} \tag{C.5}$$

$$\eta_{LI} = \frac{V_{out,max}}{V_{charge}} = \frac{C_d}{C_d + C_l} \tag{C.6}$$

When there is a (stray) inductance in the circuit this will together with the capacitance result in an oscillation and overshoot for the fast wavefronts (LI). The IEC standard specified tolerance of ±30% of the front time and less than ±5% for the overshoot. In order to comply with the IEC requirements, the relation in Equation C.7 must be satisfied. In the test setup which is used for the experiments, the inductance is expected to be low and is thus neglected in the calculations [30].

$$2 * \sqrt{\frac{L_s}{Cd} + \frac{L_s}{C_l}} \leq R_f \tag{C.7}$$

C.2. Multi-stage impulse generator

A single-stage impulse generator will be limited by the maximum voltage of the DC source and the discharge capacitor (C_d). To obtain a higher impulse voltage a multi-stage impulse generator can be used as shown in Figure C.3. The principle of a multi-stage generator is that the capacitors C_d are charged in parallel and discharged in series. The sphere gaps are positioned horizontally and in a vertical stack thus the firing of the first gap will initiate the firing of the succeeding stage causing a cascading effect and firing from the bottom to the top. When the first gap is fired the next one will follow and this way a voltage of n*V_{charge} is generated, where n is the number of stages. This way crests up to several million volts can be reached. The impulse generator which is used in this experiment has 10 stages and a maximum voltage of 1 MV. The wave shape and efficiency of the multi-stage generator will be equivalent to the single-stage if, in every stage nR'$_f$, nR'$_h$ and 1/n C'$_d$ are used. The output voltage of the multi-stage generator can be approximated by Equation C.4. The constants τ_1 and τ_2 are defined as in Equations C.2 and C.1, the other relationships are;

- $R_f = nR'_f + R_{damping}$ ($R_{damping}$ is an external damping resistor)

- $R_h = nR'_h$
- $C_d = C'_d / n$

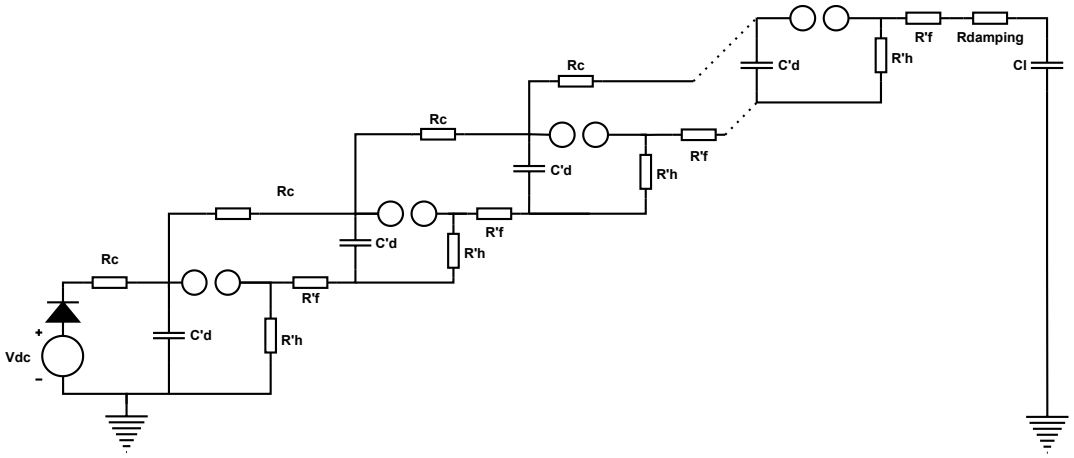

Figure C.3: Multi-stage Marx generator, 4 stages

In Figure C.3 it can be seen that there are charging resistors R_c which are required for charging the discharge capacitors (C_d). When the generator is fired these resistors will be in parallel with the front resistors R_f. The R_c value is chosen many times larger than the R_f value to not affect the output wave shape of the generator.

D

Measurement Data

Content:

Measurement DATA:			Protrusions 50cm Neg		
number	Uload [kV]	Upeak [kV]	Ucorrected [kV]	Flashover	puls #
1	405	389,70	392,48	Yes	579
2	400	385,50	388,25	No	580
3	405	389,50	392,28	Yes	581
4	400	385,40	388,15	No	582
5	405	390,40	393,19	No	583
6	410	395,10	397,92	No	584
7	415	399,82	402,68	No	585
8	420	404,10	406,99	Yes	586
9	415	399,80	402,66	No	587
10	420	405,00	407,89	No	589
11	425	408,80	411,72	Yes	590
12	420	404,10	406,99	Yes	591
13	415	398,80	401,65	Yes	592
14	410	394,20	397,02	Yes	593
15	405	389,70	392,48	Yes	594
16	400	385,30	388,05	No	595
17	405	390,40	393,19	No	596
18	410	395,10	397,92	No	597
19	415	398,80	401,65	Yes	598
20	410	394,00	396,81	Yes	599
21	405	389,40	392,18	Yes	600
22	400	385,20	387,95	No	601
23	405	390,40	393,19	No	602
24	410	394,10	396,92	Yes	603
25	405	389,50	392,28	Yes	604
26	400	384,50	387,25	Yes	605
27	395	379,80	382,51	Yes	606
28	390	375,90	378,59	No	607
29	395	380,70	383,42	No	608

Protrusions 50cm Neg				
Upeak(i) [l\	# pulses	# Flashovers	V50 [kV]	
378,59	1	0	min	359,0
382,97	2	1	opt	394,0
387,93	5	1	max	425,3
392,66	8	5		
397,32	5	3	confidence interval = 95%	
402,16	4	2		
407,29	3	2		
411,72	1	1		

Figure D.1

Measurement DATA:			Protrusions 50cm Pos		
number	Uload [kV]	Upeak [kV]	Ucorrected [kV]	Flashover	puls #
1	355	340,61	344,23	Yes	540
2	350	336,17	339,74	Yes	541
3	345	331,37	334,90	Yes	542
4	340	323,88	327,32	Yes	543
5	335	321,62	325,04	Yes	544
6	330	316,92	320,29	Yes	545
7	325	312,48	315,80	No	546
8	330	316,90	320,27	Yes	547
9	325	311,83	315,15	Yes	548
10	320	306,12	309,37	Yes	549
11	315	299,92	303,11	Yes	550
12	310	296,55	299,71	No	551
13	315	303,20	306,42	No	552
14	320	307,31	310,58	Yes	553
15	315	303,18	306,41	No	554
16	320	307,96	311,23	No	555
17	325	311,99	315,31	Yes	556
18	320	307,99	311,27	No	557
19	325	311,96	315,27	Yes	558
20	320	306,75	310,01	No	559
21	325	312,59	315,91	No	560
22	330	317,00	320,37	Yes	561
23	325	310,89	314,19	Yes	565
24	320	307,95	311,22	No	566
25	325	312,11	315,42	Yes	567
26	320	307,90	311,17	No	568
27	325	311,96	315,28	Yes	569
28	320	307,93	311,20	No	570
29	325	311,81	315,13	Yes	571
30	320	308,0	311,2	No	572

Protrusions 50cm Pos				
Upeak(i) [l\	# pulses	# Flashovers	V50 [kV]	
299,71	1	0	min	305,7
305,31	3	1	opt	312,1
310,81	9	2	max	316,9
315,27	9	7		
320,31	3	3	confidence interval = 95%	
325,04	1	1		
327,32	1	1		
334,90	1	1		
339,74	1	1		
344,23	1	1		

Figure D.2

Measurement DATA:			Protrusions 40cm Neg		
number	Uload [kV]	Upeak [kV]	Ucorrected [kV]	Flashover	puls #
1	340	327,80	330,38	No	619
2	345	332,30	334,92	Yes	620
3	340	327,90	330,48	No	621
4	345	332,10	334,71	Yes	622
5	340	327,20	329,78	Yes	623
6	335	322,30	324,84	Yes	624
7	330	317,50	320,00	Yes	625
8	325	313,30	315,77	No	626
9	330	318,40	320,91	No	627
10	335	322,40	324,94	No	628
11	340	327,90	330,48	No	629
12	345	332,30	334,92	Yes	630
13	340	327,90	330,48	No	631
14	345	332,80	335,42	No	632
15	350	336,90	339,55	Yes	633
16	345	332,00	334,61	Yes	634
17	340	327,10	329,68	Yes	635
18	335	322,90	325,44	No	638
19	340	327,10	329,68	Yes	639
20	335	322,30	324,84	Yes	640
21	330	318,20	320,71	No	641
22	335	322,30	324,84	No	642
23	340	327,10	329,68	Yes	643
24	335	322,10	324,64	Yes	644
25	330	318,20	320,71	No	645
26	335	322,90	325,44	No	646
27	340	327,70	330,28	No	647
28	345	332,10	334,71	Yes	648
29	340	327,10	329,68	Yes	649
30	335	322,3	324,8	Yes	650

Protrusions 40cm Neg				
Upeak(i) [l\	# pulses	# Flashovers	V50 [kV]	
315,77	1	0	min	312,9
320,58	4	1	opt	327,3
324,98	8	4	max	338,6
330,06	10	5		
334,88	6	5	confidence interval = 95%	
339,55	1	1		

Figure D.3

Measurement DATA:			Protrusions 40cm Pos		
number	Uload [kV]	Upeak [kV]	Ucorrected [kV]	Flashover	puls #
1	270	259,70	260,45	Yes	658
2	265	255,50	256,24	No	659
3	270	260,30	261,05	No	660
4	275	264,70	265,46	Yes	661
5	270	259,70	260,45	Yes	662
6	265	255,70	256,44	No	663
7	270	260,20	260,95	No	664
8	275	264,70	265,46	Yes	665
9	270	259,70	260,45	Yes	666
10	265	255,60	256,34	No	667
11	270	259,60	260,35	Yes	668
12	265	255,50	256,24	No	669
13	270	260,30	261,05	No	670
14	275	264,70	265,46	Yes	671
15	270	260,20	260,95	No	672
16	275	265,00	265,76	No	673
17	280	269,50	270,28	Yes	674
18	275	264,70	265,46	Yes	675
19	270	260,30	261,05	No	676
20	275	262,90	263,66	Yes	677

Protrusions 40cm Pos				
Upeak(i) [l\	# pulses	# Flashovers	V50 [kV]	
256,31	4	0	min	257,3
260,75	9	4	opt	261,6
265,21	6	5	max	266,0
270,28	1	1		
			confidence interval = 95%	

Figure D.4

Measurement DATA:			Protrusions 30cm Neg		
number	Uload [kV]	Upeak [kV]	Ucorrected [kV]	Flashover	puls #
1	270	259,70	261,96	Yes	711
2	265	255,50	257,73	No	712
3	270	259,40	261,66	Yes	713
4	265	255,00	257,22	Yes	714
5	260	250,70	252,88	No	715
6	265	255,50	257,73	No	716
7	270	260,30	262,57	No	717
8	275	264,70	267,01	Yes	718
9	270	260,20	262,47	No	719
10	275	264,80	267,11	Yes	720
11	270	259,60	261,86	Yes	721
12	265	255,60	257,83	No	722
13	270	259,60	261,86	Yes	723
14	265	254,90	257,12	Yes	724
15	260	250,70	252,88	No	725
16	265	254,80	257,02	Yes	726
17	260	250,10	252,28	Yes	727
18	255	246,10	248,24	No	728
19	260	250,80	252,98	No	729
20	265	255,60	257,83	No	730

Protrusions 30cm Neg				
Upeak(i) [l\	# pulses	# Flashovers	V50 [kV]	
248,24	1	0	min	247,7
252,76	4	1	opt	258,4
257,49	7	3	max	269,1
262,06	6	4		
267,06	2	2	confidence interval = 95%	

Figure D.5

Measurement DATA:			Protrusions 30cm Pos		
number	Uload [kV]	Upeak [kV]	Ucorrected [kV]	Flashover	puls #
1	215	207,80	208,75	No	682
2	220	211,90	212,87	Yes	683
3	215	207,70	208,65	No	684
4	220	212,00	212,97	Yes	285
5	215	207,60	208,55	No	286
6	220	211,90	212,87	Yes	687
7	215	207,70	208,65	No	688
8	220	211,90	212,87	Yes	689
9	215	207,20	208,15	Yes	691
10	210	202,60	203,53	No	692
11	215	207,70	208,65	No	693
12	220	212,00	212,97	Yes	694
13	215	207,70	208,65	No	695
14	220	211,90	212,87	Yes	697
15	215	207,60	208,55	No	698
16	220	212,50	213,48	No	699
17	225	216,70	217,70	Yes	700
18	220	211,90	212,87	Yes	701

Protrusions 30cm Pos				
Upeak(i) [l\	# pulses	# Flashovers	V50 [kV]	
203,53	1	0	min	208,3
208,58	8	1	opt	210,8
212,97	8	7	max	213,2
217,70	1	1		
			confidence interval = 95%	

Figure D.6

Measurement DATA:			Protrusions 25cm Neg		
number	Uload [kV]	Upeak [kV]	Ucorrected [kV]	Flashover	puls #
1	240	231,00	233,20	Yes	733
2	235	226,90	229,06	No	734
3	240	231,20	233,41	Yes	735
4	235	226,40	228,56	Yes	736
5	230	221,80	223,92	No	737
6	235	226,45	228,61	Yes	738
7	230	221,80	223,92	No	739
8	235	226,10	228,26	Yes	740
9	230	220,90	223,01	Yes	741
10	225	217,10	219,17	No	742
11	230	221,30	223,41	Yes	743
12	225	217,00	219,07	No	744
13	230	221,60	223,71	No	745
14	235	226,80	228,96	No	746
15	240	231,00	233,20	Yes	747
16	235	226,70	228,86	No	748
17	240	231,60	233,81	No	749
18	245	235,60	237,85	Yes	750
19	240	231,10	233,30	Yes	751
20	235	226,90	229,06	No	752

Protrusions 25cm Neg				
Upeak(i) [l\	# pulses	# Flashovers	V50 [kV]	
219,12	2	0	min	216,3
223,59	5	2	opt	228,1
228,77	7	3	max	240,0
233,39	5	4		
237,85	1	1	confidence interval = 95%	

Figure D.7

Measurement DATA:			Protrusions 25cm Pos		
number	Uload [kV]	Upeak [kV]	Ucorrected [kV]	Flashover	puls #
1	185	178,10	179,07	Yes	756
2	180	171,70	172,64	No	757
3	185	178,50	179,48	No	758
4	190	183,30	184,30	No	759
5	195	188,10	189,13	No	760
6	200	193,30	194,36	No	761
7	205	197,40	198,48	Yes	762
8	200	192,80	193,85	Yes	763
9	195	187,60	188,63	Yes	764
10	190	182,90	183,90	Yes	765
11	185	176,70	177,67	No	766
12	190	183,30	184,30	No	767
13	195	187,70	188,73	Yes	768
14	190	181,70	182,69	Yes	769
15	185	177,50	178,47	No	770
16	190	183,20	184,20	No	771
17	195	187,60	188,63	Yes	772
18	190	182,90	183,90	Yes	773
19	185	178,20	179,17	Yes	774
20	180	173,90	174,85	No	775
21	185	178,20	179,17	Yes	776
22	180	173,90	174,85	Yes	777
23	175	168,20	169,12	No	778
24	180	172,80	173,74	No	779
25	185	178,60	179,58	No	780
26	190	183,00	184,00	Yes	781
27	185	178,60	179,58	No	782
28	190	182,90	183,90	Yes	783
29	185	178,60	179,58	No	784
30	190	183,3	184,3	No	785

Protrusions 25cm Pos				
Upeak(i) [l\	# pulses	# Flashovers	V50 [kV]	
169,12	1	0	min	167,5
174,02	4	1	opt	183,6
179,08	9	3	max	204,1
183,94	9	5		
188,78	4	3	confidence interval = 95%	
194,11	2	1		
198,48	1	1		

Figure D.8

Measurement DATA:			Protrusions 20cm Neg		
number	Uload [kV]	Upeak [kV]	Ucorrected [kV]	Flashover	puls #
1	190	182,60	184,39	Yes	488
2	185	178,20	179,95	No	489
3	190	183,00	184,80	No	490
4	195	187,70	189,54	No	491
5	200	192,10	193,99	Yes	492
6	195	187,30	189,14	Yes	493
7	190	183,03	184,83	No	494
8	195	187,69	189,53	No	495
9	200	191,91	193,79	Yes	496
10	195	187,29	189,13	Yes	497
11	190	182,61	184,41	Yes	498
12	185	178,26	180,02	No	499
13	190	183,00	184,79	Yes	500
14	195	187,32	189,16	Yes	501
15	190	182,99	184,78	No	502
16	195	187,31	189,15	Yes	503
17	190	183,00	184,79	No	504
18	195	187,38	189,22	Yes	505
19	190	182,99	184,79	No	506
20	195	187,30	189,14	Yes	507

Protrusions 20cm Neg				
Upeak(i) [l\	# pulses	# Flashovers	V50 [kV]	
179,98	2	0	min	179,6
184,70	8	3	opt	186,3
189,25	8	6	max	191,1
193,89	2	2		
			confidence interval = 95%	

Figure D.9

Measurement DATA:			Protrusions 20cm Pos		
number	Uload [kV]	Upeak [kV]	Ucorrected [kV]	Flashover	puls #
1	170	163,80	165,28	No	196
2	175	168,50	170,03	No	797
3	180	172,90	174,46	Yes	798
4	175	168,20	169,72	Yes	199
5	170	163,80	165,28	No	800
6	175	168,60	170,13	No	801
7	180	173,00	174,57	Yes	802
8	175	168,60	170,13	No	803
9	180	173,70	175,27	No	804
10	185	177,60	179,21	Yes	805
11	180	173,70	175,27	No	806
12	185	178,30	179,91	No	807
13	190	183,10	184,76	No	808
14	195	185,80	187,48	Yes	809
15	190	182,70	184,35	Yes	810
16	185	178,00	179,61	Yes	811
17	180	172,00	173,56	No	812
18	185	178,30	179,91	No	813
19	190	182,70	184,35	Yes	814
20	185	177,60	179,21	Yes	815

Protrusions 20cm Pos				
Upeak(i) [l\	# pulses	# Flashovers	V50 [kV]	
165,28	2	0	min	164,2
170,00	4	1	opt	177,6
174,63	5	2	max	195,5
179,57	5	3		
184,49	3	2	confidence interval = 95%	
187,48	1	1		

Figure D.10

Measurement DATA:			Protrusions 15,34cm Neg		
number	Uload [kV]	Upeak [kV]	Ucorrected [kV]	Flashover	puls #
1	155	148,80	149,94	Yes	466
2	150	144,50	145,60	No	467
3	155	149,10	150,24	No	468
4	160	153,90	155,08	Yes	469
5	155	149,20	150,34	No	470
6	160	153,90	155,08	Yes	471
7	155	149,10	150,24	No	472
8	160	153,70	154,87	Yes	473
9	155	148,50	149,63	Yes	474
10	160	154,30	155,48	No	475
11	165	158,60	159,81	Yes	476
12	160	153,90	155,08	Yes	477
13	155	149,10	150,24	No	478
14	160	153,90	155,08	Yes	479
15	155	149,10	150,24	No	480
16	160	153,90	155,08	Yes	481
17	155	148,80	149,94	Yes	482
18	150	144,40	145,50	No	483
19	155	148,70	149,84	Yes	484
20	150	144,40	145,50	No	485

Protrusions 15,34cm Neg				
Upeak(i) [l\	# pulses	# Flashovers	V50 [kV]	
145,54	3	0	min	145,4
150,07	9	4	opt	151,0
155,10	7	6	max	155,0
159,81	1	1		
			confidence interval = 95%	

Figure D.11

Measurement DATA:			Protrusions 15,34cm Pos		
number	Uload [kV]	Upeak [kV]	Ucorrected [kV]	Flashover	puls #
1	160	154,00	155,18	Yes	442
2	155	149,30	150,44	No	443
3	160	153,20	154,37	Yes	444
4	155	149,20	150,34	No	445
5	160	154,00	155,18	Yes	446
6	155	149,00	150,14	Yes	446
7	150	144,50	145,60	Yes	448
8	145	139,80	140,87	No	449
9	150	144,50	145,60	No	450
10	155	148,90	150,04	Yes	451
11	150	144,50	145,60	No	452
12	155	149,00	150,14	Yes	453
13	150	144,50	145,60	No	454
14	155	149,20	150,34	No	455
15	160	153,60	154,77	No	456
16	165	158,80	160,01	Yes	457
17	160	153,60	154,77	Yes	458
18	155	149,30	150,44	No	459
19	160	154,30	155,48	No	460
20	165	159,10	160,32	No	461

Protrusions 15,34cm Pos				
Upeak(i) [l\	# pulses	# Flashovers	V50 [kV]	
140,87	1	0	min	133,2
145,60	4	1	opt	153,0
150,27	7	3	max	176,4
154,96	6	4		
160,16	2	1	confidence interval = 95%	

Figure D.12

Measurement DATA:			Sphere-Sphere 15,1cm Neg		
number	Uload [kV]	Upeak [kV]	Ucorrected [kV]	Flashover	puls #
1	386	371,72	372,87	No	349
2	388	372,90	374,06	Yes	350
3	386	371,56	372,72	No	351
4	388	372,79	373,95	Yes	352
5	386	371,73	372,88	No	353
6	388	372,79	373,95	Yes	354
7	386	371,69	372,85	No	355
8	388	372,89	374,05	Yes	356
9	386	371,89	373,04	No	357
10	388	372,76	373,92	Yes	358

Sphere-Sphere 15,1cm Neg				
Upeak(i) [l\	# pulses	# Flashovers	V50 [kV]	
372,87	5	0	min	371,8
373,99	5	5	opt	373,4
			max	375,0
			confidence interval = 95%	

Figure D.13

Measurement DATA:		Sphere-Sphere 15,1cm Pos			
number	Uload [kV]	Upeak [kV]	Ucorrected [kV]	Flashover	puls #
1	402	386,00	387,20	Yes	320
2	400	384,62	385,82	No	321
3	402	386,10	387,29	Yes	322
4	400	384,63	385,82	No	323
5	402	385,90	387,10	Yes	324
6	400	384,60	385,80	No	325
7	402	385,96	387,16	Yes	326
8	400	384,57	385,76	No	327
9	402	385,89	387,09	Yes	328
10	400	383,70	384,89	Yes	329
11	398	382,67	383,86	No	330
12	400	384,61	385,80	No	331
13	402	385,91	387,11	Yes	332
14	400	384,53	385,72	No	333
15	402	385,93	387,12	Yes	334
16	402	385,74	386,94	Yes	336
17	400	384,52	385,72	No	337
18	402	385,91	387,11	Yes	338
19	400	384,53	385,73	No	339
20	402	385,85	387,04	Yes	340

Sphere-Sphere 15,1cm Pos				
Upeak(i) [l\	# pulses	# Flashovers	V50 [kV]	
383,86	1	0	min	385,3
385,67	9	1	opt	386,2
387,12	10	10	max	387,0
			confidence interval = 95%	

Figure D.14

Measurement DATA:			Sphere-Sphere 9,6cm Neg		
number	Uload [kV]	Upeak [kV]	Ucorrected [kV]	Flashover	puls #
1	260	250,00	251,91	Yes	397
2	255	245,80	247,67	No	398
3	260	249,90	251,81	Yes	399
4	255	245,80	247,67	No	400
5	260	250,00	251,91	Yes	401
6	255	245,80	247,67	No	402
7	260	250,00	251,91	Yes	403
8	255	245,70	247,57	No	404
9	260	250,50	252,41	No	405
10	265	250,55	252,46	Yes	406

Sphere-Sphere 9,6cm Neg				
Upeak(i) [l\	# pulses	# Flashovers	V50 [kV]	
247,65	4	0	min	249,2
251,99	5	4	opt	251,1
252,46	1	1	max	253,1
			confidence interval = 95%	

Figure D.15

Measurement DATA:		Sphere-Sphere 9,6cm Pos			
number	Uload [kV]	Upeak [kV]	Ucorrected [kV]	Flashover	puls #
1	260	250,00	251,91	Yes	383
2	255	245,90	247,77	No	384
3	260	250,00	251,91	Yes	385
4	255	245,80	247,67	No	386
5	260	250,00	251,91	Yes	388
6	255	245,00	246,87	No	389
7	260	250,00	251,91	Yes	390
8	255	245,90	247,77	No	391
9	260	250,00	251,91	Yes	392
10	255	245,81	247,68	No	393

Sphere-Sphere 9,6cm Pos				
Upeak(i) [l\	# pulses	# Flashovers	V50 [kV]	
247,55	5	0	min	247,7
251,91	5	5	opt	249,7
			max	251,7
			confidence interval = 95%	

Figure D.16

Measurement DATA:			Sphere-Sphere 7,1cm Neg		
number	Uload [kV]	Upeak [kV]	Ucorrected [kV]	Flashover	puls #
1	195	187,60	189,03	No	413
2	200	192,70	194,17	Yes	414
3	195	187,60	189,03	No	415
4	200	192,80	194,27	Yes	416
5	195	187,60	189,03	No	417
6	200	192,80	194,27	Yes	418
7	195	187,70	189,13	No	419
8	200	191,10	192,56	Yes	420
9	195	187,70	189,13	No	421
10	200	192,80	194,27	Yes	422

Sphere-Sphere 7,1cm Neg				
Upeak(i) [l\	# pulses	# Flashovers	V50 [kV]	
189,07	5	0	min	189,5
193,91	5	5	opt	191,5
			max	193,5
			confidence interval = 95%	

Figure D.17

Measurement DATA:			Sphere-Sphere 7,1cm Pos		
number	Uload [kV]	Upeak [kV]	Ucorrected [kV]	Flashover	puls #
1	195	187,70	189,13	No	426
2	200	192,60	194,07	Yes	427
3	195	187,70	189,13	No	428
4	200	192,60	194,07	Yes	429
5	195	187,70	189,13	No	430
6	200	192,60	194,07	Yes	431
7	195	187,70	189,13	No	432
8	200	192,60	194,07	Yes	433
9	195	187,60	189,03	No	434
10	200	193,10	194,57	Yes	435

Sphere-Sphere 7,1cm Pos				
Upeak(i) [l\	# pulses	# Flashovers	V50 [kV]	
189,11	5	0	min	189,6
194,17	5	5	opt	191,6
			max	193,6
			confidence interval = 95%	

Figure D.18

Measurement DATA:			Rod-Rod 50cm Neg		
number	Uload [kV]	Upeak [kV]	Ucorrected [kV]	Flashover	puls #
1	440	422,20	424,36	Yes	147
2	430	412,50	414,61	Yes	148
3	420	404,10	406,17	No	149
4	430	413,40	415,52	No	150
5	440	422,20	424,36	Yes	151
6	430	412,50	414,61	Yes	152
7	420	403,90	405,97	No	153
8	430	413,40	415,52	No	154
9	440	422,10	424,26	Yes	155
10	430	413,30	415,42	No	156
11	440	422,00	424,16	Yes	157
12	430	412,20	414,31	Yes	158
13	420	403,80	405,87	No	159
14	430	412,20	414,31	Yes	160
15	420	403,70	405,77	No	161
16	430	412,30	414,41	Yes	162
17	420	403,20	405,27	Yes	163
18	410	394,10	396,12	No	164
19	420	403,80	405,87	No	165
20	430	413,30	415,42	No	166

Rod-Rod 50cm Neg				
Upeak(i) [l\	# pulses	# Flashovers	V50 [kV]	
396,12	1	0	min	404,3
405,82	6	1	opt	413,1
414,91	9	5	max	422,0
424,29	4	4		
			confidence interval = 95%	

Figure D.19

Measurement DATA:			Rod-Rod 50cm Pos		
number	Uload [kV]	Upeak [kV]	Ucorrected [kV]	Flashover	puls #
1	325	312,20	315,47	Yes	175
2	315	303,70	306,88	No	176
3	325	312,90	316,18	No	177
4	335	319,80	323,15	Yes	178
5	325	312,80	316,08	No	180
6	335	321,90	325,27	Yes	181
7	325	312,10	315,37	Yes	182
8	315	303,40	306,58	No	183
9	325	313,00	316,28	No	184
10	335	321,90	325,27	Yes	185
11	325	312,90	316,18	No	186
12	335	322,60	325,98	No	187
13	345	331,70	335,17	Yes	188
14	335	321,90	325,27	Yes	189
15	325	312,90	316,18	No	190
16	335	321,90	325,27	Yes	191
17	325	313,00	316,28	No	192
18	335	320,30	323,66	No	193
19	345	331,80	335,28	Yes	194
20	335	321,90	325,27	Yes	195

Rod-Rod 50cm Pos				
Upeak(i) [l\	# pulses	# Flashovers	V50 [kV]	
306,73	2	0	min	312,0
316,00	8	2	opt	320,5
324,89	8	6	max	329,0
335,22	2	2		
			confidence interval = 95%	

Figure D.20

Measurement DATA:			Rod-Rod 40cm Neg		
number	Uload [kV]	Upeak [kV]	Ucorrected [kV]	Flashover	puls #
1	370	356,30	357,29	No	72
2	380	365,00	366,01	Yes	73
3	370	356,30	357,29	No	74
4	380	364,90	365,91	Yes	75
5	370	356,30	357,29	No	76
6	380	364,90	365,91	Yes	77
7	370	356,30	357,29	No	78
8	380	365,70	366,72	No	79
9	390	374,60	375,64	Yes	80
10	380	364,90	365,91	Yes	81
11	370	356,30	357,29	No	82
12	380	365,70	366,72	No	83
13	390	375,50	376,54	No	84
14	400	383,70	384,77	Yes	85
15	390	375,30	376,34	No	86
16	400	383,00	384,06	No	87
17	410	393,40	394,49	Yes	88
18	400	385,60	386,67	Yes	89
19	390	375,40	376,44	No	90
20	400	383,90	384,97	Yes	91

Rod-Rod 40cm Neg				
Upeak(i) [l\	# pulses	# Flashovers	V50 [kV]	
357,29	5	0	min	348,0
366,20	6	4	opt	373,6
376,24	4	1	max	407,6
385,12	4	3		
394,49	1	1	confidence interval = 95%	

Figure D.21

Measurement DATA:			Rod-Rod 40cm Pos		
number	Uload [kV]	Upeak [kV]	Ucorrected [kV]	Flashover	puls #
1	275	264,40	269,53	Yes	95
2	260	250,40	255,25	No	96
3	265	255,00	259,94	No	97
4	270	259,30	264,33	Yes	98
5	265	254,50	259,43	Yes	99
6	260	250,30	255,15	No	100
7	265	255,10	260,05	No	101
8	270	259,70	264,73	No	102
9	275	264,40	269,53	Yes	103
10	270	259,30	264,33	Yes	104
11	265	255,10	260,05	No	105
12	270	259,70	264,73	No	106
13	275	264,20	269,32	Yes	107
14	270	259,20	264,22	Yes	108
15	265	255,10	260,05	No	109
16	270	259,40	264,43	Yes	110
17	265	255,20	260,15	No	111
18	270	259,40	264,43	Yes	112
19	265	254,50	259,43	Yes	113
20	260	248,16	252,97	Yes	114

Rod-Rod 40cm Pos				
Upeak(i) [l\	# pulses	# Flashovers	V50 [kV]	
254,46	3	1	min	248,8
259,87	7	2	opt	261,0
264,46	7	5	max	270,2
269,46	3	3	confidence interval = 95%	

Figure D.22

Measurement DATA:			Rod-Rod 30cm Neg		
number	Uload [kV]	Upeak [kV]	Ucorrected [kV]	Flashover	puls #
1	310	297,34	298,30	Yes	230
2	305	292,53	293,48	Yes	231
3	300	288,69	289,62	No	232
4	305	292,37	293,31	Yes	233
5	300	288,63	289,56	No	234
6	305	292,57	293,51	Yes	235
7	300	287,97	288,89	Yes	236
8	295	283,94	284,86	No	237
9	300	288,63	289,56	No	238
10	305	292,15	293,09	Yes	239
11	300	287,75	288,67	Yes	240
12	295	283,98	284,90	No	241
13	300	288,68	289,61	No	242
14	305	292,70	293,64	Yes	243
15	300	288,63	289,56	No	244
16	305	292,69	293,64	Yes	245
17	300	288,57	289,50	No	246
18	305	292,55	293,50	Yes	247
19	300	288,56	289,49	No	248
20	305	292,37	293,31	Yes	249

Rod-Rod 30cm Neg				
Upeak(i) [l\	# pulses	# Flashovers	V50 [kV]	
284,88	2	0	min	288,8
289,39	9	2	opt	290,1
293,43	8	8	max	292,1
298,30	1	1		
			confidence interval = 95%	

Figure D.23

Measurement DATA:			Rod-Rod 30cm Pos		
number	Uload [kV]	Upeak [kV]	Ucorrected [kV]	Flashover	puls #
1	210	202,00	203,73	Yes	203
2	205	197,34	199,03	Yes	204
3	200	190,49	192,12	No	205
4	205	197,52	199,21	No	206
5	210	202,19	203,92	No	207
6	215	207,21	208,98	No	208
7	220	211,37	213,19	Yes	209
8	215	206,76	208,53	Yes	210
9	210	202,19	203,92	Yes	211
10	205	197,37	199,07	No	212
11	210	202,21	203,94	No	213
12	215	207,25	209,03	No	214
13	220	211,88	213,70	No	215
14	225	214,48	216,32	Yes	216
15	220	211,84	213,66	No	217
16	225	216,63	218,49	No	218
17	230	220,85	222,74	Yes	219
18	225	216,17	218,03	Yes	220
19	220	211,44	213,26	Yes	221
20	215	206,68	208,45	Yes	222

Rod-Rod 30cm Pos				
Upeak(i) [l\	# pulses	# Flashovers	V50 [kV]	
192,12	1	0	min	175,4
199,10	3	1	opt	208,5
203,88	4	2	max	241,6
208,75	4	2		
213,45	4	2	confidence interval = 95%	
217,61	3	2		
222,74	1	1		

Figure D.24

Measurement DATA:			Rod-Rod 25cm Neg		
number	Uload [kV]	Upeak [kV]	Ucorrected [kV]	Flashover	puls #
1	230	221,11	221,97	No	255
2	235	225,67	226,54	Yes	256
3	230	221,28	222,13	No	257
4	235	225,85	226,72	Yes	258
5	230	221,27	222,12	No	259
6	235	225,66	226,53	Yes	260
7	230	221,26	222,12	No	261
8	235	225,63	226,50	Yes	262
9	230	220,74	221,59	Yes	263
10	225	216,04	216,87	Yes	264
11	220	211,78	212,60	No	265
12	225	216,48	217,32	No	266
13	230	221,22	222,08	No	267
14	235	226,25	227,13	No	268
15	240	231,05	231,94	No	269
16	245	234,90	235,81	Yes	270
17	240	231,08	231,97	No	271
18	245	235,06	235,97	Yes	272
19	240	231,06	231,95	No	273
20	245	235,05	235,96	Yes	274

Rod-Rod 25cm Neg				
Upeak(i) [l\	# pulses	# Flashovers	V50 [kV]	
212,60	1	0	min	204,4
217,10	2	1	opt	227,7
222,00	6	1	max	255,7
226,68	5	4		
231,95	3	0	confidence interval = 95%	
235,91	3	3		

Figure D.25

Measurement DATA:			Rod-Rod 25cm Pos		
number	Uload [kV]	Upeak [kV]	Ucorrected [kV]	Flashover	puls #
1	210	201,59	202,77	Yes	281
2	205	197,34	198,50	No	282
3	210	201,53	202,71	Yes	283
4	205	197,30	198,46	No	284
5	210	201,48	202,66	Yes	285
6	205	196,96	198,11	Yes	286
7	200	192,01	193,13	Yes	287
8	195	186,52	187,62	No	288

Rod-Rod 25cm Pos				
Upeak(i) [l\	# pulses	# Flashovers	V50 [kV]	
187,62	1	0	min	183,0
193,13	1	1	opt	195,6
198,35	3	1	max	208,5
202,71	3	3		
			confidence interval = 95%	

Figure D.26

Measurement DATA:			Rod-Rod 20cm Neg		
number	Uload [kV]	Upeak [kV]	Ucorrected [kV]	Flashover	puls #
1	180	172,94	173,72	Yes	291
2	175	168,32	169,08	No	292
3	180	173,08	173,87	Yes	293
4	175	168,35	169,12	No	294
5	180	172,92	173,71	Yes	295
6	175	168,28	169,05	No	296
7	180	172,97	173,76	Yes	297
8	175	168,33	169,10	No	298
9	180	172,99	173,78	Yes	299
10	175	168,30	169,06	No	300
11	180	173,49	174,28	No	301
12	185	177,61	178,41	Yes	302
13	180	173,00	173,78	Yes	303
14	175	168,37	169,13	No	304
15	180	172,95	173,74	Yes	305
16	175	168,31	169,08	No	306
17	180	172,99	173,77	Yes	307
18	175	167,96	168,73	Yes	308
19	170	163,59	164,34	No	309
20	175	168,36	169,12	No	310

Rod-Rod 20cm Neg				
Upeak(i) [l\	# pulses	# Flashovers	V50 [kV]	
164,34	1	0	min	169,2
169,05	9	1	opt	171,4
173,82	9	8	max	173,7
178,41	1	1		
			confidence interval = 95%	

Figure D.27

Measurement DATA:			Rod-Rod 20cm Pos		
number	Uload [kV]	Upeak [kV]	Ucorrected [kV]	Flashover	puls #
1	190	182,60	183,16	No	37
2	195	187,20	187,77	Yes	38
3	190	182,80	183,36	No	39
4	195	185,50	186,07	No	40
5	200	191,80	192,39	Yes	41
6	195	187,20	187,77	Yes	42
7	190	182,90	183,46	No	43
8	195	186,90	187,47	Yes	44
9	190	182,50	183,06	Yes	45
10	185	177,70	178,24	Yes	46
11	180	173,50	174,03	No	47
12	185	178,20	178,74	No	48
13	190	181,40	181,95	Yes	49
14	185	178,20	178,74	No	50
15	190	182,40	182,96	Yes	51
16	185	177,20	177,74	No	52
17	190	182,90	183,46	No	53
18	195	187,10	187,67	Yes	54
19	190	182,90	183,46	No	55
20	195	186,20	186,77	Yes	56

Rod-Rod 20cm Pos				
Upeak(i) [l\	# pulses	# Flashovers	V50 [kV]	
174,03	1	0	min	175,6
178,37	4	1	opt	183,4
183,11	8	3	max	191,2
187,25	6	5		
192,39	1	1	confidence interval = 95%	

Figure D.28